Heliyon 10 (2024) e40571

Contents lists available at ScienceDirect

Heliyon

journal homepage: www.cell.com/heliyon

Review article

Recent advances in heterogeneous porous Metal–Organic Framework catalysis for Suzuki-Miyaura cross-couplings

Ravulakollu Srinivasa Rao [a,b,1], Mahira Bashri [a,b,1], Mohamed Infas Haja Mohideen [a,b], Ibrahim Yildiz [a,c], Dinesh Shetty [a,b,**], Janah Shaya [a,b,*]

[a] Department of Chemistry, College of Engineering and Physical Sciences, Khalifa University of Science and Technology, Abu Dhabi, P.O. Box 127788, United Arab Emirates
[b] Center for Catalysis and Separations, Khalifa University of Science and Technology, Abu Dhabi, P.O. Box 127788, United Arab Emirates
[c] Functional Biomaterials Group, Khalifa University of Science and Technology, Abu Dhabi, P.O. Box 127788, United Arab Emirates

ARTICLE INFO

Keywords:
MOF
Palladium
Catalysis
Suzuki-miyaura coupling

ABSTRACT

Suzuki-Miyaura coupling (SMC), a crucial C–C cross-coupling reaction, is still associated with challenges such as high synthetic costs, intricate work-ups, and contamination with homogeneous metal catalysts. Research intensely focuses on strategies to convert homogeneous soluble metal catalysts into insoluble powder solids, promoting heterogeneous catalysis for easy recovery and reuse as well as for exploring greener reaction protocols. Metal-Organic Frameworks (MOFs), recognized for their high surface area, porosity, and presence of transition metals, are increasingly studied for developing heterogeneous SMC. The molecular fence effect, attributed to MOF surface functionalization, helps preventing catalyst deactivation by aggregation, migration, and leaching during catalysis. Recent reports demonstrate the enhanced catalytic activity, selectivity, stability, application scopes, and potential of MOFs in developing greener heterogeneous synthetic methodologies. This review focuses on the catalytic applications of MOFs in SMC reactions, emphasizing developments after 2016. It critically examines the synthesis and incorporation of active metal species into MOFs, focusing on morphology, crystallinity, and dimensionality for catalytic activity induction. MOF catalysts are categorized based on their metal nodes in subsections, with comprehensive discussion on Pd incorporation strategies, catalyst structures, optimal SMC conditions, and application scopes, concluding with insights into challenges and future research directions in this important emerging area of MOF applications.

TABLE OF ABBREVIATIONS:

Abdc	2-amino-benzene-1,4-dicarboxylate

(*continued on next page*)

* Corresponding author. Department of Chemistry, College of Arts and Sciences, Khalifa University, Abu Dhabi, P.O. Box 127788, United Arab Emirates.
** Corresponding author. Department of Chemistry, College of Arts and Sciences, Khalifa University, Abu Dhabi, P.O. Box 127788, United Arab Emirates.
E-mail addresses: Dinesh.shetty@ku.ac.ae (D. Shetty), shaya.janah@ku.ac.ae (J. Shaya).
[1] SRR and MBK contributed equally to this work and shall be considered Co-First authors.

https://doi.org/10.1016/j.heliyon.2024.e40571
Received 27 July 2024; Received in revised form 18 November 2024; Accepted 19 November 2024
Available online 22 November 2024

(*continued*)

Abdc	2-amino-benzene-1,4-dicarboxylate
AP	Aminopyridine
ArX	Aryl halide
ATA	2-aminoterephthalate
AZDC	Azobenzene-4,4′-dicarboxylic acid
BDC	1,4-benzenedicarboxylate
BET	Brunauer-Emmett-Teller
BI	2-benzyl-imine
Bpe	1,2-bis(4-ypridyl)ethane
BPY	Bipyridine
bpydc	2,2-bipyridine-5,5-dicarboxylic acid
Cat.	Catalyst
CTAB	Cetyltrimethylammonium bromide
CUSs	Coordinately unsaturated metal sites
DABCO	1,4-diazabicyclo[2.2.2]octane
DCID	Dichloroimidazolidinedione
DMF	Dimethylformamide
EDG	Electron donating group
EtOH	Ethyl alcohol
EWG	Electron withdrawing group
GlcA	Gluconic acid
H_2BDP	1,4-bis(1Hpyrazol- 4-yl)benzene
H_3BTC	1,3,5-benzenetricarboxylic acid
K_2CO_3	Potassium carbonate
K_2PdCl_4	Potassium tetrachloropalladate(II)
LMCT	Ligand to metal charge transfer
Ln	Lanthanide
MeOH	Methyl alcohol
MIL	Material Institute Lavoisier
MOFs	Metal-Organic Frameworks
MOPs	Metal-organic polyhedras
MW	Microwave
NDISA	Naphthalene diimide salicylic acid
NHC	N-heterocyclic carbene
NPC	Nanoporous carbon
NPs	Nanoparticles
OMS	Ordered mesoporous silica
OTf	Triflate
PAN	Polyacrylonitrile
PDA	Polydopamine acid
PI	Pyridylimine
PSM	Postsynthetic modification
py-SI	Pyridyl-salicylimine
Pyta	Pyridyltriazol
Pza	2,3-pyrazinedicarboxylic acid
rt	Room temperature
SA	Surface area
SBUs	Secondary building units
SI	Salicylaldehyde
SMC	Suzuki-Miyaura coupling
TEOS	Tetraethyl orthosilicate
TOF	Turnover frequency
TON	Turnover number
UiO	University of Oslo
wt%	Percentage by weight
2-pymo	2-Hydroxypyrimidinolate

1. Introduction

The advent of metal-catalyzed cross-coupling reactions marked a paradigm shift in modern organic synthesis, enabling versatile formation of a wide range of C–C bonds [1–4]. The primary advantage of cross-coupling reactions lies in using minimal loadings of metal catalysts under relatively mild conditions achieving a variety of important substrates and functionalities in high yields. Advances in coupling reactions have enabled the syntheses of products that are very challenging to prepare via conventional methods or even otherwise unattainable from nonactivated or deactivated substrates such as aryl chlorides [5–7]. Cross-coupling reactions specifically consist of joining two substrates with complementary functional groups such as an organic halide as the electrophile with an organometallic compound as the nucleophile. Among the most important classes of coupling reactions are Suzuki-Miyaura couplings (SMC) [2,3,6,8–11], which produce biaryl products via coupling of aryl boronic moieties (acids, esters, etc.) with aryl halides or

pseudohalides. Other examples of coupling reactions involve the Heck-Mizoroki reaction [12] between aryl halides and activated C=C functional groups, and Sonogashira coupling [13–15] of alkynes with aryl halides (Scheme 1).

Pd complexes remain among the most common and efficient systems implemented in homogeneous catalysis of cross-coupling reactions. Palladium's efficiency in these reactions, including SMC, has led to its widespread use at very low catalytic loadings, sometimes reaching parts per billion [16–18]. Nickel also demonstrates effective catalytic activity, particularly with difficult substrates like aryl chlorides/mesylates, and offers advantages such as lower cost and easier removal from reaction mixtures [19]. Other metal catalytic systems such as Fe, Co, Ru, Cu, and Ag complexes have been explored for SMC reactions, but their use is less common compared to Pd and Ni [9,20]. Mechanistically, Pd-catalyzed SMCs comprise an oxidative addition of the Pd (0) species across the C–X bond of the electrophile, followed by a transmetallation step with the main group of the organometallic nucleophile, and a final reductive elimination that forms C–C bonds (Scheme 2) [1]. Transmetallation can proceed through one or both distinct/competitive pathways (A and B) [21]. The boronate pathway (A) consists of in-situ formation of the nucleophilic boronate species (III), which substitutes the halide ligand of Pd intermediate (I). Pathway B (oxo-palladium) involves the substitution of the halide of intermediate (I) by RO^- bases forming oxo-palladium (II), which acts as a nucleophile towards the boronic species, leading to the same intermediate (IV).

Ongoing research continuously focuses on developing new approaches to transform efficient soluble homogeneous catalysts into insoluble solids in liquid reaction mixtures in order to promote reactions in a heterogeneous manner [22–26]. This strategy of employing the catalyst in a different phase than the reaction medium facilitates easy recovery and reuse of the active catalytic species in sequential batch or flow reactions. Consequently, this heterogenization of homogeneous catalysis simplifies tedious purifications and enables synthesis of products with minimal metal contamination, particularly in adducts designed for biomedical and optoelectronic applications. Several active heterogeneous palladium catalysts have been developed for C–C couplings including single-atom palladium and Pd immobilized on solid supports such as zeolites and silica [27–30]. In particular, Metal-Organic Frameworks (MOFs) are widely studied in heterogeneous catalysis [24,31–33], offering a set of advantages such as high surface area, greater porosity and easy access to a large density of active sites. The inherent presence of metal nodes with strong Lewis acidity in flexible frameworks, along with the possibility of incorporating additional metals, makes MOFs promising candidates for several catalytic applications, including coupling reactions (Scheme 3). Despite the numerous reports demonstrating their efficiency in organic transformations, MOF catalysis can still be challenged by the deactivation of the catalyst in many cases. This deactivation generally occurs by the loss of the structural integrity of the MOF or by aggregation, migration, and leaching of the active metal species in the catalytic process. Recent studies and new MOF designs demonstrate improved stability and efficiency in preventing the deactivation of active metal species due to the molecular fence effect generated by MOF surface functionalization [32,34]. Considering SMC typically relying on Pd active species, reports on monometallic (intrinsic) Pd-MOFs are scarce due to synthetic and stability challenges. This research area is still is in its infancy, and advances in Pd-MOFs will greatly benefit SMC as well as other MOF applications. Till now, effective MOF-catalyzed SMCs depend on bi- or multimetallic MOFs, where the MOF scaffold acts as the heterogeneous support for further incorporation of Pd active species.

As mentioned, research on MOF-based catalysis and other applications has increased tremendously in recent years [35–39]. Although several reviews on MOFs have been published [40–48], there is no review exclusively dedicated to the catalytic application of MOFs in the widely-used Suzuki-Miyaura coupling, despite its important synthetic uses. For instance, Gascon et al. reviewed the general applications of MOFs in heterogeneous catalysis in 2020 [33]. Ji et al. described the use of MOF materials for electrochemical supercapacitors in 2022 [49]. In 2023, Wei et al. reviewed the recent advances in MOF catalysis for electrochemical ammonia synthesis [50]. This review discusses the catalysis of Suzuki-Miyaura coupling (SMC) using the reported MOF catalysts after 2016, while avoiding repetition of the excellent existing reviews on MOFs or coupling reactions discussed in this introduction for readers'

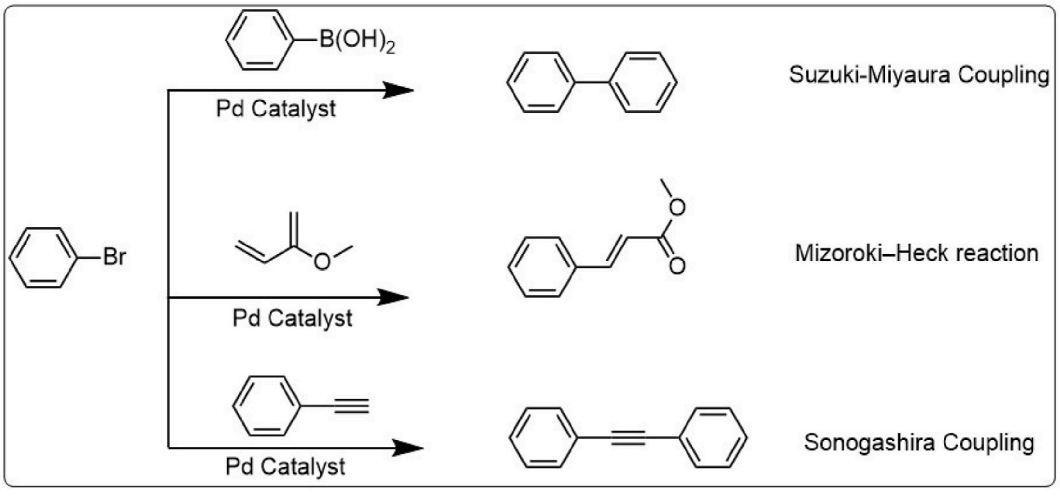

Scheme 1. Examples of Pd-catalyzed cross-coupling reactions.

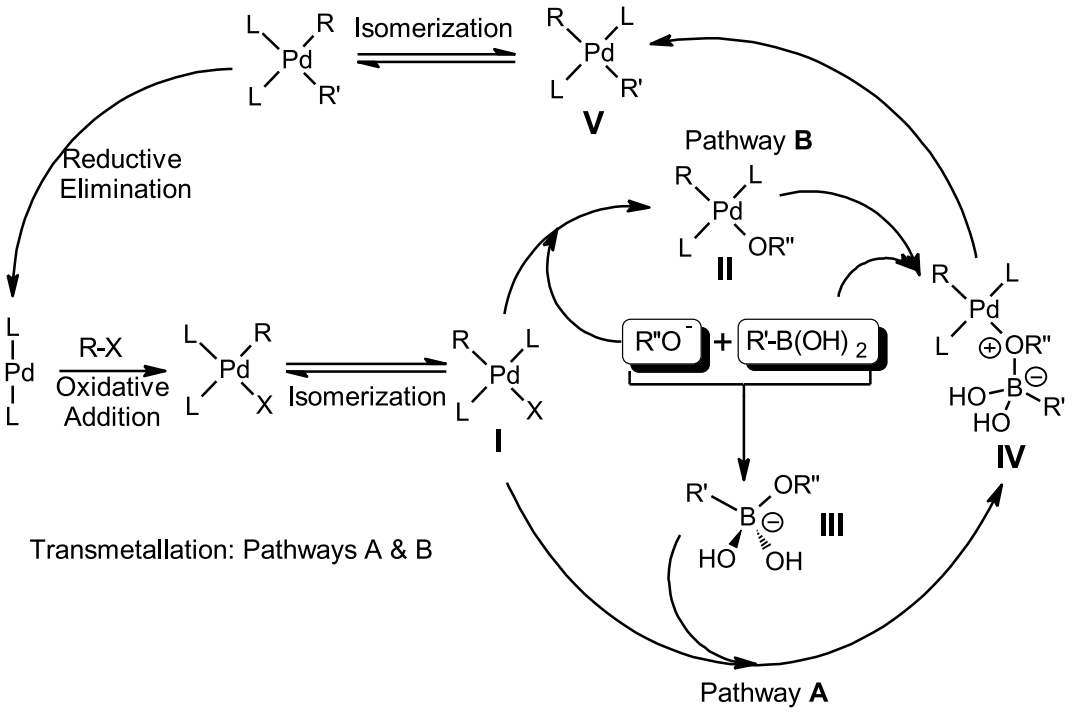

Scheme 2. The general mechanism of SMC.

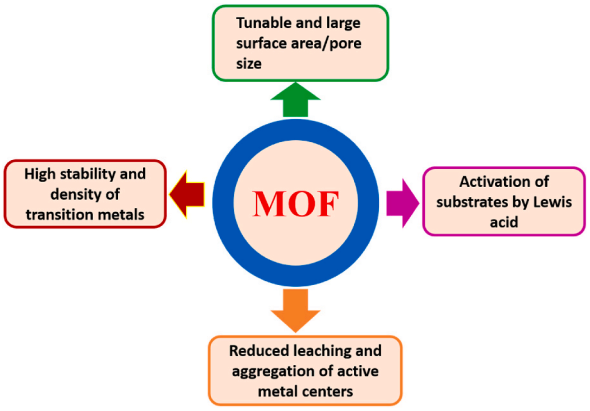

Scheme 3. Advantages of using MOFs as heterogenous catalysts particularly in coupling reactions.

reference. The first part of the review covers the morphology and engineering strategies for catalytic activity induction of MOFs. In the second part, we discuss the general aspects of MOF-catalyzed SMCs. Then, we categorize MOF catalysts reported for SMC after 2016 based on the metal nodes in subsections. It is noteworthy to re-emphasize that regardless of the metal node, most MOFs require the introduction of Pd active species for SMC catalysis. Therefore, the strategies used for Pd incorporation into the heterogenous MOF framework and the role of the different linkers/ligands are critically examined for each MOF catalyst. The structures of the obtained catalysts, the optimal SMC conditions, and the scope/applications of the catalytic methods are comprehensively discussed and summarized in detailed tables in each section. The review concludes with a discussion on the challenges and future directions for MOF-based catalysis for SMC.

2. MOF; structure and role as catalyst

2.1. MOFs and their advantages as catalyst support

Metal-organic frameworks (MOFs) are porous hybrid materials developed to take advantage of the properties of both organic and

inorganic counterparts. MOFs are made up of a regular array of positively charged metal ions that are surrounded by organic 'linker' molecules to create crystalline porous materials [51]. This combination creates two or three-dimensional structures with a network of channels and uniform pores. Scheme 4 illustrates the structural units and the formation of the lattice through the combination of nodes and linkers. The rich library of inorganic and organic building blocks offers the potential for infinite combinations and networks. The construction of such robust porous frameworks involves the strategic use of the concept of secondary building units (SBUs). It is defined as cluster entities in which ligands and metal coordination modes and environments can be utilized in transforming the fragments into porous networks via polytopic linkers. Furthermore, the structure and properties of MOFs can be adjusted and finely tuned via external stimuli adjustments, making them adaptable for several applications [52]. A key objective in MOF development is to synthesize well-defined crystalline structures with tailored properties by selecting appropriate ligands and metals [53]. In comparison to other conventional inorganic porous materials, MOFs offer the unique advantage of tunable pore size and functionality, achieved by selecting the metal ion or cluster, organic ligand, functional group, and activation processes [54]. These intriguing properties, including large surface area, low density, large porosity, tunable pore size and structural diversity, have attracted considerable attention making MOFs ideal candidates for a wide range of applications.

It is well recognized that both the morphology and size of the MOF are critical in determining their properties and catalytic activity. Therefore, developing concise methods to synthesize MOF-based catalysts with controlled size and structure is essential. Currently, MOF synthesis techniques are diverse, including solvothermal, hydrothermal, electrochemical, microwave, ultrasonic synthesis, and mechanochemical methods [56]. Several distinctions exist among these methodologies. These variances are not only represented in the reaction phase but also in the preparation's economics and yields. Moreover, using different synthesis methods for MOFs with similar raw materials, in terms of the employed metal and organic ligands, can result in different crystal structures for the synthesized MOFs. The formation of MOFs and their subsequent properties are highly sensitive to the energy source used and the synthesis technique employed. Various synthetic parameters, such as the pH, type of linker, concentration of the metal ion, and the solvent used, can affect the resultant MOF's type, size distribution, and morphology, influencing their utility and applicability. Although the synthesis of MOFs by the interaction between metal clusters and ligands appears to be a simple process, achieving the desired structure and properties is extremely challenging [57,58].

The structures of MOFs are significantly more diverse than traditional porous catalysts such as zeolites and activated carbon. This renders the pore sizes of MOFs highly tunable with a pore size gap between microporous zeolites (<2 nm) and mesoporous (2–50 nm) substances. Introducing uniformity in the porosity enhances the selectivity of MOF catalysts by allowing the reaction substrates or products to enter the locations of specific size or shape. In addition, the high surface area facilitates the adsorption of substrate molecules and their activation due to their contact with the catalytic active sites, achieving higher catalytic efficiencies. Moreover, the well-defined structures (i.e., crystallinity) of MOFs would help in better understanding of the mechanistic aspects, and subsequently the structure-catalytic performance relationships [59]. Therefore, these special solid catalysts constitute very promising candidates in metal-catalyzed cross-coupling reactions.

MOFs as supports even though relatively newer than other solid supports, promote excellent catalytic activity, and selectivity, while demonstrating stability, facile recovery and recycling unmatched by traditional solid supports like zeolites, activated carbon, and metal oxides [24]. Through rational selection of ligands and/or post-synthetic modifications, MOFs offer greater control over the architecture and functionality of their pores as well as the modulation of electronic properties of the active site, greater than that offered by other supports [29]. Hence, MOFs can be carved to perfection to bring out the best catalytic activity of the catalyst they are supporting.

The pore size of other porous materials like zeolites is largely limited (≤ 1 nm), whereas MOFs can have pore size >9.0 nm enabling greater diffusivity of reactants and consequent activity enhancement. Moreover, MOFs also exhibit some of the largest pore volumes (>1 cm^3) which can accommodate a greater number of catalytic particles such as metals like Pd [31]. Conversely, zeolites can only support few and are also sometimes quite chemically unstable, with deactivation occurring post first run itself [28]. MOFs also feature higher surface area than zeolites and metal oxides even though not as high as that of activated carbon. However, MOFs have the relative advantage of crystallinity compared to activated carbon, which leads to an ordered active site arrangement in addition to the homogeneity in the active site microenvironment. This homogenous and periodic distribution of active sites renders MOFs as 'single-site catalysts', which offers an advantage over the uniform, yet randomly distributed active sites found in zeolites [31]. Even though metal oxides also support homogeneity and orderliness of the active sites, the microenvironment can be tailored to a greater extent in MOFs. These unique microenvironments within MOFs promote substrate-selective and synergistic catalysis, enhancing

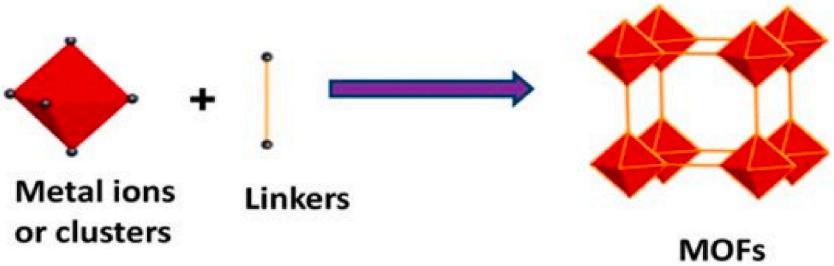

Scheme 4. Structure and components of MOFs [55]. Copyright 2014, with permission from American Chemical Society.

overall catalytic performance as opposed to other traditional supports [24].

The stability, coordination environment, and surface area of the MOFs have great influence on incorporated Pd stability and overall catalytic activity. Framework stability is crucial for preserving the integrity of the Pd active sites for continued catalytic performance. As Pd has a great tendency to be reduced and leach out, MOF stability is crucial to prevent this. As an example, Pd@OX-1 MOF NSs demonstrated robustness under a variety of conditions in addition to excellent recyclability without loss in activity [60]. As MOFs have a well-ordered network of metal nodes and organic linkers, this provides a homogenous and periodic distribution of the incorporated Pd as well [31]. The coordination environment of the Pd can be tuned to better stabilize the Pd atoms. This involves usage of ligands such as amino or bipyridyl groups that can coordinate with Pd [61]. Alternatively, using ligands that have Pd in them (metalloligand) can yield framework with more uniform and stabilized distribution of Pd centers. This can enhance the interaction with reactants and improve catalytic performance. Finally, a MOF with a higher surface area can provide more sites for Pd incorporation in addition to facilitating easier access for reactants, both of which enhance catalytic performance [62].

2.2. *Engineering strategies of MOF catalysts*

Due to the high porosity of MOFs, different species can easily integrate within the pore structure. When designing an active catalyst, different strategies are adopted for the introduction of active species (metal catalysts) inside the MOFs. The catalytic centers involved in MOFs are usually the coordinatively unsaturated metal sites (CUSs) – Lewis acid centers or the active groups on the organic linkers. This approach has certain limitations. If we consider the Pd metal incorporation for the aforementioned cross-coupling reactions, the metal undergoes successive changes in its oxidation state, which might affect the stability of the framework due to changes in the size of the active site in such locations. This explains the scarcity of reports on stable monometallic Pd-MOF that found practical applications. This situation can be well addressed by using one of the following methodologies (Fig. 1) due to the tunability of these solids: (i) functionalized modification – to graft the desired active sites onto either the metal nodes or the organic linkers by using multivariate functionality approach including mixed (multiple) linkers [63] or postsynthetic modification/metalation (PSM) [64]; (ii) encapsulation/pore confinement – to accommodate a variety of additional active species as guests and act as nanoreactors to host catalytic reactions. These active species involve the Pd moieties for SMC, but can also include other needed organic molecules, inorganic nanoparticles, metal complexes, enzymes, etc. for other applications.

Apart from the major PSM and encapsulation strategies for incorporating Pd active species for SMC, other MOF features were invested to design active catalysts such as: (iii) leveraging the material's optoelectronic properties and charge transfer for photocatalysis; (iv) acting as precursors for nanoparticles or single-site catalysts through controlled decomposition; and (v) integrating two or more of the described MOF features to enhance catalytic functionality [33,36,67]. It is worth mentioning lastly that MOFs are finding increasing applications in organocatalysis via their organic linkers or their covalent-organic framework equivalents [36, 68–71].

Impregnation/encapsulation technique involves soaking of the MOF in Pd precursor solution followed by drying and Pd(II) reduction [29,72]. On the other hand, in *in-situ* encapsulation, Pd component is encapsulated during the MOF synthesis itself, yielding Pd NPs/clusters incorporated MOF [73]. In PSM, the MOF is modified post synthesis with groups that can chelate Pd after which Pd is introduced through suitable precursors [74–78].

MOFs with basic groups such as amino or bipyridyl groups are best suited for Pd incorporation as they can coordinate well with Pd metal. To introduce other basic groups such as NHC through PSM method, strong bases are used which can damage the MOFs [79]. Incorporation through PSM technique, if not optimized properly can also potentially lead to pore blockage due to bulky organic groups

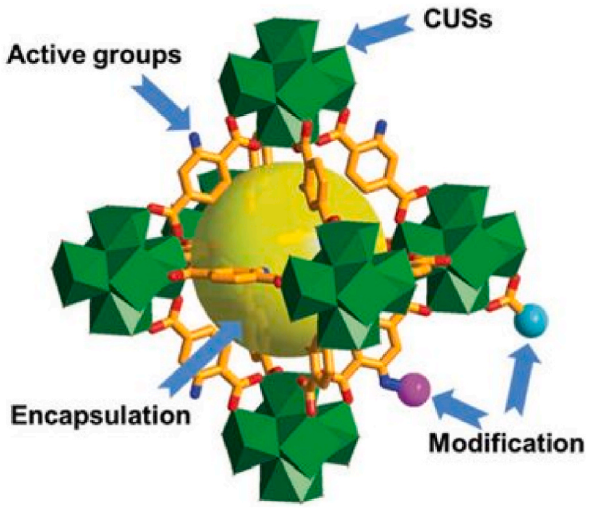

Fig. 1. Strategies adopted to introduce active species into MOFs [65,66].

which limit catalytic activity. When carefully optimized, however, PSM technique can achieve an excellent dispersion of Pd through wide variety of modification options [62]. Impregnation is quite facile and usually allows introduction of Pd without significant impact on the framework. However, the reduction step in it can compromise MOF stability and even lead to catalyst leaching [80]. Also, the chance for non-selective surface deposition and pore blockage exists for incorporation through this technique. On the contrary, *in-situ* encapsulation leads to excellent Pd-MOF integration with reduced particle aggregation which boosts catalytic activity and ensures greater stability. However, precise reaction control is required to achieve this and not all MOFs are suitable for this method [73].

Based on the above findings, PSM and impregnation methods appear to be the most widely applicable and convenient technique while *in-situ* encapsulation yields the best results given that its applicable to the MOF is carried out carefully.

3. MOFs for suzuki-miyaura coupling reaction

3.1. General aspects of MOF-catalyzed SMC

The primary goal of MOF catalysis for SMC is to harness the activity of efficient homogeneous palladium complexes within a solid-state framework material. As mentioned previously, the MOF plays the role of the catalyst support system in most cases, rather than being a primary catalyst for SMC in few reports of monometallic Pd-MOF catalysts for SMC (section 3.2). Both Pd(II) and Pd(0) species have been incorporated into MOFs via postsynthetic MOF modification or encapsulation of nanoparticles as summarized in the subsequent tables. The selection of MOF for this purpose is largely based on its flexibility as well as the thermal stability of the framework. Therefore, frameworks with basic groups such as amino or bipyridyl sites are recommended for coordinating Pd since they can withstand consecutive cycles of heating without considerable framework damage [61]. Moreover, these frameworks ensure much better coordination with the Pd metal. In the case of palladized MOF catalysts used for SMC, the underlying mechanism mainly involves the interaction of the supported Pd species with the aryl halide substrate in a manner similar to the homogeneous SMC coupling. It is generally accepted that Pd(0) is the active catalytic species in the SMC that facilitates the oxidative addition of alkyl halides to initiate the catalytic cycle. In the case of Pd(II)-MOF, Pd(II) species acts as the precatalyst that is reduced to Pd(0) before SMC commences via interaction with a base or a reductant present in the reaction mixture.

Pd-functionalized Zr-MOFs (UiO-66/67 and MOF808) are among the most employed systems in SMC due to their high stability, large surface area, ability to incorporate Pd species effectively, potential for milder and greener couplings, among other properties (Section 3.3). Pd/Cr-MOFs involved MIL topology with wide pore apertures and small pore window, which helps in reducing metal leaching (Section 3.4). Sections 3.5 onward discusses Zn, Ni, lanthanide, and other MOFs reported for this reaction, highlighting the versatility of MOFs in catalysis. Bimetallic NPs/MOFs and bifunctional MOFs with mixed linkers and different catalytic sites are emerging areas. These systems also found applications in SMC benefiting from the synergistic effects of different components for increasing catalytic efficiency and SMC scope and developing sequential reactions such as carbonylative SMC and one-pot alkyne hydration/SMC [81–83].

The majority MOF-catalyzed SMCs could be carried out in environment-friendly solvents such as water and alcohols and under relatively mild conditions such as low temperatures [8]. MOF-based catalysts can achieve the coupling process without the assistance of organic phosphine ligands at atmospheric pressure conditions. Carbonates are generally preferred as the bases in these reactions due to the slower release of hydroxide groups in the reaction media, which avoids generation of unreactive boronate species such as $ArB(OH)_3$. Some developed MOF-catalyzed SMCs demonstrated selectivity in dihaloaromatics with conditions favoring C–I coupling to boronic substrates in the presence of F, Cl, and even Br groups (e.g., Pd@MOF-808) [84]. MOF catalysts were also used in large-scale synthesis (gram-scale) of commercial pharmaceuticals such as Pd@MOF-808 in synthesis of Fenbufen, an anti-inflammatory and antirheumatic product [84,85]. Some reports also showed significant improvement in coupling of the more challenging yet economic aryl chloride substrates, and to much lesser extent, aryl fluorides (e.g., Pd@MOF-808-Pza) [72,74]. Aryl chlorides and fluorides are more stable and resistant to coupling reactions due to the strong electronegativity and poor leaving capacity of these halogen atoms. Such coupling partners (Cl and F) mostly need higher catalytic loadings, inert conditions, and longer reaction times. MOF-catalyzed SMCs were also developed with arenediazonium salts as electrophilic coupling alternatives to aryl halides. These salts are more economic electrophilic substrates that allow base-free and less energy-demanding coupling conditions such as lower temperatures [86,87]. It is worthy to note that some reports demonstrated the efficiency of MOF catalytic systems used for SMC in similar coupling reactions such as Heck coupling, carbonylative SMC and sometimes in other classes of reactions such as reduction reactions [34,88,89].

MOFs are increasingly being explored as promising photocatalysts due to their unique properties. The combination of metal catalysis and MOF photocatalysis aids in developing renewable energy-based processes. Light-induced SMCs using MOFs are greener than conventional SMCs and operate under milder conditions, avoiding the formation of byproducts at elevated temperature [82,90]. MOFs can exhibit photocatalytic properties by using their metal clusters as semiconductor quantum dots activated by light-absorbing organic linkers. Alternatively, MOF photocatalysts can be developed by incorporating photoactive metalloligands or dyes or by encapsulating photoactive metal complexes, especially in cases where charge transfer from the ligand to the metal is weak, such as in UiO-66(Zr) MOFs [91]. Several interesting reviews have discussed various applications of MOF-based photocatalysis [90,92–94].

In the following sections, we discuss the strategies for introducing Pd into MOFs with various metal centers for Suzuki-Miyaura coupling reactions, the properties of these catalysts, and the conditions and scope of the target reactions.

3.2. Palladium (Pd-MOFs)

The catalytic utility of Pd-MOFs in SMC was documented in the earliest reports of MOF-catalyzed SMC [95]. Nevertheless, only a

few studies exist on the direct synthesis of monometallic Pd-MOFs, and even fewer on the complete exchange (substitution/metathesis) of metal nodes in MOFs with Pd(II) ions without losing the structural integrity [96–98]. This is mainly due to the enormous associated synthetic and postsynthetic challenges, which often lead to the formation of less active Pd side products and amorphous adducts [99]. From a thermodynamic perspective, Pd(II), as a noble metal ion, can form strong bonds with N-donating coordination groups of ligands, enabling robust MOFs that meet catalysis requirements, particularly under alkaline conditions [97,100,101]. However, the balance between the reversibility of coordination bonds and their strength renders the synthesis of noble-metal MOFs challenging by conventional solvothermal methods [97]. Considering the kinetic perspective, noble metal ions generally possess significantly low ligand exchange rates, further limiting the reversibility of coordination bond formation. This often results in amorphous or poorly crystallized products under solvothermal conditions. Furthermore, noble metal cations have strong oxidative abilities that facilitate their reduction in classical solvents used for MOF synthesis, such as amide-types and alcohols, which also challenge their incorporation into crystalline framework as building units. Lastly, during the catalytic cycle of coupling reactions, the Pd species undergoes successive changes in its oxidation state, which may affect the stability and crystallinity of the framework due to alterations in the metal ion size at the active sites [96,102].

As mentioned, one of the initial reports on MOF catalysis of SMC (Scheme 5A) involved the palladium(II)-based system $[Pd(2\text{-pymo})_2]_n$ (Fig. 2) prepared via the solvothermal method by Xamena et al. [95,103] The catalyst was stable under the reaction conditions and even up to 330 °C under air [95]. In 2019, Liu et al., used the same $[Pd(2\text{-pymo})_2]_n$ system (BET surface area = 600 $m^2 g^{-1}$) to investigate a scope of base-free SMC using arenediazonium tetrafluoroborate salts derivatives with aryl boronic acid (Scheme 5B) [87]. The conditions tolerated a variety of electron-withdrawing and donating groups (EWG and EDG) and were selective on the diazonium tetrafluoroborate moiety in the presence of all halogens with very good yields. The framework stability of $[Pd(2\text{-pymo})_2]_n$ was retained up to 4 consecutive catalytic cycles only as the yield got diminished to almost half in the fourth run.

He et al., reported the construction of robust azolate-based Pd-MOF (BUT-33(Pd)) via metal metathesis (substitution) in which the Ni-MOF underwent metal exchange by the guidance of reticular chemistry (Scheme 6) [97]. Isoreticular MOFs represent a series of MOFs with similar topology, which can be produced by the homologation of the organic linkers or through extrapolation of the SBU in three dimensions [104–107]. SBUs refer to the metal cluster core used for the construction of MOFs commonly. The ability to proliferate an SBU is important in catalysis. The significance of this is mainly due to the increment in the surface activity of the catalyst. Moreover, it eases the accessibility of more sterically hindered entities into the catalytic system. The homologation of the linker will also help in enhancing the surface area.

This metal substitution approach with Ni-MOF was also helpful in exploring the facile synthesis of other noble metal-based MOFs such as Pt [97]. BUT33(Pd) was obtained with well-maintained crystallinity and was isoreticular with the that of BUT-33(Ni) parent

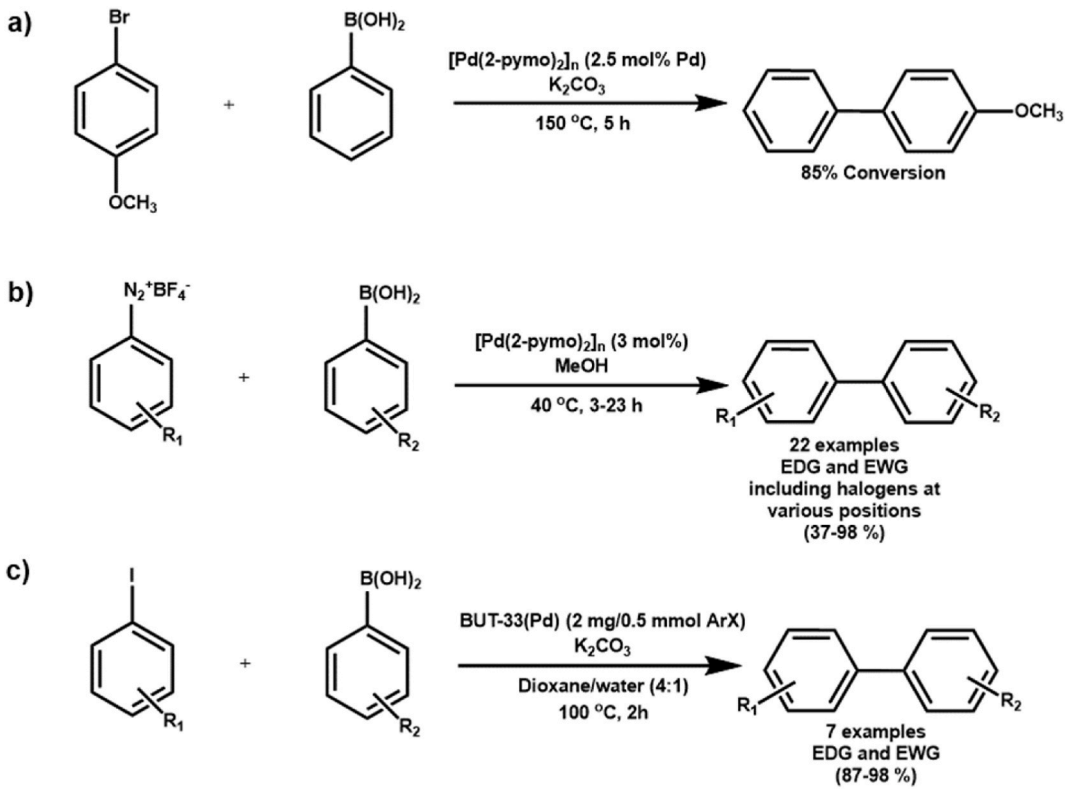

Scheme 5. SMC catalyzed by Pd-MOF.

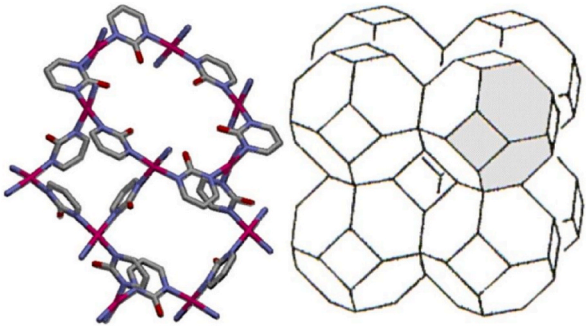

Fig. 2. (Left) $[Pd(2\text{-pymo})_2]_n$ (2-pymo = 2-hydroxypyrimidinolate; $C_4H_3N_2O$) showing the 4-membered and the two 6-membered rings. Atom colors: C = gray, N = blue, O = red and Pd = pink. (Right) 3D arrangement of the sodalite cages in sodalite-type frameworks [95]. Copyright 2007, with permission from Elsevier.

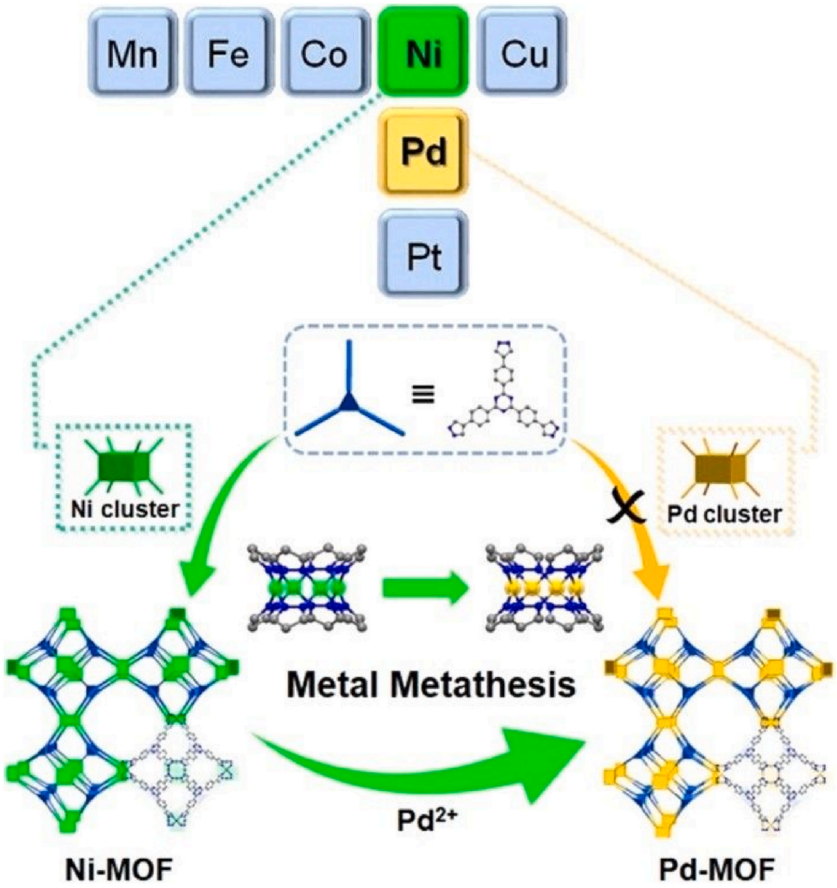

Scheme 6. Synthetic route to sodalite-type mesoporous BUT-33(Pd) through Pd(II) exchange in BUT33(Ni); BUT-33(Pd) is built from Pd_4 cluster and pyrazolate ligand (2,4,6-tris(4-(pyrazolate-4-yl)phenyl)-1,3,5-triazine ($TPTA^{3-}$)) [97]. Copyright 2021, with permission from American Chemical Society.

MOF. The synthesized BUT33(Pd) maintained cubic nanocrystals ranging in size from 100 to 400 nm and possessed a pore volume of 984 $cm^3\ g^{-1}$. Furthermore, the Pd element exhibited a uniform distribution across the entire nanocrystals following the metathesis process. The Pd-MOF was very efficient catalyst for SMC (Scheme 5C), and it was stable for 5 runs without significant decrease in yields.

In sum, less than a handful of monometallic Pd-MOFs with intrinsic catalytic activity for SMC are reported till now for the challenges described above. Further research is strongly needed to advance this area and develop stable Pd-MOFs that maintain their structural integrity while being involved in SMC. Such advances will reduce the synthetic costs of postsynthetic modifications and

expedite adopting MOF-catalyzed SMC on a large scale in pharmaceutical and industrial sectors.

3.3. Zirconium (Zr-MOFs)

Functionalized zirconium-MOFs have shown outstanding activity among all metal nodes in terms of versatility and efficiency of MOF catalysis in cross-coupling reactions. Table 1 summarizes the different reported Zr-based MOF catalysts after 2016 for SMC as well as their synthetic approaches, optimal SMC catalytic conditions, and scope of the investigated coupling reactions.

The majority of Zr-MOFs used for SMC involved MOF-808 and UiO-type (UiO-66 and 67) families. MOF-808 ($Zr_6O_4(OH)_4(BTC)_2(HCOO)_6$) is prepared with the tritopic BTC linker using 1,3,5-benzenetricarboxylic acid (H_3BTC) (Fig. 3). Tetrahedral cages are formed with the inorganic SBUs at the vertices and the BTC linkers at the faces of the tetrahedron. These octahedral crystals have the advantages of large pore sizes and the grafting ability of ligands by active formic acid sites [117].

Zr-UiO-66 and 67 landscapes (UiO stands for University of Oslo) have been recently reviewed showing the different used linkers and metalation strategies [118,119]. Considering UiO-66 Zr-based MOF, Cavka et al. were among the first groups who demonstrated their unusual high thermal stability and surface area in 2008 [120]. UiO-66, or Zr(IV)-terephthalate MOFs (Fig. 4), consists of $Zr_6O_4(OH)_4(CO_2)_{12}$ clusters joined through benzene fragments with the $–CO_2$ originating from the benzenedicarboxylate linker [72]. Several pre- and post-synthetic modifications have been proposed to enhance their surface and functional properties. A notable finding was reported by Vermoortele et al. by using acids like CF_3COOH in the synthesis which led to a more open scaffold by partial replacement of terephthalate ions with trifluoroacetate ions [121]. This modification has resulted in increasing the density of Lewis acidity in the structure, which drastically enhanced the catalytic activity.

Pd incorporation into most of Zr-based MOFs are being carried out by versatile immobilization/post synthetic metalation over functionalized organic linkers [84,122], resulting in active catalysts for SMC (e.g., Table 1, entries 1–2) [75,84]. For instance, Pourkhosravani et al. reported SMC using Pd/UiO-66 (entry 3) prepared by palladization of UiO-66 using $Pd(OAc)_2$, and they demonstrated the retainment of phase purity upon activation and functionalization (Scheme 7) [72]. Most of the studies focused on selective adsorption of Pd into organic groups containing nitrogen moieties due to their high affinity towards Pd. Coordination of Pd with N-containing MOFs was reported in SMC using the following functionalities: imidazole-α-diimines (entry 4) [108], azobenzene (entry 5) [109], pyrazine (entry 6) [74], bipyridine (entries 7–8) [110,111], guanidine (entry 9) [112,123], pyridyltriazole (entry 10) [113], and N-heterocyclic carbene (NHC, entry 17) [83,124]. The Zr-MOF with pyridyltriazole moieties (entry 10) was used for adsorption of Pd ions from wastewater showing selectivity over many other cations (Zn^{2+}, Cu^{2+}, Pb^{2+}, Fe^{3+}, Ni^{2+}, Co^{2+}, among others) and high efficiency in SMC after wastewater adsorption [113].

The azobenzene-bearing MOF catalyst developed by Chen et al., (PCN-160-Pd, entry 5) possesses a UiO-type structure where the 12-connected Zr_6 cluster is linked to 12 AZDC (azobenzene-4,4′-dicarboxylic acid) molecules, forming a cubic open pocket [109]. PCN-160-Pd was further applied in catalysis under microflow conditions within a packed column, attesting the potential of MOF catalysts in industrial continuous and portable production. $PdCl_2$/UiO-67-bpydc (entry 7) showed classical SMC selectivity for C–Cl over C–F substituents. The MOF catalyst also demonstrated phenyl-selectivity over bi- and multi-phenyl substrates which did not form coupling products due to the controlled pore size of the MOF, in contrast to classical Pd catalyst which have limited size selectivity [110].

Kim et al. reported SMC (entry 8) using a Zr-based metal-organic polyhedra (MOPs) with similar porous structure to MOFs [111]. The difference is that in MOPs, each cell exists as a discrete independent cage since it is made from organic linkers and inorganic joints with terminated interconnecting sites. The catalytic activity of MOP-BPY(Pd) was found to be superior to unsupported molecular Pd and MOF-867(Pd) catalysts.

The impact of the stereoelectronic characteristics of the metal-binding linker units on the catalytic performance of MOF-based systems and the critical role of their engineering in catalytic reactions are demonstrated by many studies (entries 11–13) [114–116]. Several studies revealed the multifold advantages of mixed-linker MOFs in addition to stability and high surface area. Chen et al. demonstrated that the incorporation of a substantial amount of the H_2bpdc ligand (90 mol% of the mixed ligands), which does not chelate the Pd complex, facilitated the creation of isolated, uniformly distributed Pd single active sites within the MOF network. The as-synthesized Pd(II)-doped UiO-67 retains the same structure as the original UiO-67 framework, with a high surface area and pore volume. This material demonstrated high efficiency in catalyzing the conversion of aryl chlorides, exhibiting significantly greater activity than homogeneous Pd catalysts [125,126]. Sun et al. (entry 11) synthesized amine-functionalized mixed-linker MOFs, namely UiO-66-Mix and UiO-67-Mix, and the free amino groups were post-synthetically modified using pyridine-2-carboxaldehyde [114]. The structures of the MOFs with mixed linkers are depicted in Scheme 8. The pyridylimine moieties in the MOF structure acted as the ligands for the Pd metal centers. Catalysts with varied Pd contents and linker ratios were reported for SMC and Heck reactions. The optimal catalytic activity was achieved with UiO-67-3-PI-Pd (2-amino-1,4-benzenedicarboxylate/1,4-benzenedicarboxylate ratio of 1:1.52; Pd = 0.054 mol%, BET = 1321 m^2/g). UiO-67-3-PI-Pd had much larger BET surface area than UiO-66-Mix-PI-Pd BET (611 m^2/g).

Considering mixed linkers with bipyridine for Pd coordination, existing sites without bipyridine serve to enhance the separation of the active Pd centers in MOFs, preventing their dimerization and deactivation [115]. Li et al. demonstrated that m-6,6′-Me_2bpy-MOF-$PdCl_2$ with UiO-67 isoreticular crystalline structures showed higher catalytic activity (entry 12) than m-bpy-MOF-$PdCl_2$ and m-4,4′Me_2bpy-MOF-$PdCl_2$ by 110- and 496-fold in SMC, respectively. It is worth noting that these metalated MOFs required toluene solvent in SMC to prevent the catalyst decomposition observed within 4 h in more common polar, protic solvents [115]. The same group also demonstrated the same enhancement in Pd(0) NP (entry 13) similar to Pd(II) catalytic sites using the same mixed-linker MOF scaffold of the previous study (m-6,6′-Me_2bpyMOF-Pd) [116]. The size of Pd NPs (~2 nm) were slightly larger than the dimension of the MOF

Table 1
Reports of SMC using Zr-based MOFs after 2016.

Entry	Catalyst	Synthesis	BET surface area, Pore volume, Mean particle or pore[a] size	Coupling reagents	Catalytic conditions	SMC scope (yield or conversion)	SMC of aryl chlorides	TOF (h^{-1}) TON[b]	Recycling catalytic runs	Ref.
1	Pd@MOF-808 Pd(0)	PSM and chemical reduction of Pd(II)	~220 cm^3/g 7 nm	(Hetero)aryl mono/di-halide (I, Br, Cl) (Hetero)aryl boronic acid	Cat. (3 mol%) K_2CO_3 MeOH 40 °C 1.5–16 h	>35 examples EWG & EDG at various positions (29–99 %)	4 examples (0–21 %)	–	6	[84]
2	UiO-66-NH_2@cyanuric chloride@2-aminopyrimidine@PdNPs Pd(0)	PSM and chemical reduction of Pd(II)	155 cm^3/g	Aryl halide (I, Br, Cl) Aryl boronic acid	Cat. (25 mg/1 mmol ArX) K_2CO_3 H_2O 60 °C 1–1.5 h	20 examples EDG & EWG at various positions (76–99 %)	94 %		10	[75]
3	Pd/UiO-66 Pd(0)	Wet impregnation	1030 m^2/g 0.46 cm^3/g ~8 nm	Aryl halide (I, Br, Cl) Phenyl boronic acid	Cat. (0.59 mol%) Na_2CO_3 EtOH–H_2O (1:2) 80 °C 0.5–20 h	13 examples EWG & EDG at various positions (63–100 %)	70 %	305-339 h^{-1} (109–172)[b]	5	[72]
4	$PdCl_2$@Zr-UiO-66-L_1/L_2 Pd(II) L_1 = 2-aminoterephthalic L_2 = imidazole α-diimine	PSM	548 m^2/g	Aryl halide (I, Br) Phenyl boronic acid	Cat. (10.0 mg per 0.33 mmol ArX) K_2CO_3 H_2O 25 °C 10 h	3 examples (99 %)	–	28[bk]	5	[108]
5	PCN-160-Pd Pd(II) PCN = Zr-AzoBDC azobenzene-4,4′-dicarboxylic acid	PSM	200 cm^3/g	Aryl bromide Phenyl boronic acid	Cat. (2 mol%) K_2CO_3 Toluene 90 °C 12h	11 examples EWG & EDG (50–96 %)		14 h^{-1} (16)[b]	4	[109]
6	Pd@MOF-808-Pza Pd(II) Pza = 2,3-pyrazinedicarboxylic acid	PSM	616 m^2/g	Aryl halides (I, Br, Cl, F) Phenyl boronic acid	Cat. (10 mg per 0.5 mmol Ar-X) K_2CO_3 DMF 80 °C 4h	8 examples Cascade SMC/ hydrogenation (78–99 %)	Ar-Cl (32 %) Ar-F (21 %)	7-9 h^{-1}	–	[74]
7	$PdCl_2$/UiO-67- bpydc Pd(II) bpydc = 2,2-bipyridine-5,5-dicarboxylic acid	PSM	1436 m^2/g 1 nm[a]	Aryl chlorides Aryl boronic acids	Cat. (1.0 mol%) Cs_2CO_3 EtOH/H_2O (29:1) rt 36 h	–	12 examples EWG & EDG at various positions (85–95 %)	–	5	[110]
8	MOP-BPY(Pd) Pd(II) BPY = bipyridine	PSM	~6 nm	Aryl bromide Phenyl boronic acids	Cat. (0.01 mol%) Na_2CO_3 MeOH/ H_2O (1:1) 80 °C 6–12 h	8 examples EWG & EDG (86–99 %)		718-822 h^{-1}	3	[111]

(*continued on next page*)

Table 1 (*continued*)

Entry	Catalyst	Synthesis	BET surface area, Pore volume, Mean particle or pore[a] size	Coupling reagents	Catalytic conditions	SMC scope (yield or conversion)	SMC of aryl chlorides	TOF (h^{-1}) TON[b]	Recycling catalytic runs	Ref.
9	UiO-66-biguanidine/Pd Pd(II)	PSM	629 m^2/g 0.41 cm^3/g 0.51 nm[a]	Aryl halides (I, Br, Cl) Phenyl boronic acid	Cat. (0.1 mol%) K_2CO_3 EtOH/H_2O (1:1) 50 °C 0.15–2 h	14 examples Phenyl & 2-thienyl halides (82–98 %)	3 examples (40–50 %)	11,870 h^{-1} (I), 3920 h^{-1} (Br)	9	[112]
10	UiO-66-Pyta-Pd Pd(II) Pyta = pyridyltriazol	PSM (azide-alkyne cycloaddition) followed by selective Pd(II) adsorption from wastewater	70–100 nm	Bromobenzene Phenyl boronic acid	Cat. (10 mg per 1 mmol ArBr) K_2CO_3 EtOH 80 °C 2 h	One example (80 %)		–	3	[113]
11	UiO-67-3-PI-Pd Pd(II) PI = pyridylimine	PSM	1321 m^2/g 1.2–1.5 nm[a]	Aryl halide (I, Br, Cl) Phenyl boronic acid	Cat. (0.054 mol %) K_2CO_3 EtOH–H_2O (4:1) 80 °C 1–10 h	11 examples EDG & EWG (86–100 %)	2 examples (86–100 %)	861-1235 h^{-1} 185 h^{-1} (Cl)	10	[114]
12	m-6,6′-Me_2bpy-MOF-$PdCl_2$ Pd(II) Mixed linker (0.42:0.58)	PSM	2100 m^2/g 0.71 cm^3/g	Iodobenzene Phenyl boronic acid	Cat. (1.0 mol %) K_2CO_3 Toluene 85 °C 11 h	One example (~80 %)	–	–	3	[115]
13	m-6,6′-Me_2bpy-MOF-Pd Pd(0) Mixed linker (0.4:0.6)	PSM and chemical reduction of Pd(II)	2000 m^2/g 0.76 cm^3/g 2 nm	Iodobenzene Aryl boronic acid	Cat. (1.0 mol %) K_2CO_3 Toluene 85 °C 12 h	2 examples (70–75 %)	–	–	3	[116]
14	Pd@UiO-66 Pd(0)	MW-assisted PSM and chemical reduction of Pd (II)	895.9 m^2/g 0.4864 cm^3/g 5 nm	Aryl halide (I, Br, Cl) Aryl boronic acid	Cat. (0.075mol%) K_2CO_3 EtOH–H_2O (1:1) rt 0.5–6 h	12 examples EWG & EDG at various positions (78–99 %)	29 %	1266.7 h^{-1}	5	[65]
15	Pd@NH_2−UiO-66(Zr) Pd(0)	Double-solvent impregnation and photoreduction of Pd(II)	1.2 nm	Aryl halide (I, Br) Aryl boronic acid	Cat. (5 mg per 0.1 mmol of ArX) Triethylamine DMF/H_2O (1/1) Visible light 0.75–2 h	10 examples EWG & EDG at various positions (63–99 %)	–	2514[b]	3	[80]
16	Bimetallic Cu_1Pd_2@NH_2-UiO66(Zr)	Double-solvent impregnation and chemical reduction	0.9 nm	Aryl iodide Aryl boronic acid	Cat. (5 mg per 0.1 mmol of ArX) Triethylamine DMF/H_2O (1/1) Visible light 4 h	9 examples EWG & EDG at various positions (42–99 %)	–	–	3	[82]
17	Au/Pd@UiO-66-NH_2 Pd(0)	Adsorption-reduction technique	526 m^2/g 0.46–0.86 nm	Aryl halide (I, Br, Cl)	Cat. (0.02 g per 1.8 mmol of ArX) K_2CO_3	4 examples (85–99 %)	81 %	242-433 h^{-1}	3	[83]

(*continued on next page*)

Table 1 (*continued*)

Entry	Catalyst	Synthesis	BET surface area, Pore volume, Mean particle or pore[a] size	Coupling reagents	Catalytic conditions	SMC scope (yield or conversion)	SMC of aryl chlorides	TOF (h^{-1}) TON[b]	Recycling catalytic runs	Ref.
				Phenyl boronic acid	$EtOH/H_2O$ (1/1) Visible light 1 h					

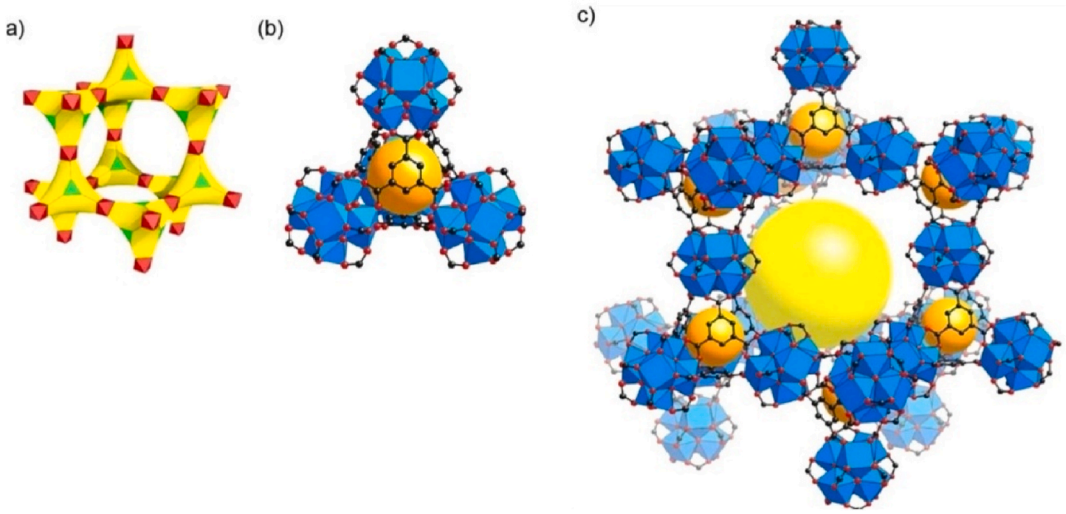

Fig. 3. Representation of the MOF-808 topology (a) built with octahedral (red) and triangular (green) units, resulting in the formation of tetrahedral cage (b) and large adamantane pores (c). Atom color scheme: C, black; O, red; Zr, blue polyhedra. H atoms are omitted for clarity. Yellow and orange balls indicate the space in the framework [117]. Copyright 2014, with permission from American Chemical Society.

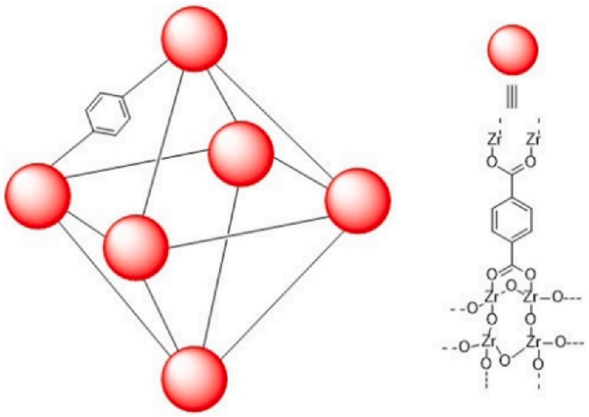

Fig. 4. Illustration of UiO-66 [120]. Copyright 2008, with permission from American Chemical Society.

cavities (~1.6 nm), as generally obtained in other NPs@MOFs composites, mostly due to deformations or local defects of the host MOFs.

Different synthetic methods were reported thereafter. For instance, a microwave-assisted polymerization strategy for synthesis of the efficient Pd@UiO-66 catalyst was described by Dong et al. (entry 14) [65]. Another successful synthetic strategy involved the encapsulation of Pd nanoparticles (Fig. 5a) into the MOF cavities via a double-solvent approach followed by reduction [80]. In this strategy, the MOF is dissolved in the organic phase whereas the aqueous Pd(II) solution is added dropwise to facilitate controlled impregnation of Pd into the pores via capillary action in the organic medium. However, the use of reducing agents in the latter step compromised the framework stability and was raised as a disadvantage in this method. Photoreduction of Pd^{2+}/amine-functionalized UiO-66 MOF was reported by Sun et al., in 2016 as an effective alternative to avoid the use of reducing agents to retain the MOF stability and achieve greener and milder synthesis [80]. The catalyst was successfully used in visible-light promoted SMC (entry 15) using the attributes of MOF-based photocatalysis with metal-based catalysis. The plausible mechanism is depicted in Fig. 5a involving the excitation of the catalyst upon irradiation generating electrons that transfer from the amine-MOF ligand to the encapsulated Pd metal center (ligand to metal charge transfer, LMCT). This results in electron-rich Pd(0) state that promotes the cleavage of C-X bond in aryl halides leading to aryl radicals, which is the rate-determining step in the coupling process. On the other hand, the photogenerated positive holes help to activate the boronic acids by cleavage of the C−B bond of the formed $RB(OH)_3^-$ species in the basic reaction medium to form another aryl radical. Lastly, the two aryl radicals couple to produce the desired biaryl product.

The same group reported bimetallic CuPd nanoclusters encapsulation inside the cavities of the same MOF (NH_2-UiO-66(Zr)) via the double-solvent approach followed by reduction with $NaBH_4$ in 2018 [82]. As the rate-determining step in the reaction is the activation of aryl halide by the Pd(0) catalyst, they explored the idea of incorporating a better electron-transferring mediator in between MOF

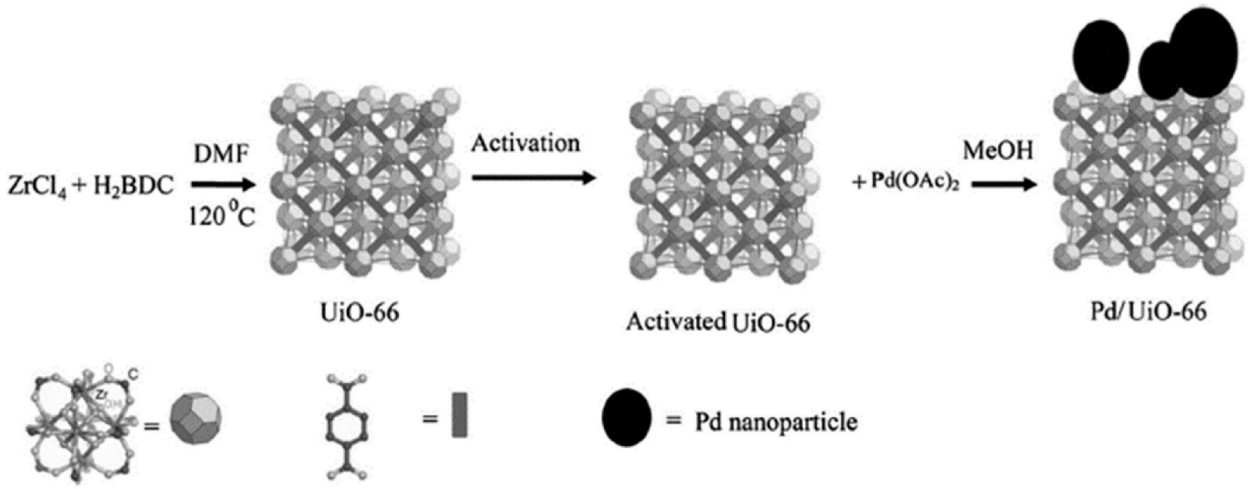

Scheme 7. Synthesis of Pd/UiO-66 MOF [72]. Copyright 2015, with permission from Springer Science Business Media, New York.

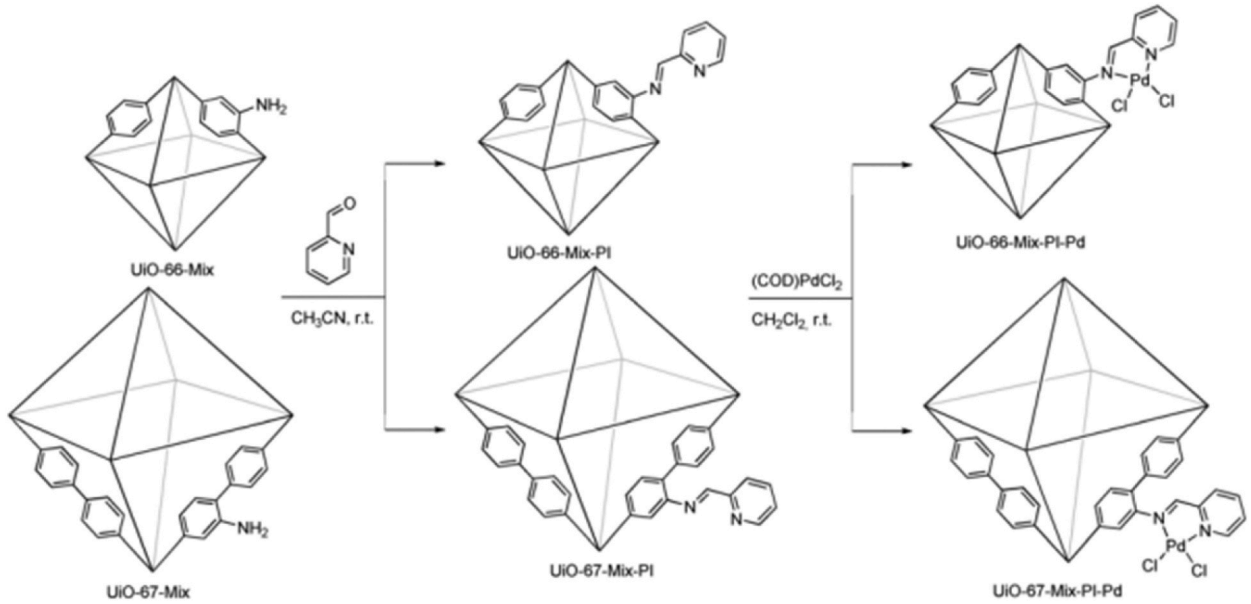

Scheme 8. PSM of mixed ligands used by Sun et al. [114] Copyright 2016, with permission from Wiley.

system and noble Pd(II) metal. For that, they introduced copper (Cu) nanoparticles along with Pd by considering its larger fermi energy level than Pd and prepared bimetallic CuPd nanoclusters (<0.9 nm) with various ratios encapsulated inside the same MOF cavities (Fig. 5b). The optimal photocatalyst for SMC (entry 16) was Cu_1Pd_2@NH_2-UiO66(Zr) (1:2 Cu/Pd ratio).

Similarly, Dong et al. demonstrated that different NHC–M (M = Au and Pd) species can be simultaneously introduced into a single MOF by direct assembly of NHC–M-decorated ligands and metal ions under solvothermal conditions (Scheme 9a) [124]. The dual catalyst (UiO-67-Au/Pd-NHBC MOF) was efficient in sequential Au-catalyzed alkyne hydration/Pd-catalyzed SMC (Scheme 9b) with a broad scope (18 examples of 4a, 81–99 %). The catalyst was reusable in 6 runs. Syntheses and applications of bimetallic nanoparticles/MOFs (e.g., Au/Pd@UiO-66-NH_2 in entry 17) [83] have been reviewed in 2020 [81].

Zr-MOFs as sacrificial templates were also reported by Li et al. [127] The MOF scaffold (e.g., UiO-66-NH_2) was used for growing Pd nanocluster catalysts with small size (~1.1 nm). The catalysts were successfully tested on a model SMC reaction [127]. In line, Alsalahi et al. developed using Pd catalysts using pyrolysis and post-pyrolytic encapsulation strategies (Fig. 6a). Pd was introduced into amino-functionalized UiO-66 via solution-impregnation method to form Pd-1 catalyst [128]. Pd-1 was subjected to pyrolysis in both inert and air conditions resulting in Pd-4 and Pd-2, respectively. Pd-3 was prepared by impregnation of Pd-2 with palladium (II) acetate solution. Pd-2 performed the best in both SMC and carbonylative SMC. This study also found that the presence of both Pd(0) and PdO species in the catalyst increases catalytic efficiency, where PdO activates the aryl halide and Pd(0) enhances the adsorption and

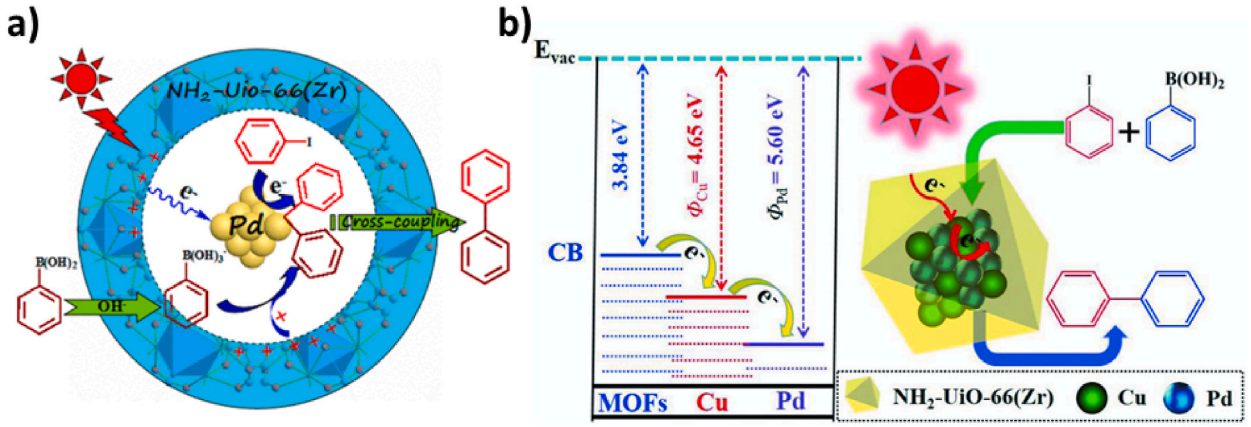

Fig. 5. a) Encapsulation of Pd into UiO-66 via double-solvent approach photoreductive catalysis [80]. b) Incorporation of bimetallic nanoparticle in MOF cavity to enhance photocatalytic activity [82]. Copyright 2018, with permission from Wiley.

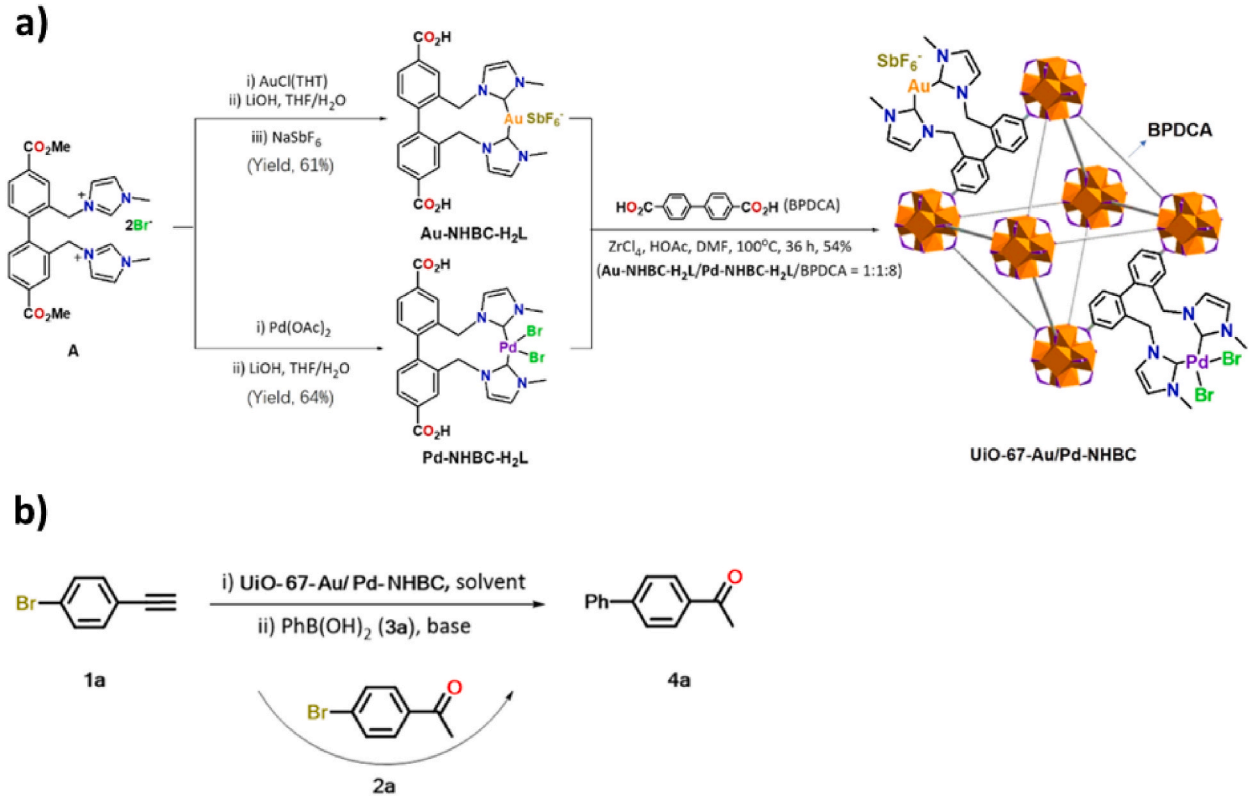

Scheme 9. a) Synthesis of UiO-67-Au/Pd-NHBC. b) Model Au-catalyzed alkyne hydration Pd−catalyzed Suzuki coupling reaction [124]. Copyright 2021, with permission from American Chemical Society.

activation of CO (Fig. 6b).

In conclusion, extensive studies on Pd incorporation into stable, high surface area Zr-MOFs show enhanced catalytic efficiency in SMC. Recent advances involve microwave-assisted polymerization, double-solvent methods, bimetallic NPs/MOFs, and mixed-linker strategies, boosting catalytic activity and enabling one-pot and photocatalytic SMC methods.

3.4. Chromium (Cr-MOFs)

Cr-containing MOFs were initially developed for gas storage applications [49,129]. Subsequently, several Cr-MOFs have been

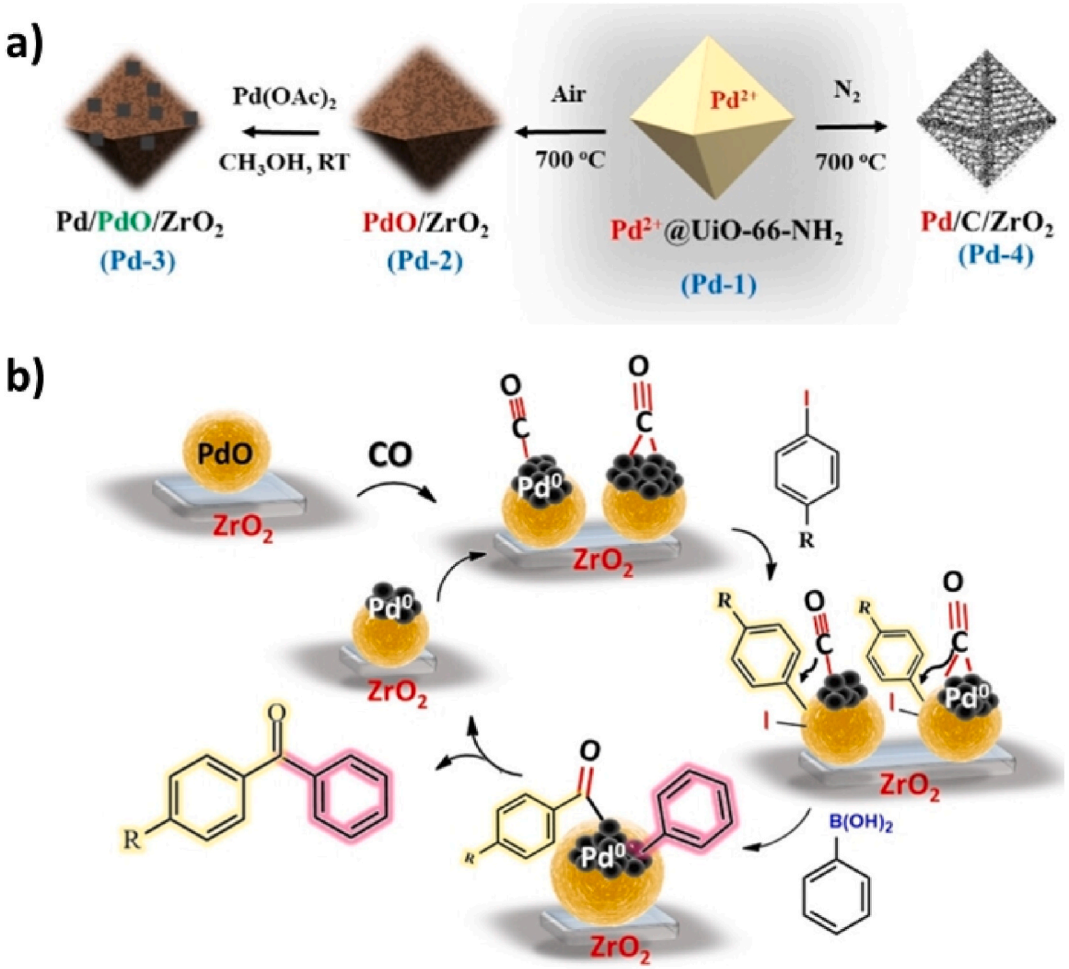

Fig. 6. a) Synthesis of Pd1-4 catalysts and b) the mechanistic role of Pd-2 in carbonylative SMC [128]. Copyright 2016, with permission from Wiley.

reported for catalytic utility due to their large surface areas and enhanced linker functionalities. The toxic nature of the chromium metal remains a major drawback that hinders their practical catalytic applications, particularly in synthesis related to bio-applications. Table 2 presents the Cr-MOFs used in SMC after 2016.

The typical Cr-MOF used for coupling reactions involves MIL-101(Cr), (MIL, Matérial Institut Lavoisier), which is made of trimeric Cr(III) octahedral clusters interconnected by 1,4-benzenedicarboxylates (Scheme 10). The active catalyst is generally prepared by palladization and subsequent borohydride reduction. MIL-Pd NP was used in the very first SMC reports of challenging aryl chlorides with phenyl boronic acids in aqueous media [134]. Many studies of palladized MIL-101(Cr) scaffolds were reported for C–C coupling reactions before 2016 in both batch and continuous processes [135–137]. This can be attributed to the chemical stability of MIL-101 (Cr) and their large surface area (BET, ca. 4000 $m^2\ g^{-1}$), mesoporous cavities, and wide pore apertures with smaller pore windows. These large cavities render them ideal candidates as host materials for nanosized guests, whereas the small pore windows prevent the leaching and aggregation of the guest molecules [138,139]. Among these nanosized guests, polyoxo-noble-metalate (POM) was reported by Bhattacharya et al. by impregnation of MIL-101 with discrete, cuboid-shaped polyoxopalladate $[Pd_{13}Se_8O_{32}]^{6-}$ (Fig. 7). This approach was successful in reducing the leaching and aggregation of guest molecules. The POM-containing MOF was efficient in SMC (Table 2, entry 1) [130].

PSM has also been reported on functionalized Cr-MOFs with triphenyl phosphines (PPh_3) [34] (Table 2, entry 2), mono-NHC (entry 3) [131], and bis-NHC ligands (entries 4–5) [132,133]. Scheme 11A&B illustrates the two main ligands and the SMC mechanism involving NHC-MOF. Pd/MIL-101-PPh_3 was reported by Wu et al. with excellent catalytic activity in SMC of both aryl chlorides and bromides (entry 2) as well as in other reactions (Heck and three-component reaction of 2-iodoaniline, CO_2, and isocyanide). The activity of Pd/MIL-101-PPh_3 far exceeded other tested catalysts such as amino-functionalized Pd/MIL-101-NH_2, naked Pd/MIL-101, and other commercial-supported Pd catalysts, as shown in Scheme 11A [34]. It is worth noting that the three Pd/MIL-101 catalysts resulted in more than 50 % yields in the SMC of the challenging aryl chlorides.

NHCs play important roles in metal catalysis due to their structural flexibility, the ease of tuning their electronic and steric properties, and the strength of the NHC–metal bond. The imidazolium moieties in such MOF scaffolds were also proposed to act as

Table 2
Reports of SMC using Cr-based MOFs after 2016.

Entry	Catalyst	Synthesis	BET surface area, Pore volume, Mean particle or pore[a] size	Coupling reagents	Catalytic conditions	SMC scope (yield or conversion)	SMC of aryl chlorides	TOF (h^{-1}) TON[b]	Recycling catalytic runs	Ref.
1	$Pd_{13}Se_8$@MIL-101 Pd(II/0)	Wet impregnation	1596 m^2/g 0.96 cm^3/g	Aryl bromide Phenyl boronic acid	Cat. (2 mol%) K_2CO_3 $MeOH/H_2O$ (1:1) rt 3 h	8 examples EWG & EDG (29–100 %)	–	–	4	[130]
2	Pd/MIL-101-PPh_3 Pd(0)	PSM and chemical reduction of Pd(II)	1805 m^2/g ~0.1 cm^3/g 2.5 nm	Phenyl halide (Br, Cl) Phenyl boronic acid	Cat. (0.15 mol%) K_2CO_3 $EtOH/H_2O$ (4:1) 80 °C 2–10 h	One example (99 %)	99 %	–	5	[34]
3	Pd-NHC-MIL-101 (mono-NHC) Pd(II)	PSM, Ag/Pd transmetalation	657 m^2/g 0.59 cm^3/g 0.6–2.1 nm	Aryl halide (I, Br, Cl) Aryl boronic acid	Cat. (0.1 mol%) K_2CO_3 dioxane/H_2O (3:1) 60 °C 3–6 h	7 examples EDG (73–99 %)	90 %	136-330 h^{-1}	3	[131]
4	Pd−NHC−MIL-101 (bis-NHC) Pd(0)	PSM (reduction of Pd(II) attributed to NHC)	1583 m^2/g	Aryl halide (I, Br, Cl) Aryl boronic acid	Cat. (0.6 mol%) K_2CO_3 H_2O 85 °C 0.25–3 h	>35 examples EWG & EDG Thienyl & polyaryl (80–97 %)	3 examples (55–90 %)	–	8	[132]
5	MIL-101(Cr)-NH_2-bis (NHC)-Pd Pd(0/II)	PSM followed by Pd(II) coordination	1335 m^2/g 0.7259 cm^3/g 3.383 nm[a]	Aryl halide (I, Br, Cl) Aryl boronic acid	Cat. (25 mg/0.5 mmol ArX) K_2CO_3 DMF/H_2O (2:1) 60 °C 0.5–24 h	9 examples EWG & EDG (40–100 %)	7 examples 30–100 % (0.5–24 h)	62-625 h^{-1} (9000)[b]	15	[133]

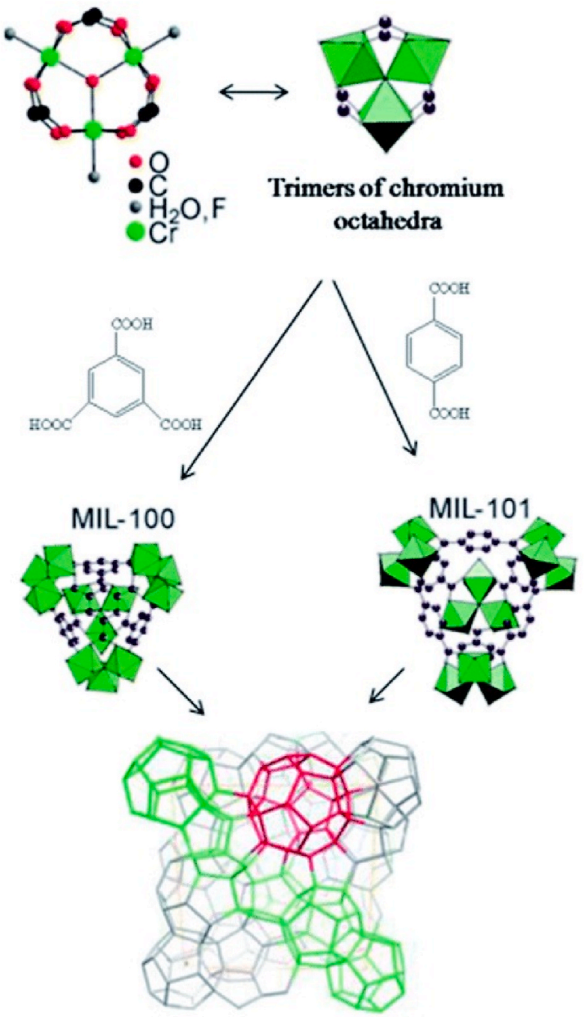

Scheme 10. MIL(Cr) and general synthetic routes [138,140]. Copyright 2014, with permission from Royal Society of Chemistry; 2021, HAL open sciences.

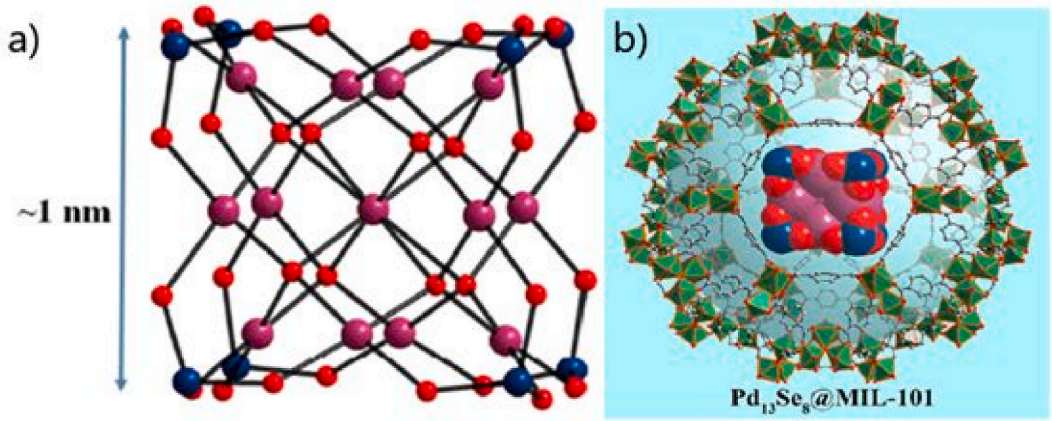

Fig. 7. Encapsulation of polyoxopalladate guest (a) into the MIL-101 pore (b). Color code: Pd(II) purple, Se(IV) blue, O red, Cr(III)O_6 green octahedra, C gray, and O red [130]. Copyright 2020, with permission from American Chemical Society.

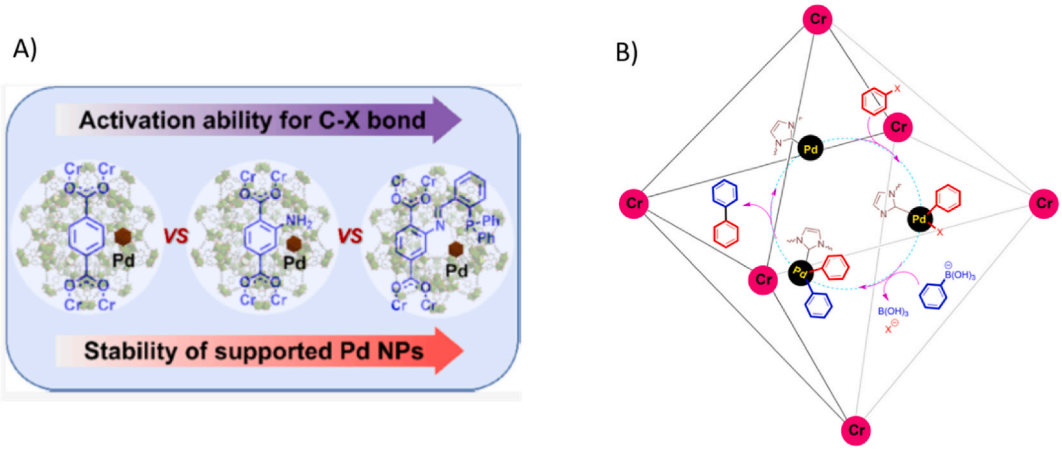

Scheme 11. Cr-MOFs functionalized with PPh_3 (A) [34] and NHC involving proposed SMC mechanism (B) [132]. Copyright 2022, with permission from American Chemical Society; 2020, with permission from Wiley.

reducing agents, generating Pd(0) NP from Pd(II) species [132]. Modifications of MOFs comprising NHCs have been reviewed in 2016 [79], and they can be classified into two general approaches (Scheme 12). The first is postsynthetic modification of imidazolium-based MOFs and incorporation of NHC moieties in the MOF structure using an organic reaction followed by Pd complexation. This protocol generally needs strong bases, which can damage most of the MOF structures. Therefore, Ag_2O was used in this strategy to prepare Ag–NHC, which is subsequently transformed to M–NHC by transmetalation. Soluble silver salts (e.g., $AgOC(CF_3)_3$) can also be used to enhance the synthetic efficiency and overcome the solubility issues of Ag_2O and MOF in this method [131]. The second approach consists of ligand pre-modification in which MOFs can be directly generated by combining Pd−NHC-functionalized organic spacers and metal ions (direct assembly). The disadvantage of the second approach is the sensitivity of M-NHC moieties to oxygen and water, which limits its use in most solvothermal methods and restricts its applications. It is worth mentioning that there are several important reviews on postsynthetic modifications of MOFs that readers can refer to [64,79,141,142].

MIL-101 was also used in bimetallic catalysis. Dhankhar et al. synthesized NiPd/MIL-101 and CuPd/MIL-101 nanoparticles (M/Pd atomic ratio = 95:5, M = Ni and Cu). The bimetallic catalysts demonstrated considerable enhancement in catalytic activity with about 20 times higher TOF than Pd/MIL-101 in SMC and excellent yields (11 examples). The observed higher catalytic activity was attributed to the synergistic effect due to electronic charge transfer from Ni or Cu to Pd and to the high dispersion of the bimetallic nanoparticles on MIL-101 framework [143].

Using catalysts in continuous-flow processes is dependent on the stability of the MOF supports and on avoiding their collapse, as mentioned previously. In line, Carson and co-workers studied the effect of bases on decomposition of MOFs in SMC using an amino-

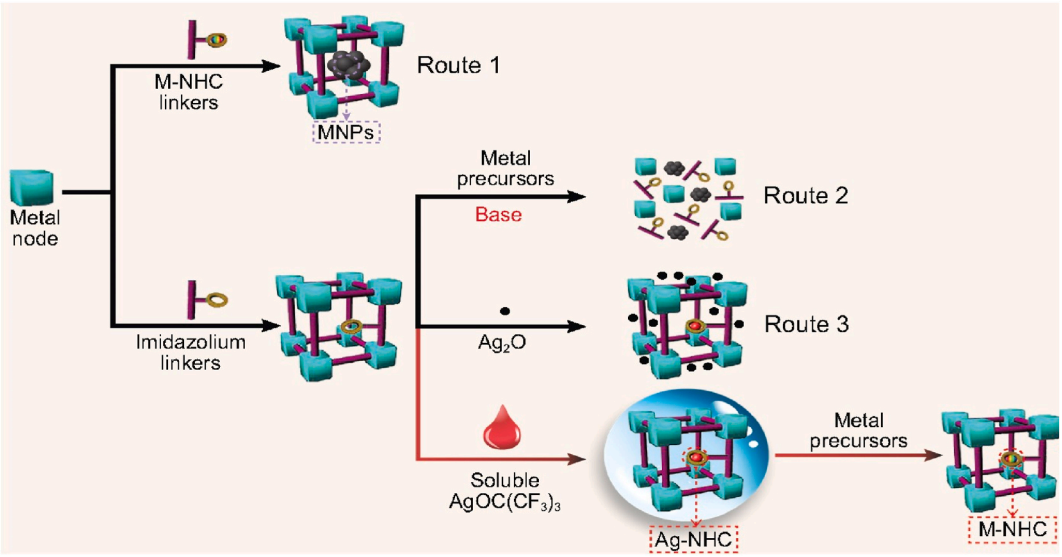

Scheme 12. Preparation of M–NHC-functionalized MOFs [131]. Copyright 2021, with permission from Oxford University Press on behalf of China Science Publishing & Media Ltd.

functionalized MIL-101 (Pd@MIL-101-NH_2(Cr)) and a control reaction with ethyl-4-bromobenzoate and p-tolyl boronic acid [144]. Significant Pd leaching was observed when organic bases were used in this study. The frame integrity was retained by employing fluoride bases, particularly CsF which has a lower degree of solvation and ion-pairing compared to other alkali metal salts. Carbonates showed the highest catalytic activities and yields of SMC products in shortest reaction times, but they were paralleled with the degradation of the MOF catalysts.

3.5. Zinc (Zn-MOFs)

Zn has a major advantage over other metal nodes used in MOFs due to its isoreticular nature, making Zn-MOFs among the most commonly studied isoreticular systems, particularly in forming useful composites with zeolites and other porous materials for

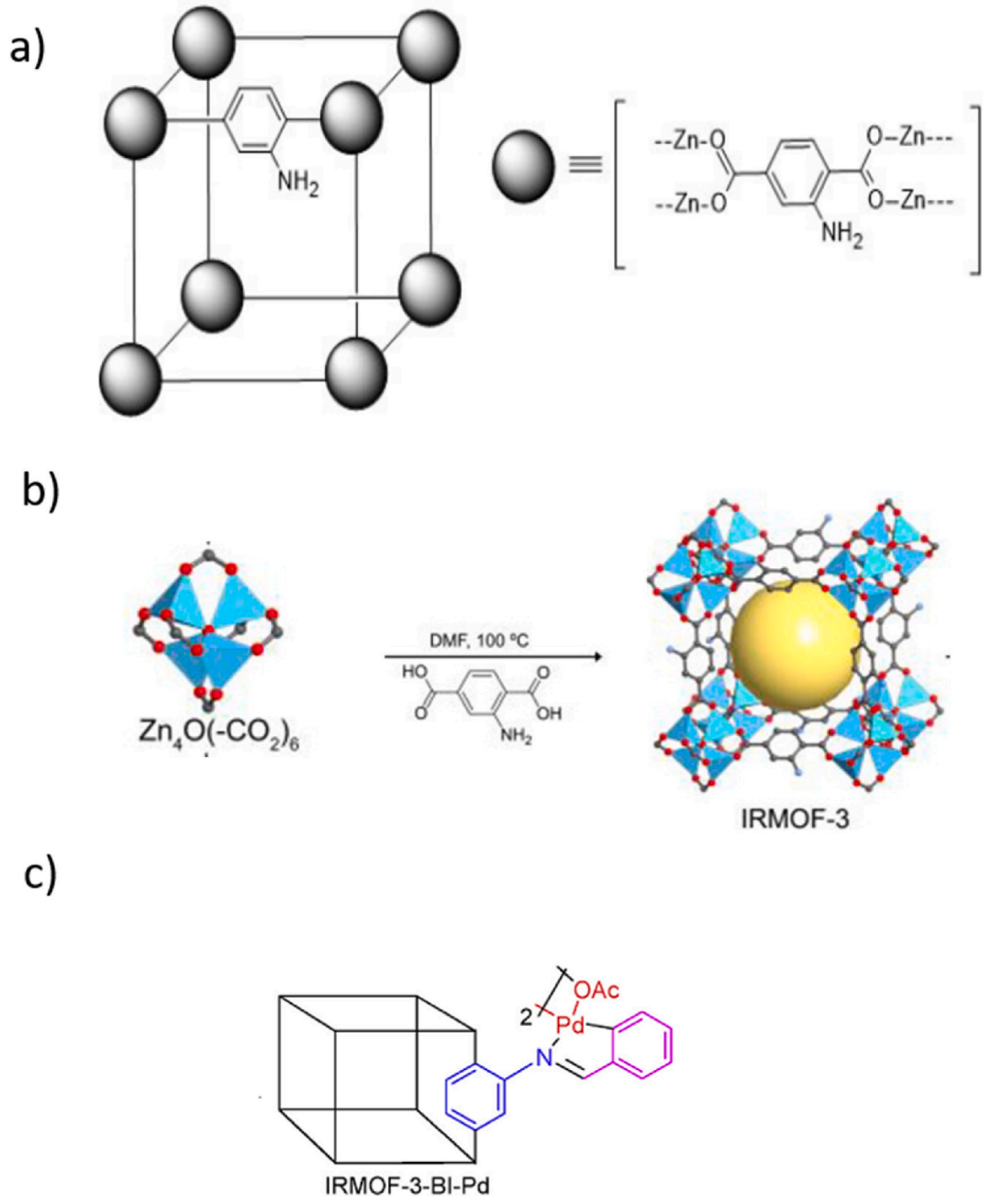

Fig. 8. a) Structure of IRMOF-3 ($Zn_4O(ATA)_3$); ATA = 2-aminoterephthalate [106], b) synthesis of IRMOF [106], c) IRMOF-3-BI-Pd [148]. Copyright 2018, with permission from American Chemical Society; 2017, with permission from Elsevier.

Table 3
Reports of SMC using Zn-based MOFs after 2016.

Entry	Catalyst	Synthesis	BET surface area, Pore volume, Mean particle or pore[a] size	Coupling reagents	Catalytic conditions	SMC scope (yield or conversion)	SMC of aryl chlorides	TOF (h^{-1}) TON[b]	Recycling catalytic runs	Ref.
1	IRMOF-3-BI-Pd Pd(II) BI = 2-benzyl-imine	PSM	594 m^2/g 0.43 cm^3/g 2.6 nm[a]	Aryl halide (I, Br, Cl) Aryl boronic acid	Cat. (0.065 mol %) K_2CO_3 EtOH–H_2O (1:1) rt 0.3–1 h	12 examples EWG & EDG at various positions (92–98 %)	4 examples (92–98 %)	~2950 h^{-1} (1480)[b]	5	[148]
2	IRMOF-3-SI-Pd(0) SI = salicylaldehyde	PSM and chemical reduction of Pd (II)	4–12 nm	Aryl halide (I, Br) Aryl boronic acid	Cat. (0.5 mol%) K_2CO_3 DMF–H_2O 80 °C 1.5–24 h	14 examples EWG & EDG at various positions (82–100 %)	–	–	4	[150]
3	Pd-NPs@Zn-MOF Pd(0)	One-step encapsulation/ reduction via temperature-controlled reaction	30 m^2/g 9.5 nm	17-haloandrosta-5,16-dien-3-ol (Br, I, OTf) Pyridine-3-boranyl derivatives	Cat. (0.2 mol%) K_2CO_3 MeOH/H_2O (2:1) reflux 3–6 h	15 examples (50–72 %)	–	59.20 h^{-1} (355)[b]	5	[151]
4	Zn-free MOF-5-NPC-900-Pd NPC = nanoporous carbon	Carbonization of MOF, Pd precursor impregnation, and chemical reduction	2200 m^2/g and 2.65 cm^3/g 2.7 nm	Aryl halide (Br, Cl) Aryl boronic acid	Cat. (0.1–0.5 mol%) K_2CO_3 EtOH–H_2O (1:1) rt 0.75–5h	12 examples EWG & EDG at various positions (91–99 %)	4 examples (25–75 %)	–	5	[66]
5	OMS@Pd-ZnMOF-5% OMS = ordered mesoporous silica	Cooperative template-directed self-assembly	239 m^2/g 0.308 cm^3/g	Aryl iodide Phenyl boronic acid	Cat. (0.05 g/ mmol Ar-X) K_3PO_4 EtOH 80 °C 2 h	6 examples EWG & EDG at various positions (63–92 %)	–	55-79 h^{-1}	5	[146]

synthetic applications [104–107,145,146]. Zn-containing IRMOF-3, synthesized using zinc nitrate and aminoterphthalic acid (Fig. 8a and b), was used in the first reports of efficient MOF catalysis in SMC [147].

More recently, IRMOF-3 was post-synthetically modified using iminopalladacycle complexes leading to an efficient heterogenous catalyst (IRMOF-3-BI-Pd, Fig. 8c) for SMC (Table 3, entry 1) [148]. The Zn-iminopalladacycle assembly was formed by treating IRMOF-3 with benzaldehyde for imine formation followed by anchoring Pd(II) using $Pd(OAc)_2$. The obtained catalytic system with a cubic geometry exhibited good crystallinity retention, with major framework degradation observed only at temperatures above 400 °C. Similar PSM approaches have been reported by different groups by using the advantage 3D extrapolation ability and subsequent enhancement in catalytic activities [60,149–151]. Among these studies, Taghavi et al. used modified IRMOF-3 (entry 2) and demonstrated its utility in SMC with two major findings. First, both Pd(0) NP and its IRMOF-Pd(II) precursor have almost the same SMC catalytic efficiency with differences only in the reaction durations. Second, reduction using $NaBH_4$ generated smaller NPs positioned into the pores of IRMOF-3 with reduced leaching (<0.6 %) in contrast to ethanol reductant that resulted in dispersed Pd NPs between the layers of the catalyst and more leaching (1.2 %) [150]. Shirazi et al. reported one-step encapsulation/reduction of Pd(II) via temperature-controlled reaction with DMF to prepare Pd-NPs@Zn-MOF with less than 0.1 % leaching. The catalyst was efficient and reusable in the synthesis of abiraterone, a prostate cancer drug, via new SMC method using both halogenated and triflate (OTf) adducts and pyridine-3-boranyl derivatives (entry 3) [151].

Zn-MOFs (particularly MOF-5: $Zn_4O(H\text{-}BDC)_3$) were also employed as sacrificial templates to produce Zn-free MOF-5-NPC-900-Pd catalyst (entry 4) [66]. The synthesis is outlined in Scheme 13. The Zn-free Pd catalyst outperformed the other tested MOF-Pd catalysts containing Zn (see Scheme 14).

An interesting catalytic composite was reported using mesoporous silica and Pd-decorated MOF(Zn) (OMS@Pd-ZnMOF-x; x = Pd/Pd + Zn molar ratio) via template-directed self-assembly by Yang and coworkers [146]. A supramolecular aggregation was obtained with the help of cetyltrimethyl ammonium bromide (CTAB) and tetraethyl orthosilicate (TEOS), through which solutions of varied molar ratio of Pd/Zn were introduced. The optimal Pd content for SMC was found to be OMS@Pd-ZnMOF-5% with ~1.2 wt % Pd (entry 5). The crystalline mesoporous composite was obtained by the hydrothermal growth of framework followed by calcination (Scheme 14). Slight contraction on the framework and decrease of crystallinity were observed upon calcination with retention of the microcrystalline networks. The catalytic activity decreased gradually upon reuse in SMC for up to five cycles.

As previously mentioned, the framework stability constitutes an important aspect for encapsulation of Pd nanoparticles. Mao et al. utilized proteins as surfactants to anchor metal nanoparticles into the MOF precursor solution [152]. The selection of protein instead of other commonly used amphiphilic polymers led to efficient hybridization of metal nanoparticles into the MOF structure with increased stability. SMC was carried out using the prepared catalysts, albeit low yields (3 examples, 12–25 %).

3.6. Copper (Cu-MOFs)

Copper-based frameworks exhibit high catalytic activity in several organic transformations attributed to their unsaturated open copper metal sites [153,154]. Tahmasebi et al. reported Pd-functionalized-$Cu_2(BDC)_2DABCO$ (Table 4, entry 1) [155] in 2017. The coordination cross-section of the MOF is shown in Scheme 15a. In 2020, the same catalyst was used in one-pot SMC of phenols (Scheme 15b) using phenols dichloroimidazolidinedione (DCID) to generate the electrophile for coupling with aryl boronic acids. The reaction showcased over 15 examples with moderate to excellent yields and selectivity for the hydroxyl group in the presence of chlorine atoms in reacting substrates [88].

Similarly, Panahi et al. employed amine-functionalized BDC linker-containing MOF ($Pd@Cu_2(NH_2\text{-}BDC)_2(DABCO)$), which was used in an ultrasound-assisted SMC of aryl halides including aryl chlorides (entry 2) [156]. Rostmania et al. immobilized Pd atoms by

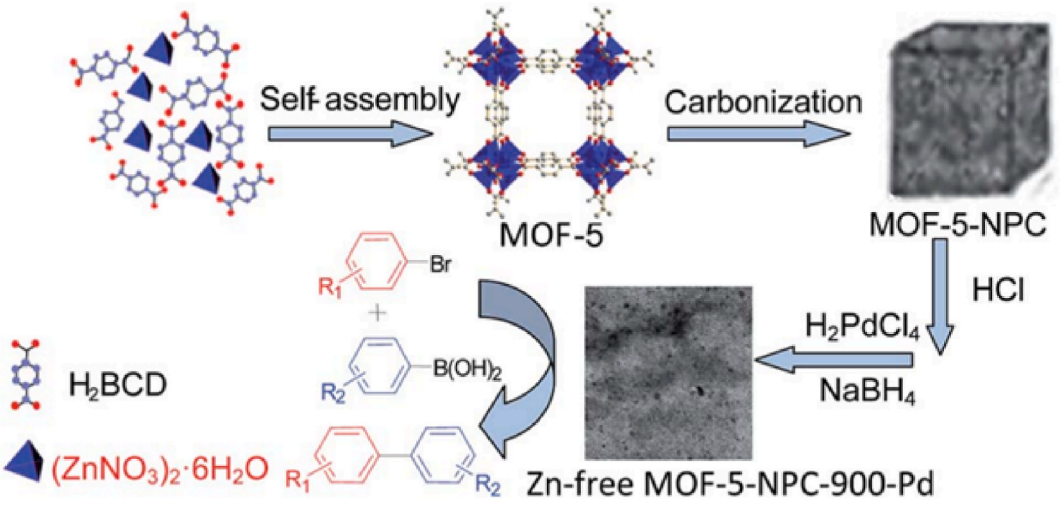

Scheme 13. Synthesis of Zn-free MOF-5-NPC-900-Pd [66]. Copyright 2016, with permission from Royal Society of Chemistry.

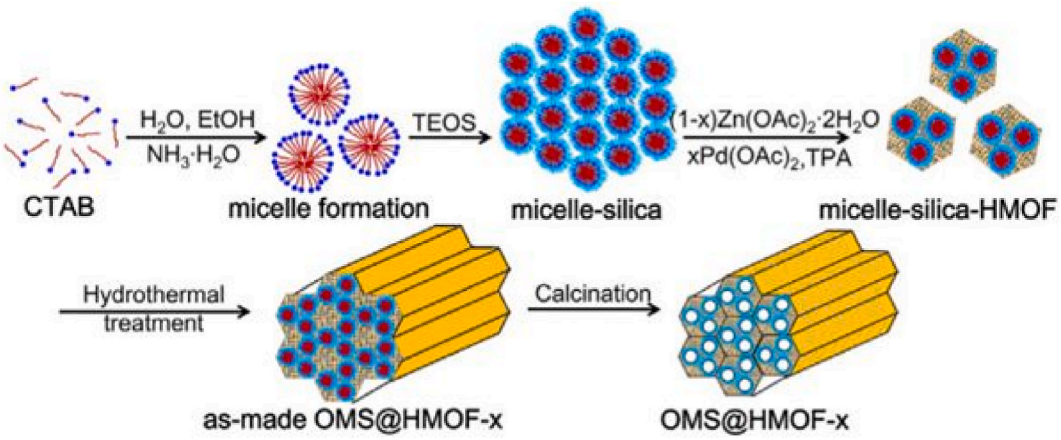

Scheme 14. Synthesis of OMS@Pd-ZnMOF-x [146]. Copyright 2016, with permission from Wiley.

grafting onto open coordination site Cu-BDC MOF. The synthesized Cu-MOF was reacted with pyridyl-salicylimine (py-SI) and subsequently palladized with $PdCl_2$ (Scheme 16). The final catalyst (entry 3) exhibited thermal stability between 130 and 255 °C [157].

A core-shell structured magnetic nanocomposite catalyst Fe_3O_4@PDA-Pd@MOF was fabricated via a layer-by-layer assembly method (Scheme 17). The structure consists of a core of polydopamine (PDA)-modified Fe_3O_4 NPs, a layer of Pd NPs, and a porous outer shell of Cu-MOF ($Cu_3(btc)_2$) with controlled thickness via the number of assembly cycles [89]. This approach with magnetic particles induced efficient catalyst recovery with less complicated magnetic separation. In addition to its application in SMC (entry 4), the catalyst was efficient in reduction of nitrophenols on the condition that both Pd and Cu moieties are present in the catalytic system.

The previous SMC examples and other reports in Fig. 9 and Table 4 (entries 5–8) [149,158–160] clearly show the excellent topology and functional diversity of Cu-based MOFs. A minimal functional modification over the linker groups can greatly impact the Lewis acidity of the nodal metals, making them a resourceful subject for PSM possibilities and adaptation of functionalities for various catalytic reactions.

3.7. Nickel (Ni-MOFs)

Ni-based MOFs have similar functionalities to Cu-MOFs described in the previous section. In terms of their applications in C–C couplings, Augustyniak et al. used a strong donor pyrazolato-based Ni-MOF containing sulfonate functionalities for Pd immobilization (Scheme 18) [161]. Nitrogen-donor ligands are valid alternatives to O-donors [101,162]. Palladization of the isoreticular Ni-MOF was done by treatment with $PdCl_2(CH_3CN)_2$ in methanol, demonstrating crystallinity retainment of the parent structure with thermal stability up to 350 °C. The catalyst was efficient in SMC (Table 5, entry 1), and it further demonstrated excellent selectivity to diarylketone products via carbonylative coupling in the presence of CO (10 examples, 21–71 % yield). This work was among the first MOF reports in carbonylative SMC [161].

Recently, the first covalent PSM of defective Ni-MOF-74 (DEMOF-1) was reported via a novel solvothermal approach using fragmented aminosalicylic acid (Scheme 19) [166]. Fragmented ligands in MOF synthesis are generally utilized as defect-generating dopants or modulators. Considering MOF-74, functionalized 2,5-dioxido-1,4-benzenedicarboxylic acid are very difficult to synthesize, and this type of MOF was only suitable for dative PSM. The incorporation of the functionalized fragmented organic ligand was only successful with Ni, and attempts to synthesize other M-MOF-74 with Mg, Zn, Co, and Mn were not fruitful. Ni-MOF-74 exhibited highly efficient and recyclable catalytic activity up to 5 runs in SMC (3 examples with excellent yields).

Large-pore MOFs, particularly mesoporous ones, continue to face problems with pore collapse upon activation. Polymer reinforcement is widely studied in many applications such as gas adsorption, demonstrating improved mechanical stability under harsh conditions. Hybridization of MOFs with polymers was reviewed in 2017 [167]. In 2019, Peng et al. investigated such reinforcement effect as shown in Scheme 20 [163]. Ni_2(NDISA)-PDA was efficient catalyst for SMC (entry 2) Loaded only with 6.8 wt% polydopamine, the BET SA of the Ni-MOF dramatically increased to 2276 m^2/g, about 5 times that of the parent structure. This increase reached ~50 times with other metal nodes such as Mg. The improved pore volume was further employed as active site for Pd incorporation and successful catalyst development [163].

The catalytic utility of Ni-based MOFs is primarily influenced by the properties of the linkers (entries 3–4) [164,165]. Despite their thermal stability and polyfunctionality, fewer reports on SMC using Ni-MOFs exist compared to other metal nodes. This is likely due to the advancements in Cu-MOF catalysis and their more economical perspective.

3.8. Lanthanides (Ln-MOFs)

Lanthanide (III) complexes exhibit good catalytic activities due to their enhanced Lewis acidity that can be retained with high coordination numbers (6–12) in contrast to conventional Lewis acids that may lose their activities due to coordinative saturation

Table 4
Reports of SMC using Cu-based MOFs after 2016.

Entry	Catalyst	Synthesis	BET surface area, Pore volume, Mean particle or pore[a] size	Coupling reagents	Catalytic conditions	SMC scope (yield or conversion)	SMC of aryl chlorides	TOF (h^{-1}) TON[b]	Recycling catalytic runs	Ref.
1	Pd-NPs@Cu_2 $(BDC)_2(DABCO)$ Pd(0) BDC = 1,4-benzenedicarboxylate DABCO = diazabicyclo [2.2.2]octane	One-step encapsulation/ reduction via temperature-controlled reaction	873 m^2/g 0.475 cm^3/g 2.7–3.1 nm	Aryl halide (Cl, Br, I) Phenyl boronic acid	Cat. (0.01 mol%) K_2CO_3 EtOH/H_2O (1:1) Rt 1 h	9 examples EWG & EDG (82–98 %)	2 examples (52–58 %)	–	5	[155]
2	Pd@$Cu_2(NH_2$-$BDC)_2(DABCO)$ Pd(0)	PSM and chemical reduction of Pd(II)	413 m^2/g 0.21 cm^3/g 9.3–9.5 nm	Aryl halide (Cl, Br, I) Aryl boronic acid	Cat. (30 mg/1 mmol ArX) K_2CO_3 EtOH ultrasonic irradiation (37 kHz, 550 W) 70 °C 1–3 h	11 examples EWG & EDG at various positions (85–99 %)	4 examples (62–80 %)	–	4	[156]
3	Pd@Cu-BDC/py-SI Pd(II) py-SI = pyridyl-salicylimine	PSM followed by open metal site grafting	–	Aryl halide (Br, I) Aryl boronic acid	Cat. (0.2 mol%) K_2CO_3 DMF/H_2O (1:1) 80 °C 0.5–1 h	13 examples EWG & EDG at various positions (93–100 %)	–	–	7	[157]
4	Fe_3O_4@PDA-Pd@ $[Cu_3(btc)_2]$ Pd(0) PDA = polydopamine	Layer-by-layer assembly of core-shell nanocomposite	51.50 m^2/g 8 nm	Aryl halide (Cl, Br) Aryl boronic acid	Cat. (0.006 mol%) K_2CO_3 EtOH/H_2O (1:1) 75 °C 0.5–6 h	9 examples EWG & EDG at various positions (82–98 %)	3 examples (83–93 %)	23429-32667 h^{-1} (Br) 2305-2583 h^{-1} (Cl)	8	[89]
5	Pd@{[Cu(1,2,3-btc)(bpe) $(H_2O)]\cdot H_2O\}_n$ Pd(0) bpe = 1,2-bis(4-ypridyl) ethane	Impregnation/reduction	2–3 nm	Aryl halide (Br, I) Phenyl boronic acid	Cat. (1.5 mg/1 mmol ArX) Cs_2CO_3 THF 65 °C 24 h	8 examples EWG & EDG at various positions (64–99 %)	–	–	4	[158]
6	Pd@HKUST-1 Pd(0)	Impregnation/reduction	461 m^2/g 0.41 cm^3/g 1.8 nm	Aryl boronic acid Elemental iodine (Tandem)	Cat. (1 mmol% Pd) K_2CO_3 EtOH 70 °C 7 h	11 examples F, Cl, and biphenyl substituents at various positions (24–93 %)	–	–	5	[159]
7	Pd/AP-MOF-199 Pd(II) AP = aminopyridine	PSM	50-100 nm[a]	Aryl bromide Aryl boronic acid	Cat. (0.3 mol%) K_2CO_3 EtOH/H_2O (2:1) 60 °C 0.5–1 h	8 examples EWG & EDG at various positions (85–98 %)	–	–	5	[160]
8	Cu-MOF-[Pd] Pd(II)	PSM on Zn-MOF-[Pd] followed by Cu transmetalation	–	Aryl/alkyl boronic acid Aryl boronic acid	Cat.(10 mg) K_2CO_3 EtOH/H_2O (1:1) 80 °C 10–60 min	14 examples EWG & EDG at various positions (58–98 %)	2 examples (10–30 %)	–	5	[149]

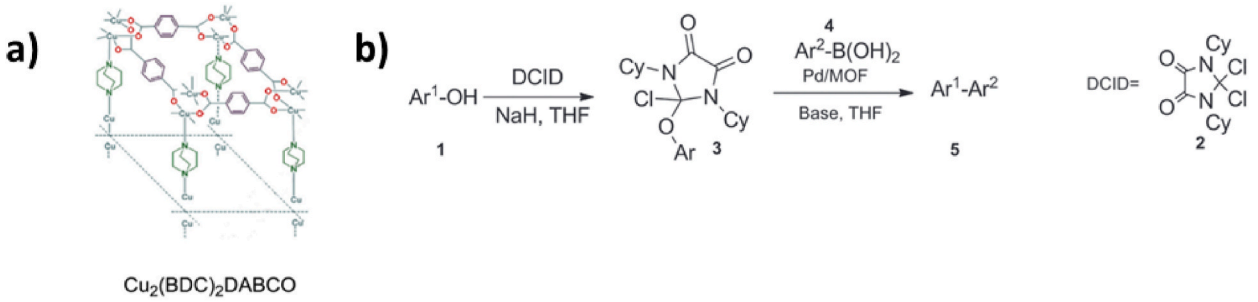

Scheme 15. a) Coordination cross-section of $Cu_2(BDC)_2DABCO$ [155], b) One-pot SMC of phenols using $Pd@Cu_2(BDC)_2(DABCO)$ [88]. Copyright 2017 and 2020, with permission from Elsevier.

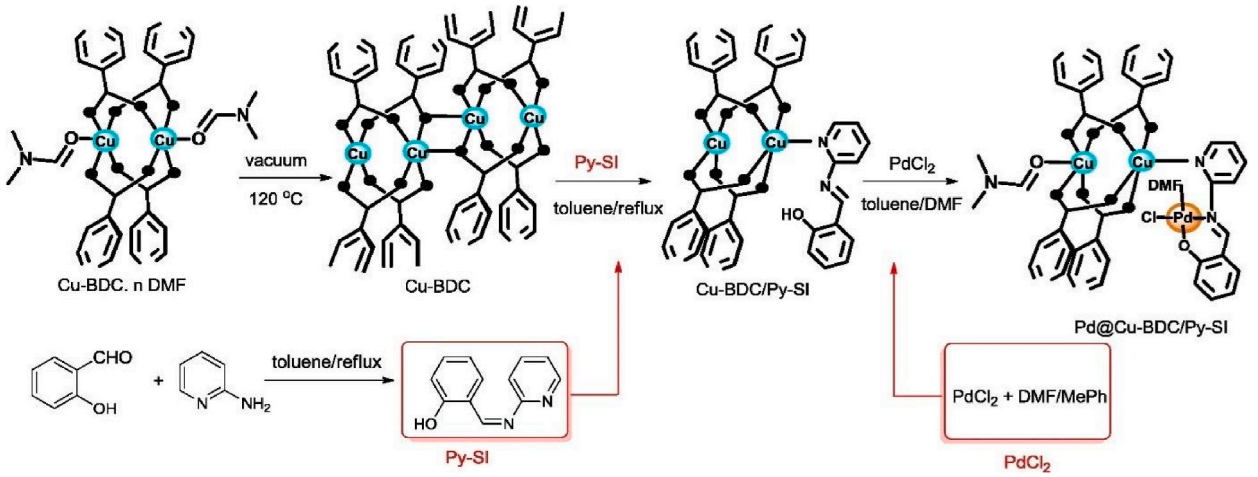

Scheme 16. Functionalization of Cu-BDC with palladium complexex [157]. Copyright 2016, with permission from Elsevier.

[168]. Few attempts have been made to convey their utility into a heterogenous environment in order to improve recyclability and product purification despite their high catalytic efficiency in homogeneous systems [169,170]. The interesting topological properties of lanthanide-MOFs arise from their large coordination spheres which helps in incorporation of more solvent molecules into their SBUs. Furthermore, removal of solvent molecules from several Ln-MOFs leads to enhance their flexibility without losing structural integrity.

Based on these rationales, You et al. synthesized a series of heterobimetallic Ln-MOFs using nitrate salts of samarium (Sm), europium (Eu), terbium (Tb), and dysprosium (Dy) [171]. The nitrate salts were treated with 1,1′-di(p-carboxybenzyl)-2,2′-diimidazole with two functionalities: carboxylates for binding Ln ions and forming a rigid structure, and N-donor diimidazole groups for Pd coordination. The four-coordinated Pd(II) atoms in the Ln-MOF had a slightly distorted quadrangular prism geometry with the eight-coordinated Ln atoms (Fig. 10). The four Pd(II)/Ln(III) MOFs showed good stability and catalytic activity in a SMC model reaction. The Pd(II)/Sm(III) MOF catalyst was used to elaborate the coupling scope (Table 6, entry 1). The used catalysts didn't show leaching and had good recyclability in solvent media based on water and ethanol.

Similarly, the efficiency of polypyridine ligands with holmium (Ho) ions for Pd(II) coordination and the catalytic applications of the post-synthetically modified structures were reported for SMC (entry 2) as well as Heck coupling [172]. Magnetically recoverable post-metalated La-MOFs were reported by Xiong et al., with good catalytic activity (entry 3), recyclability, and among the highest TOF obtained in MOF-Pd catalysis for SMC [173]. The synthetic pathways to MOFs used in entries 2,3, and 5 are illustrated in Scheme 21.

Apart from the PSM strategies, incorporation of Pd nanoclusters into Ln-MOF cavities has also been described in the literature. Mostafa et al. reported three Ce-based MOFs (MOF808, UiO66, and BTC) for the solution impregnation of ultra-small thiolated Pd nanoclusters ($Pd_n(L\text{-}Cys)_m$) and their subsequent applications as nanoreactors for SMC at room temperature (entry 4) [73]. Pd_n@Ce-MOF-808 showed considerably high TOF (132,530.1 h^{-1}) in MW-assisted SMC with extremely low Pd_n loading (0.007 mol%, 0.0224 μmol Pd). This work notably compared the in-situ growth method to high-temperature impregnation for Pd incorporation. This strategy led to higher catalytic activity compared to traditional impregnation, which was attributed to better encapsulation of the guest metals in the framework. Lin et al. also reported well-dispersed Pd NPs supported on a Ce-MOF-801 (Pd/Ce-MOF-801) via impregnation strategy (entry 5) [174]. Guo et al. reported the incorporation of Ni along with Pd into Eu-MOF cavity to improve the stability of the catalytic intermediates and achieve better activity and cost effectiveness (entry 6) [175].

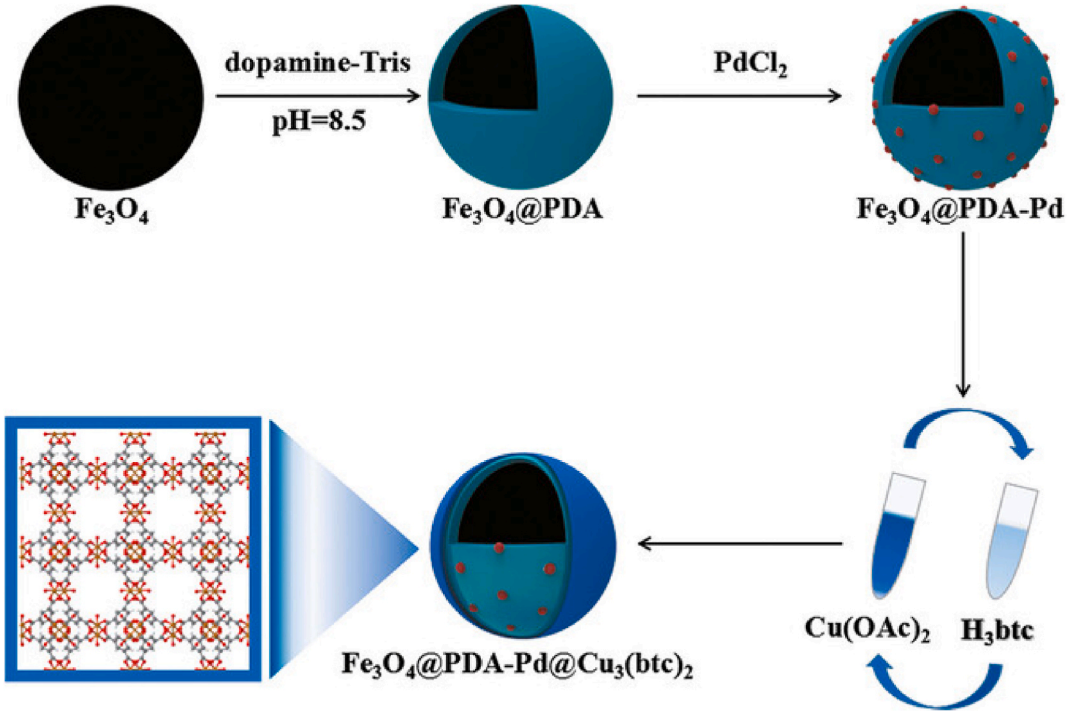

Scheme 17. Synthesis of Fe_3O_4@PDA-Pd@MOF nanocomposite [89]. Copyright 2018, with permission from Wiley.

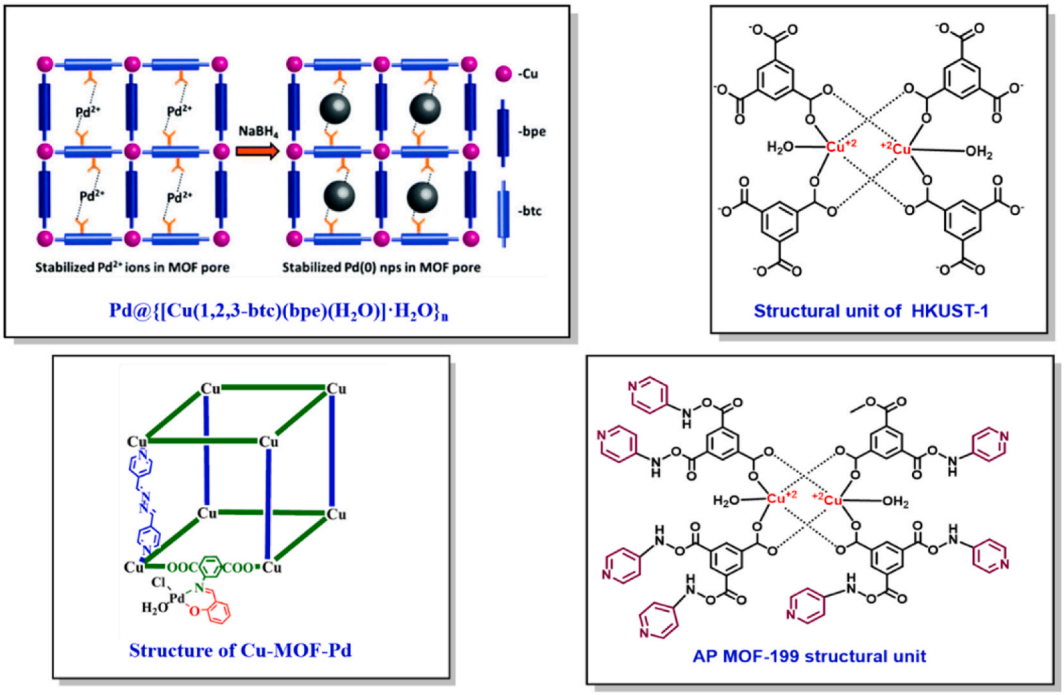

Fig. 9. Structures of MOFs used in SMC in entries 5–8 [149,158–160].

Lanthanide metal-based MOFs possess a variety of strengths such as larger coordination polyhedra and greater stability, which make them interesting for catalytic applications [176]. Nevertheless, the application of these metals in green synthesis is impeded by their toxicity, a constraint similarly encountered with the previously mentioned Cr-based MOFs.

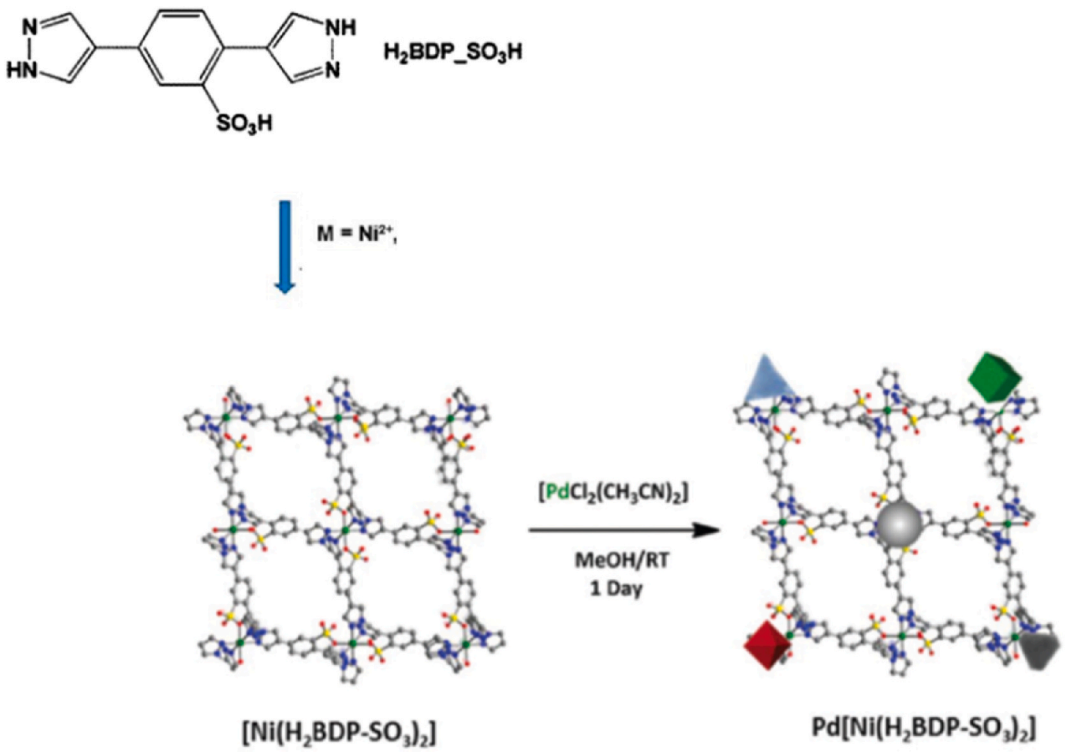

Scheme 18. Schematic representation of Pd@[Ni(H_2BDP-SO_3)$_2$] synthesis [161]. Copyright 2016, with permission from Royal Society of Chemistry.

3.9. Other metals

There are few reports on MOF-catalyzed SMC involving other metal nodes. For instance, Julian et al. reported using titanium-based MIL-125 as a sacrificial template to produce TiO_2 as cocatalyst and support for Pd(0) by photoreduction of Pd(II) [177]. The carbonized MIL-125 produces carbonaceous TiO_2 support that synergistically enhances the catalytic activity by both electron and O-transfer at the metal-oxide interface (Scheme 22a). Chen et al. reported the development of indium-based water-stable MOF solvothermally and incorporated Pd into the tetragonal pores of the framework via capillary action induced by the double-solvent approach [178]. The selectivity of coupling product was maintained by the size-selective property endowed by the confined space of the active sites (Scheme 22b). PSM strategy was reported on aluminium-based MOF LSK-15 (MIL-101 topology) containing phosphine anchoring site for Pd. The obtained catalyst outperformed the existing inorganic phosphine-based Pd complexes [179].

4. Conclusion

This review focused on the catalytic uses of Metal-Organic Frameworks (MOFs) in Suzuki-Miyaura coupling (SMC) reactions, with emphasis on advancements that have occurred since 2016. Two fundamental strategies are used for the optimization of MOF catalysts for the Pd-mediated Suzuki-Miyaura coupling reaction: enhancement of Lewis acidity and the modulation of active sites. The focus of the majority of studies significantly lies on the stability (thermal and mechanical) and surface activity of the support framework. Aspects related to the retainment of framework stability during Pd incorporation are explained in most examples. The stability, coordination environment, and surface area of MOFs are crucial for maintaining Pd stability and enhancing catalytic performance. Stable frameworks prevent Pd leaching, while tailored coordination environments, like amino or bipyridyl ligands, stabilize Pd atoms. High surface area offers more incorporation sites and improved reactant access, boosting overall catalytic efficiency. MOF catalysts were classified based on metals such as Zr, Zn, Cr, Cu, Ni. Moreover, the attempts made to synthesize different Ln-based MOFs are also discussed due to their enhanced flexibility and Lewis acidity. Most of the Suzuki-Miyaura reaction catalysts are of novel metal-organic frameworks. The SMC catalytic conditions and scopes along with the MOF characterization and synthesis are summarized in relevant tables in each metal section. MOF-based coupling catalysts targets development of a solid-state medium for anchoring of homogenous catalytic active species which mostly contains palladium. Incorporation of Pd into MOFs for SMC follows two major general approaches: postsynthetic modification or impregnation/encapsulation. The review summarized the introduction of catalysts into MOFs with minimal susceptibility to leaching, highlighting their important roles in SMC and synthetic applications.

The catalytic application of monometallic Pd-MOFs in SMC was highlighted in the earliest studies on MOF-catalyzed SMC. However, limited investigations exist on the direct synthesis of Pd-MOFs, with even fewer exploring the complete exchange

Table 5
Reports of SMC using Ni-based MOFs after 2016.

Entry	Catalyst	Synthesis	BET surface area, Pore volume, Mean particle or pore[a] size	Coupling reagents	Catalytic conditions	SMC scope (yield or conversion)	SMC of aryl chlorides	TOF (h^{-1}) TON[b]	Recycling catalytic runs	Ref.
1	Pd@[Ni(H_2BDP-SO_3)$_2$] Pd(II) and Pd(0) H_2BDP = 1,4-bis(1H-pyrazol-4-yl)benzene	One-step impregnation/reduction	583 m^2/g 0.58 cm^3/g 4–8 nm	Aryl bromide Phenyl boronic acid	Cat. (0.5 mol%) K_2CO_3 iPrOH/H_2O (1:1) rt or 60 °C 4–8 h	6 examples EWG & EDG at various positions (58–97 %)	24 %	–	7	[161]
2	Ni_2(NDISA)-PDA-Pd Pd(II) and Pd(0) NDISA = naphthalene diimide salicylic acid PDA = polydopamine	PSM	1681 m^2/g 2 nm	Aryl halide (Br, I) Phenyl boronic acid	Cat. (0.1 mol % Pd) K_2CO_3 DMF-H_2O (1:1) 50 °C 4–8 h	6 examples EWG & EDG at various positions (48–99 %)	–	5760 h^{-1}	–	[163]
3	Pd1/Ni_4-MOF@PAN(C) PAN = polyacronitrile	Electrospinning and carbonization followed by solvothermal method	–	Aryl halide (Br, I) Phenyl boronic acid	Cat. (5 mg per 0.5 mmol ArX) K_2CO_3 EtOH-H_2O (4:3) 80 °C 0.5–1.5 h	11 examples EWG & EDG at various positions (88–100 %)	–	–	6	[164]
4	Fe_3O_4@GlcA@Ni-MOF Ni(0) GlcA = gluconic acid	encapsulation of Fe_3O_4@GlcA NP	97 m^2/g 22.25 cm^3/g	Aryl halide (Cl, Br, I) Phenyl boronic acid	Cat. (60 mg/1 mmol ArX) KO*t*Bu H_2O 90 °C 2–15 h	11 examples EDG & EWG at various positions (53–88 %)	55 %	–	7	[165]

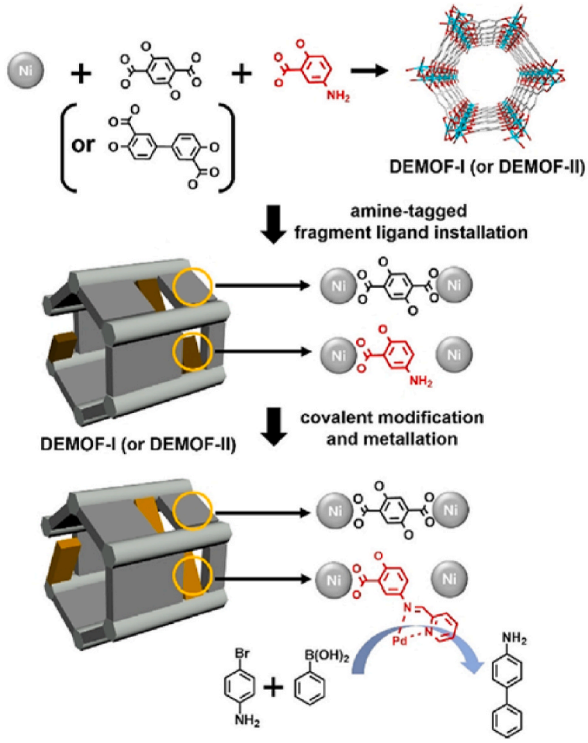

Scheme 19. Reaction scheme of fragmented MOF for efficient PSM of Pd in Ni-MOF-74 [166]. Copyright 2021, with permission from Wiley.

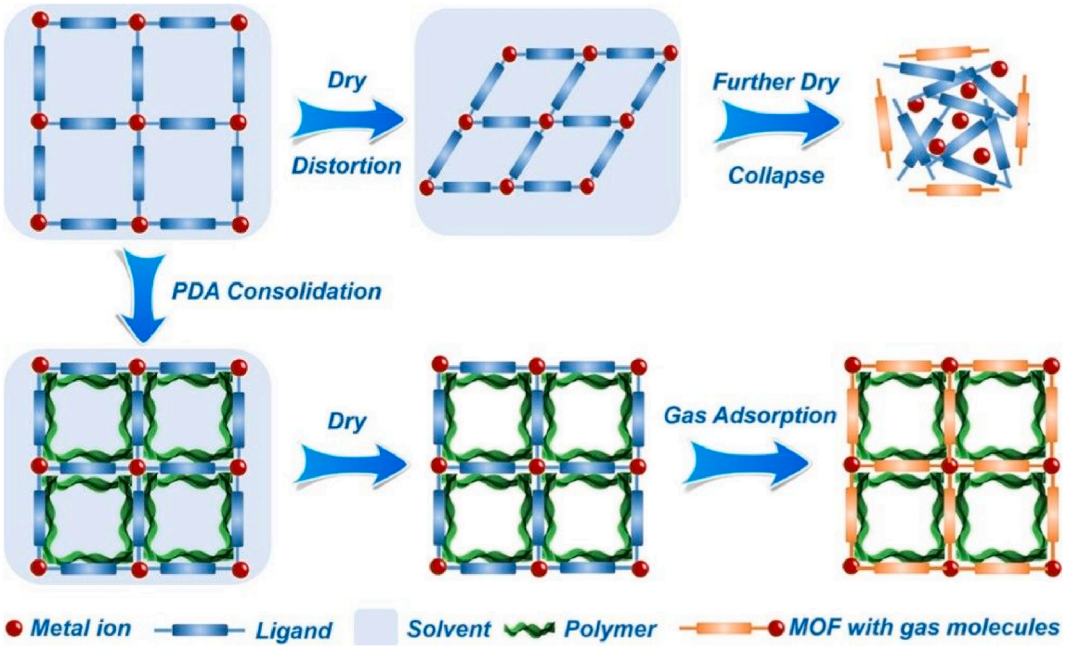

Scheme 20. Polymer introduced into the pore channel supports the porous structure, prevents the mesopores from collapsing, and enhances accessibility of molecules into pores [163]. Copyright 2019, with permission from American Chemical Society.

(substitution/metathesis) of metal nodes in MOFs with Pd(II) ions while preserving structural integrity. Zr-MOFs, such as MOF-808 and UiO-type families, have shown efficient catalytic activity in SMC as supports for active palladium species, with modifications like using acids in synthesis to enhance Lewis acidity and catalytic activity. Pd incorporation into Zr-based MOFs is typically achieved

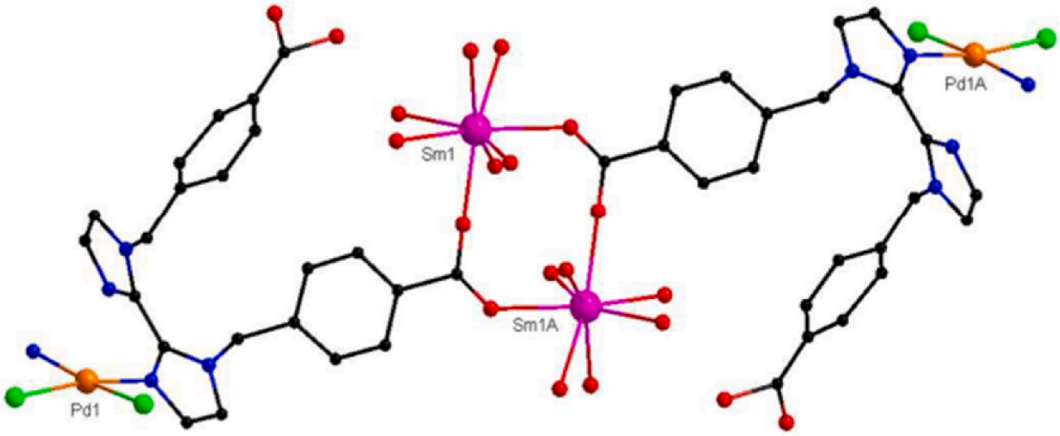

Fig. 10. Illustration of coordination environments of Sm(III) and Pd(II) ions in the Ln-MOF catalyst [171]. Copyright 2018, with permission from Royal Society of Chemistry.

through immobilization or postsynthetic metalation. Similarly, palladized Cr-based MOFs, such as MIL-101(Cr), have shown promise in C-C coupling reactions. Zn-based MOFs, including Zn-containing IRMOF-3, have demonstrated catalytic activity in SMC, with modifications like Pd(II) encapsulation and reduction improving stability and efficiency. Additionally, composite materials, such as mesoporous silica and Pd-decorated ZnMOF, have shown promising results in SMC. Copper-based MOFs display high catalytic activity, while Ni-based MOFs have shown selectivity in carbonylative SMC. Lanthanide-based MOFs exhibit enhanced Lewis acidity, with lanthanide-metal interactions improving catalytic performance. Despite the efficiency of Cr and Ln MOFs in Pd incorporation and SMC, their toxicity remains a major drawback, particularly in synthesizing biological compounds.

In summary, MOF-based catalysts show promise for offering efficient and selective C-C bond formation. Advances in enhancing catalytic performance through strategies like increasing Lewis acidity and modulating active sites have improved stability and activity. Incorporating metals like Zr, Zn, Cr, Cu, Ni, and lanthanides tailors catalyst properties, enhancing efficiency. Synthesis innovations, including functionalization and post-synthetic metalation, enable precise control over catalyst composition, leading to improved stability and activity in reactions. MOF-based catalysts demonstrate excellent activity and selectivity in SMC reactions, tolerating diverse substrates and functional groups. Composite materials combining MOFs with other supports or reinforcement materials such as polymers and surfactants show enhanced performance, expanding catalyst applicability.

Although catalytic applications of MOFs are advancing at an unprecedented pace providing more sustainable synthetic toolbox, continued research is need to streamline large-scale organic transformations such as SMC to reach industrial and pharmaceutical sector that usually operate under flow and automated conditions.

- Developing simpler and more straightforward synthetic approaches, such as one-pot syntheses, for active MOF catalysts is crucial. For instance, more research is needed to develop monometallic Pd-MOFs with intrinsic catalytic activities and improved chemical and thermal stability. This class of noble metal MOFs will greatly benefit Pd-catalyzed reactions and reduce the need for costly and complex postsynthetic palladium functionalization.
- More studies are needed to control the structural and thermal integrity of MOF catalysts under experimental conditions, often challenged by high temperatures and reagents like reducing agents, water, and bases, and to understand structure-catalytic properties relationships. It is also beneficial to synthesize and implement MOFs in automated and continuous flow systems for scaling up both MOFs synthesis and their catalytic applications.
- SMC and coupling reactions should further exploit the size-selective properties of MOFs, highlighted in few studies only, such phenyl versus naphthyl coupling, which is beneficial for multistep synthesis of complex pharmaceuticals and commercial chemicals.
- Developing more stable systems for bifunctional MOF catalysis for useful one-pot SMC/organic transformation and for photo-catalytic coupling reactions is essential.
- More precise studies on leaching of metal ions from MOF catalysts, particularly with toxic metals like Cr, are necessary to ensure their adoption in synthesis of biomedical chemicals. This will also prolong the catalyst's service life and facilitate recycling in continuous processes. Strategies to address leaching include optimizing the binding mode of metals in MOFs with suitable functional groups or ligands, surface modification, and even by developing more appropriate synthesis and catalytic conditions.
- Exploring MOF-catalyzed SMC using other efficient metal nodes, such as Ni and Fe, could expand the scope of SMC beyond Pd.
- Reducing noble metal nanoparticles from nanoscale to subnanometer clusters or atoms and exploring the influence of pore confinement can significantly improve their catalytic activity, selectivity, and recycling efficiency.
- The implementation of MOFs in automated and continuous flow synthesis systems is expected to streamline the SMC process, making it more efficient and scalable for industrial applications.

Table 6
Reports of SMC using Ln-based MOFs after 2016.

Entry	Catalyst	Synthesis	BET surface area, Pore volume, Mean particle or pore[a] size	Coupling reagents	Catalytic conditions	SMC scope (yield or conversion)	SMC of aryl chlorides	TOF (h^{-1}) TON[b]	Recycling catalytic runs	Ref.
1	Pd(II)/Sm(III) MOFs $\{[H_3O]\cdot[SmPd_2L_2Cl_4]\cdot 4H_2O\}_n$ Pd(II) L = 1,1′-di(p-carboxybenzyl)2,2′-diimidazole	Hydrothermal method	–	Aryl bromide Aryl boronic acid	Cat. (0.2 mol%) K_2CO_3 EtOH and/or H_2O 50–80 °C 4–6 h	12 examples EWG & EDG (78–99 %)	–	–	4	[171]
2	Pd-HoMOF Pd(II)	PSM	–	Aryl halide (Cl, Br, I) Phenyl boronic acid	Cat. (0.4 mol%) KOH DMF 100 °C 1–6 h	10 examples EWG & EDG (92–99 %)	3 examples (92–99 %)	–	5	[172]
3	Fe_3O_4@La-MOF-Schiff base-Pd Pd(II) La-MOF = $[La(abdc)(Habdc).9H_2O]_n$ (abdc = 2-amino-benzene-1,4-di carboxylate	PSM	532.7 m^2/g 10 nm	Aryl halide (Cl, Br, I) Aryl boronic acid	Cat. (0.066 mmol% Pd) K_2CO_3 Ethanol 80 °C 0.5–12 h	8 examples EWG & EDG (52–99 %)	3 examples (5–19 %)	42,886 h^{-1} (21,443)[b]	12	[173]
4	Pd_n@CeMOF-808 Pd(0)	Self-assembly followed by impregnation	1180 m^2/g 0.55–1 nm 0.55 cm^3/g	Aryl halide (Cl, Br, I) Aryl boronic acid	Cat. (0.3 mol% Pd) K_2CO_3 Ethanol/water (1:1) 80 °C MW 5 min	7 examples EWG & EDG (90–100 %)	2 examples (75–80 %)	4016-132,530 h^{-1} (326)[b]	5	[73]
5	Pd/Ce-MOF-801 Pd(II) and Pd(0)	Self-assembly followed by impregnation	397.1 m^2/g 0.25 cm^3/g 9 nm	Aryl halide (Br, I) Phenyl boronic acid	Cat. (0.1 mol% Pd) K_2CO_3 Ethanol/H_2O (1:1) 318–353 K 0.5–2 h	11 examples EDG & EWG at various positions (90–99 %)	–	–	8	[174]
6	Pd/Ni NPs@Eu-MOF Pd(0)	Impregnation followed by chemical reduction of Pd(II)	591.9 m^2/g 2–5 nm	Aryl halide (Cl, Br, I) Aryl boronic acid	Cat. (10 mg/1 mmol ArX) K_2CO_3 Ethanol 100–110 °C 9–12 h	6 examples EWG and EDG (85–99 %)	2 examples (15–32 %)	–	5	[175]

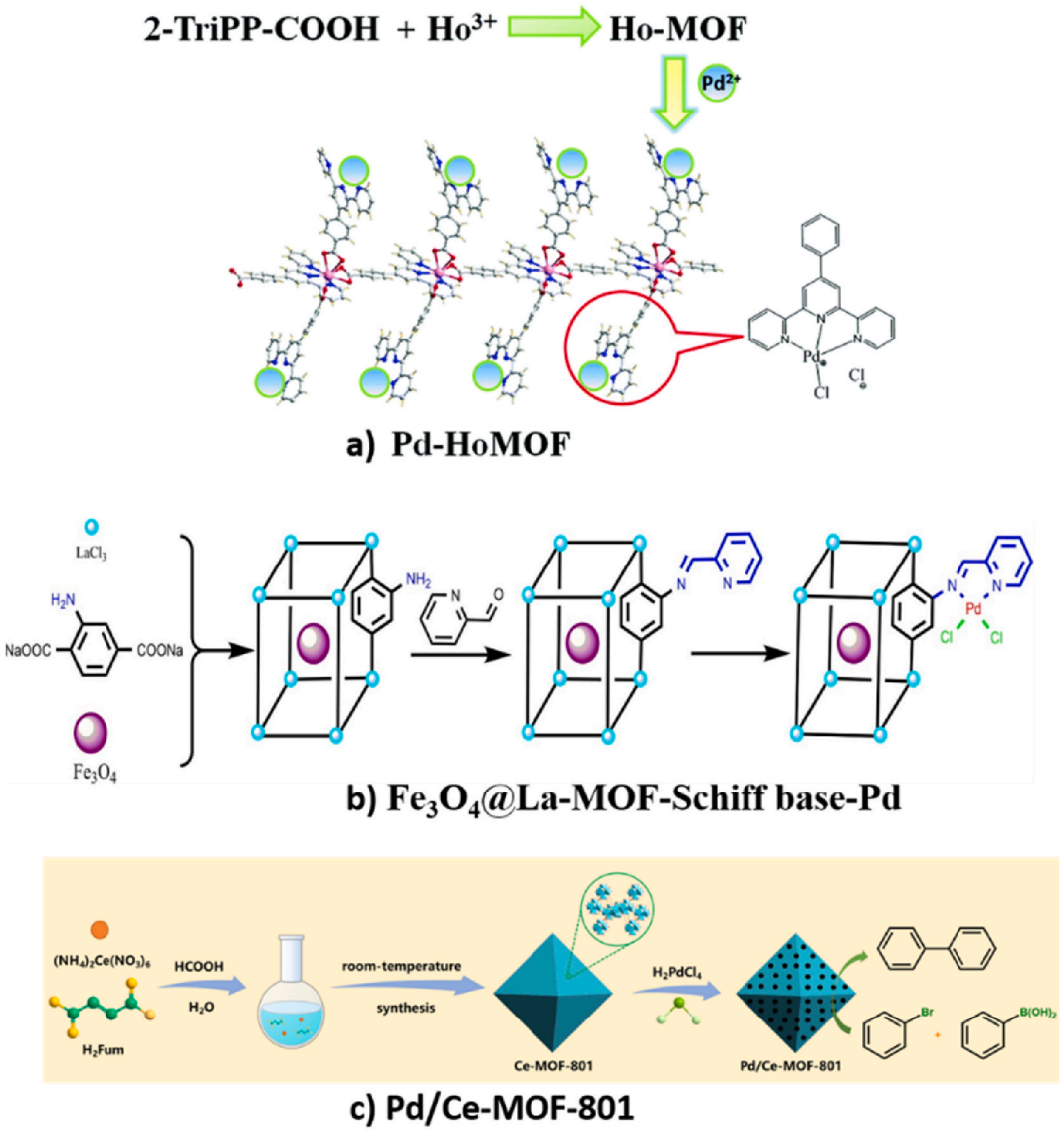

Scheme 21. Synthetic pathways to MOF catalysts in entries 2,3, and 5 [172–174].

CRediT authorship contribution statement

Ravulakollu Srinivasa Rao: Writing – original draft, Investigation. **Mahira Bashri:** , Writing – original draft, Investigation. **Mohamed Infas Haja Mohideen:** Writing – review & editing, Supervision. **Ibrahim Yildiz:** Writing – review & editing, Supervision. **Dinesh Shetty:** Writing – review & editing, Writing – original draft, Investigation. **Janah Shaya:** Writing – review & editing, Writing – original draft, Investigation, Conceptualization.

Disclosure statement

The authors have no competing interests to declare.

Data availability statement

This article is a review and does not contain original datasets generated by the authors. All data analyzed or discussed in this review are derived from publicly available studies, which are cited in the reference section.

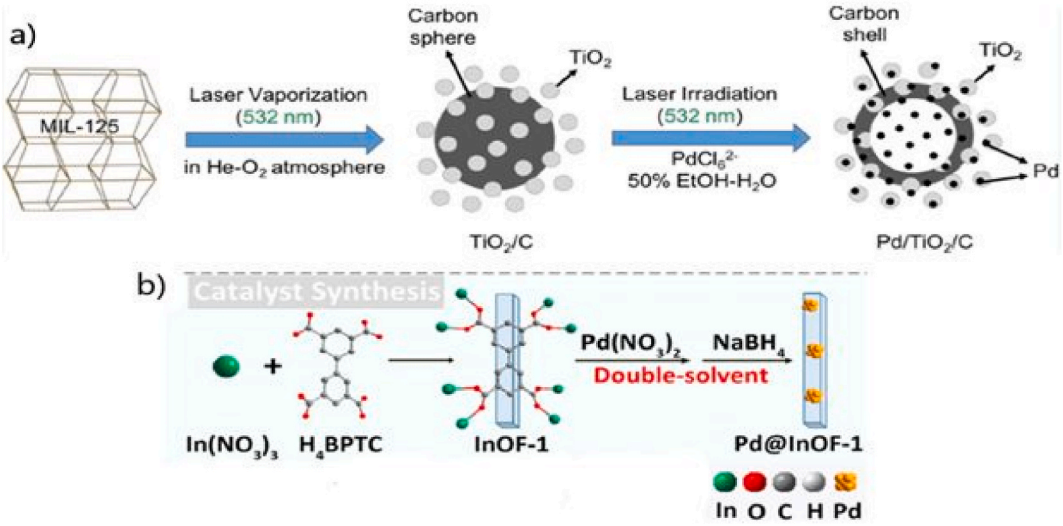

Scheme 22. a) Development of TiO_2 support from Ti-MOF for Pd adsorption [177]. b) Incorporation of Pd in tetragonal pores of Indium-organic framework [178]. Copyright 2018 and 2022, with permission from American Chemical Society.

Declaration of competing interest

The authors declare the following financial interests/personal relationships which may be considered as potential competing interests: Conflict statement.

Acknowledgment

This work was supported by the Khalifa University under Grant [FSU-2023-021], 8474000527.

References

[1] H. Li, C.C.C.J. Seechurn, T.J. Colacot, Development of preformed Pd catalysts for cross-coupling reactions, beyond the 2010 nobel prize, ACS Catal. 2 (2012) 1147–1164, https://doi.org/10.1021/cs300082f.
[2] A. Suzuki, Cross-coupling reactions of organoboranes: an easy way to construct C?C bonds (nobel lecture), Angew. Chem. Int. Ed. 50 (2011) 6722–6737.
[3] N. Miyaura, A. Suzuki, Palladium-catalyzed cross-coupling reactions of organoboron compounds, Chem. Rev. 95 (1995) 2457–2483, https://doi.org/10.1021/cr00039a007.
[4] K. Hong, M. Sajjadi, J.M. Suh, K. Zhang, M. Nasrollahzadeh, H.W. Jang, R.S. Varma, M. Shokouhimehr, Palladium nanoparticles on assorted nanostructured supports: applications for Suzuki, Heck, and Sonogashira cross-coupling reactions, ACS Appl. Nano Mater. 3 (2020) 2070–2103, https://doi.org/10.1021/acsanm.9b02017.
[5] A. Zapf, A. Ehrentraut, M. Beller, A new highly efficient catalyst system for the coupling of nonactivated and deactivated aryl chlorides with arylboronic acids, Angew. Chem. Int. Ed. 39 (2000) 4153–4155, https://doi.org/10.1002/1521-3773(20001117)39:22<;4153::aid-anie4153>3.0.co;2-t.
[6] I.P. Beletskaya, F. Alonso, V. Tyurin, The Suzuki-Miyaura reaction after the Nobel prize, Coordin Chem Rev 385 (2019) 137–173, https://doi.org/10.1016/j.ccr.2019.01.012.
[7] J. Shaya, F. Fontaine-Vive, B.Y. Michel, A. Burger, Rational design of push–pull fluorene dyes: synthesis and structure–photophysics relationship, Chem European J 22 (2016) 10627–10637, https://doi.org/10.1002/chem.201600581.
[8] S.E. Hooshmand, B. Heidari, R. Sedghi, R.S. Varma, Recent advances in the Suzuki–Miyaura cross-coupling reaction using efficient catalysts in eco-friendly media, Green Chem. 21 (2018) 381–405, https://doi.org/10.1039/c8gc02860e.
[9] J. El-Maiss, T.M.E. Dine, C.-S. Lu, I. Karamé, A. Kanj, K. Polychronopoulou, J. Shaya, Recent advances in metal-catalyzed alkyl–boron (C(sp3)–C(sp2)) suzuki-miyaura cross-couplings, Catalysts 10 (2020) 296, https://doi.org/10.3390/catal10030296.
[10] M. Farhang, A.R. Akbarzadeh, M. Rabbani, A.M. Ghadiri, A retrospective-prospective review of Suzuki–Miyaura reaction: from cross-coupling reaction to pharmaceutical industry applications, Polyhedron 227 (2022) 116124, https://doi.org/10.1016/j.poly.2022.116124.
[11] A. Ahmed, I. Mushtaq, S. Chinnam, Suzuki–Miyaura cross-couplings for alkyl boron reagent: recent developments—a review, Futur. J. Pharm. Sci. 9 (2023) 67, https://doi.org/10.1186/s43094-023-00520-1.
[12] W. Cabri, I. Candiani, Recent developments and new perspectives in the Heck reaction, Acc. Chem. Res. 28 (1995) 2–7, https://doi.org/10.1021/ar00049a001.
[13] R. Chinchilla, C. Nájera, Recent advances in Sonogashira reactions, Chem. Soc. Rev. 40 (2011) 5084, 39.
[14] R. Chinchilla, C. Nájera, The Sonogashira Reaction:~ A booming methodology in synthetic organic chemistry ag, Chem. Rev. 107 (2007) 874–922.
[15] W. Pickhardt, E. Siegfried, S. Fabig, M.F. Rappen, M. Etter, M. Wohlgemuth, S. Grätz, L. Borchardt, The Sonogashira coupling on palladium milling balls—a new reaction pathway in mechanochemistry, Angew. Chem. Int. Ed. 62 (2023) e202301490, https://doi.org/10.1002/anie.202301490.
[16] D. Roy, Y. Uozumi, Recent advances in palladium-catalyzed cross-coupling reactions at ppm to ppb molar catalyst loadings, Adv. Synth. Catal. 360 (2018) 602–625, https://doi.org/10.1002/adsc.201700810.
[17] J. Shaya, M.-A. Deschamps, B.Y. Michel, A. Burger, Air-stable Pd catalytic systems for sequential one-pot synthesis of challenging unsymmetrical aminoaromatics, J. Org. Chem. 81 (2016) 7566–7573, https://doi.org/10.1021/acs.joc.6b01248.
[18] P.M. Holstein, D. Dailler, J. Vantourout, J. Shaya, A. Millet, O. Baudoin, Synthesis of strained γ-lactams by palladium(0)-catalyzed C(sp3)−H alkenylation and application to alkaloid synthesis, Angewandte Chemie Int Ed 55 (2016) 2805–2809, https://doi.org/10.1002/anie.201511457.
[19] F.-S. Han, Transition-metal-catalyzed Suzuki–Miyaura cross-coupling reactions: a remarkable advance from palladium to nickel catalysts, Chem. Soc. Rev. 42 (2013) 5270–5298, https://doi.org/10.1039/c3cs35521g.

[20] T. Hatakeyama, T. Hashimoto, K.K.A.D.S. Kathriarachchi, T. Zenmyo, H. Seike, M. Nakamura, Iron-catalyzed alkyl–alkyl suzuki–miyaura coupling, Angew. Chem. Int. Ed. 51 (2012) 8834–8837, https://doi.org/10.1002/anie.201202797.

[21] A.J.J. Lennox, G.C. Lloyd-Jones, Transmetalation in the suzuki–miyaura coupling: the fork in the trail, Angew. Chem. Int. Ed. 52 (2013) 7362–7370, https://doi.org/10.1002/anie.201301737.

[22] A. Bourouina, V. Meille, C. de Bellefon, About solid phase vs. Liquid phase in suzuki-miyaura reaction, Catalysts 9 (2019) 60, https://doi.org/10.3390/catal9010060.

[23] M. Díaz-Sánchez, D. Díaz-García, S. Prashar, S. Gómez-Ruiz, Palladium nanoparticles supported on silica, alumina or titania: greener alternatives for Suzuki–Miyaura and other C–C coupling reactions, Environ. Chem. Lett. 17 (2019) 1585–1602, https://doi.org/10.1007/s10311-019-00899-5.

[24] C. Wu, M. Zhao, Incorporation of molecular catalysts in metal–organic frameworks for highly efficient heterogeneous catalysis, Adv. Mater. 29 (2017) 1605446, https://doi.org/10.1002/adma.201605446.

[25] A.E.C. Collis, I.T. Horváth, Heterogenization of homogeneous catalytic systems, Catal. Sci. Technol. 1 (2011) 912–919, https://doi.org/10.1039/c1cy00174d.

[26] R.A. Sheldon, Homogeneous catalysts to solid catalysts, Curr. Opin. Solid State Mater. Sci. 1 (1996) 101–106, https://doi.org/10.1016/s1359-0286(96)80017-9.

[27] Z. Chen, E. Vorobyeva, S. Mitchell, E. Fako, M.A. Ortuño, N. López, S.M. Collins, P.A. Midgley, S. Richard, G. Vilé, J. Pérez-Ramírez, A heterogeneous single-atom palladium catalyst surpassing homogeneous systems for Suzuki coupling, Nat. Nanotechnol. 13 (2018) 702–707, https://doi.org/10.1038/s41565-018-0167-2.

[28] M. Pagliaro, V. Pandarus, R. Ciriminna, F. Béland, P.D. Carà, Heterogeneous versus homogeneous palladium catalysts for cross-coupling reactions, ChemCatChem 4 (2012) 432–445, https://doi.org/10.1002/cctc.201100422.

[29] S.D.T. de Barros, J.D. Senra, E.R. Lachter, L.F.B. Malta, Metal-catalyzed cross-coupling reactions with supported nanoparticles: recent developments and future directions, Cataly Rev 58 (2016) 439–496, https://doi.org/10.1080/01614940.2016.1202640.

[30] A.D. Zotto, D. Zuccaccia, Metallic palladium, PdO, and palladium supported on metal oxides for the Suzuki–Miyaura cross-coupling reaction: a unified view of the process of formation of the catalytically active species in solution, Catal. Sci. Technol. 7 (2017) 3934–3951, https://doi.org/10.1039/c7cy01201b.

[31] J. Liang, Z. Liang, R. Zou, Y. Zhao, Heterogeneous catalysis in zeolites, mesoporous silica, and metal–organic frameworks, Adv. Mater. 29 (2017) 1701139, https://doi.org/10.1002/adma.201701139.

[32] V. Pascanu, G.G. Miera, A.K. Inge, B. Martín-Matute, Metal–organic frameworks as catalysts for organic synthesis: a critical perspective, J. Am. Chem. Soc. 141 (2019) 7223–7234, https://doi.org/10.1021/jacs.9b00733.

[33] A. Bavykina, N. Kolobov, I.S. Khan, J.A. Bau, A. Ramirez, J. Gascon, Metal–organic frameworks in heterogeneous catalysis: recent progress, new trends, and future perspectives, Chem Rev 120 (2020) 8468–8535, https://doi.org/10.1021/acs.chemrev.9b00685.

[34] Y. Wu, X. Feng, Q. Zhai, H. Wang, H. Jiang, Y. Ren, Metal–organic framework surface functionalization enhancing the activity and stability of palladium nanoparticles for carbon–halogen bond activation, Inorg. Chem. 61 (2022) 6995–7004, https://doi.org/10.1021/acs.inorgchem.2c00379.

[35] N.L. Rosi, M. Eddaoudi, J. Kim, M. O'Keeffe, O.M. Yaghi, Advances in the chemistry of metal–organic frameworks, CrystEngComm 4 (2002) 401–404, https://doi.org/10.1039/b203193k.

[36] R. Freund, O. Zaremba, G. Arnauts, R. Ameloot, G. Skorupskii, M. Dincă, A. Bavykina, J. Gascon, A. Ejsmont, J. Goscianska, M. Kalmutzki, U. Lächelt, E. Ploetz, C.S. Diercks, S. Wuttke, The current status of MOF and COF applications, Angew. Chem. Int. Ed. 60 (2021) 23975–24001, https://doi.org/10.1002/anie.202106259.

[37] S. Kumar, S. Jain, M. Nehra, N. Dilbaghi, G. Marrazza, K.-H. Kim, Green synthesis of metal–organic frameworks: a state-of-the-art review of potential environmental and medical applications, Coordin Chem Rev 420 (2020) 213407, https://doi.org/10.1016/j.ccr.2020.213407.

[38] M.I.H. Mohideen, R.S. Pillai, K. Adil, P.M. Bhatt, Y. Belmabkhout, A. Shkurenko, G. Maurin, M. Eddaoudi, A fine-tuned MOF for gas and vapor separation: a multipurpose adsorbent for acid gas removal, dehydration, and btx sieving, Chem 3 (2017) 822–833, https://doi.org/10.1016/j.chempr.2017.09.002.

[39] P.K. Allan, P.S. Wheatley, D. Aldous, M.I. Mohideen, C. Tang, J.A. Hriljac, I.L. Megson, K.W. Chapman, G.D. Weireld, S. Vaesen, R.E. Morris, Metal–organic frameworks for the storage and delivery of biologically active hydrogen sulfide, Dalton Trans. 41 (2012) 4060–4066, https://doi.org/10.1039/c2dt12069k.

[40] A.S. Lawrence, N. Martin, B. Sivakumar, F.G. Cirujano, A. Dhakshinamoorthy, Palladium-based metal organic frameworks as heterogeneous catalysts for C−C couplings, ChemCatChem 14 (2022), https://doi.org/10.1002/cctc.202200403.

[41] C.P. Raptopoulou, Metal-organic frameworks: synthetic methods and potential applications, Materials 14 (2021) 310, https://doi.org/10.3390/ma14020310.

[42] D. Yang, B.C. Gates, Catalysis by metal organic frameworks: perspective and suggestions for future research, ACS Catal. 9 (2019) 1779–1798, https://doi.org/10.1021/acscatal.8b04515.

[43] A. Dhakshinamoorthy, A.M. Asiri, H. Garcia, Formation of C–C and C–heteroatom bonds by C–H activation by metal organic frameworks as catalysts or supports, ACS Catal. 9 (2019) 1081–1102, https://doi.org/10.1021/acscatal.8b04506.

[44] A. Dhakshinamoorthy, A.M. Asiri, H. Garcia, Metal–organic frameworks catalyzed C–C and C–heteroatom coupling reactions, Chem. Soc. Rev. 44 (2015) 1922–1947, https://doi.org/10.1039/c4cs00254g.

[45] A.H. Chughtai, N. Ahmad, H.A. Younus, A. Laypkov, F. Verpoort, Metal–organic frameworks: versatile heterogeneous catalysts for efficient catalytic organic transformations, Chem. Soc. Rev. 44 (2015) 6804–6849, https://doi.org/10.1039/c4cs00395k.

[46] A. Dhakshinamoorthy, H. Garcia, Metal–organic frameworks as solid catalysts for the synthesis of nitrogen-containing heterocycles, Chem. Soc. Rev. 43 (2014) 5750–5765, https://doi.org/10.1039/c3cs60442j.

[47] K. Shen, X. Chen, J. Chen, Y. Li, Development of MOF-derived carbon-based nanomaterials for efficient catalysis, ACS Catal. 6 (2016) 5887–5903, https://doi.org/10.1021/acscatal.6b01222.

[48] P. Hajivand, J.C. Jansen, E. Pardo, D. Armentano, T.F. Mastropietro, A. Azadmehr, Application of metal-organic frameworks for sensing of VOCs and other volatile biomarkers, Coord. Chem. Rev. 501 (2024) 215558, https://doi.org/10.1016/j.ccr.2023.215558.

[49] Z. Cao, R. Momen, S. Tao, D. Xiong, Z. Song, X. Xiao, W. Deng, H. Hou, S. Yasar, S. Altin, F. Bulut, G. Zou, X. Ji, Metal–organic framework materials for electrochemical supercapacitors, Nano-Micro Lett. 14 (2022) 181, https://doi.org/10.1007/s40820-022-00910-9.

[50] D. Feng, L. Zhou, T.J. White, A.K. Cheetham, T. Ma, F. Wei, Nanoengineering metal–organic frameworks and derivatives for electrosynthesis of ammonia, Nano-Micro Lett. 15 (2023) 203, https://doi.org/10.1007/s40820-023-01169-4.

[51] S.R. Batten, N.R. Champness, X.-M. Chen, J. Garcia-Martinez, S. Kitagawa, L. Öhrström, M. O'Keeffe, M.P. Suh, J. Reedijk, Terminology of metal–organic frameworks and coordination polymers (IUPAC Recommendations 2013), Pure Appl. Chem. 85 (2013) 1715–1724, https://doi.org/10.1351/pac-rec-12-11-20.

[52] A. Chandra, A. Datta, A peptide-based fluorescent sensor for anionic phospholipids, ACS Omega 7 (2022) 10347–10354, https://doi.org/10.1021/acsomega.1c06981.

[53] H.-S. Wang, Y.-H. Wang, Y. Ding, Development of biological metal–organic frameworks designed for biomedical applications: from bio-sensing/bio-imaging to disease treatment, Nanoscale Adv. 2 (2020) 3788–3797, https://doi.org/10.1039/d0na00557f.

[54] W. Ding, L. Zhao, X. Yuan, L. Zhang, B. Chen, Q. Ju, Z. Fang, Multicolour barcoding in one MOF crystal through rational postsynthetic transmetalation, J. Mater. Chem. C 8 (2020) 3176–3182, https://doi.org/10.1039/c9tc05678e.

[55] M. Li, D. Li, M. O'Keeffe, O.M. Yaghi, Topological analysis of metal–organic frameworks with polytopic linkers and/or multiple building units and the minimal transitivity principle, Chem. Rev. 114 (2014) 1343–1370, https://doi.org/10.1021/cr400392k.

[56] V.F. Yusuf, N.I. Malek, S.K. Kailasa, Review on metal–organic framework classification, synthetic approaches, and influencing factors: applications in energy, drug delivery, and wastewater treatment, ACS Omega 7 (2022) 44507–44531, https://doi.org/10.1021/acsomega.2c05310.

[57] L. Feng, K.-Y. Wang, J. Powell, H.-C. Zhou, Controllable synthesis of metal-organic frameworks and their hierarchical assemblies, Matter 1 (2019) 801–824, https://doi.org/10.1016/j.matt.2019.08.022.

[58] S.C. McKellar, A.J. Graham, D.R. Allan, M.I.H. Mohideen, R.E. Morris, S.A. Moggach, The effect of pressure on the post-synthetic modification of a nanoporous metal–organic framework, Nanoscale 6 (2014) 4163–4173, https://doi.org/10.1039/c3nr04161a.

[59] L. Jiao, Y. Wang, H. Jiang, Q. Xu, Metal–organic frameworks as platforms for catalytic applications, Adv. Mater. 30 (2018) 1703663, https://doi.org/10.1002/adma.201703663.

[60] K. Titov, D.B. Eremin, A.S. Kashin, R. Boada, B.E. Souza, C.S. Kelley, M.D. Frogley, G. Cinque, D. Gianolio, G. Cibin, S. Rudić, V.P. Ananikov, J.-C. Tan, OX-1 metal–organic framework nanosheets as robust hosts for highly active catalytic palladium species, Acs Sustain Chem Eng 7 (2019) 5875–5885, https://doi.org/10.1021/acssuschemeng.8b05843.

[61] S. Kousik, S. Velmathi, Engineering metal–organic framework catalysts for C−C and C−X coupling reactions: advances in reticular approaches from 2014–2018, Chem European J 25 (2019) 16451–16505, https://doi.org/10.1002/chem.201901987.

[62] E. Miguel-Casañ, M.D. Darawsheh, V. Fariña-Torres, I.J. Vitórica-Yrezábal, E. Andres-Garcia, M. Fañanás-Mastral, G.M. Espallargas, Heterometallic palladium–iron metal–organic framework as a highly active catalyst for cross-coupling reactions, Chem. Sci. 14 (2022) 179–185, https://doi.org/10.1039/d2sc05192c.

[63] H. Deng, C.J. Doonan, H. Furukawa, R.B. Ferreira, J. Towne, C.B. Knobler, B. Wang, O.M. Yaghi, Multiple functional groups of varying ratios in metal-organic frameworks, Science 327 (2010) 846–850, https://doi.org/10.1126/science.1181761.

[64] S.M. Cohen, The postsynthetic renaissance in porous solids, J. Am. Chem. Soc. 139 (2017) 2855–2863, https://doi.org/10.1021/jacs.6b11259.

[65] W. Dong, C. Feng, L. Zhang, N. Shang, S. Gao, C. Wang, Z. Wang, Pd@UiO-66: an efficient catalyst for suzuki–miyaura coupling reaction at mild condition, Catal. Lett. 146 (2016) 117–125, https://doi.org/10.1007/s10562-015-1659-4.

[66] W. Dong, L. Zhang, C. Wang, C. Feng, N. Shang, S. Gao, C. Wang, Palladium nanoparticles embedded in metal–organic framework derived porous carbon: synthesis and application for efficient Suzuki–Miyaura coupling reactions, Rsc Adv 6 (2016) 37118–37123, https://doi.org/10.1039/c6ra00378h.

[67] H.A.A. Almheiri, N. Singh, D. Shetty, K. Polychronopoulou, A.A. Alhammadi, A Mo–salicylaldehyde-linker (Mo–Tp) based 2D MOF as a single-atom catalyst for the nitrogen reduction reaction, J. Mater. Chem. A 12 (2024) 7058–7066, https://doi.org/10.1039/d3ta06666e.

[68] S.M.J. Rogge, A. Bavykina, J. Hajek, H. Garcia, A.I. Olivos-Suarez, A. Sepúlveda-Escribano, A. Vimont, G. Clet, P. Bazin, F. Kapteijn, M. Daturi, E.V. Ramos-Fernandez, F.X.L. i Xamena, V.V. Speybroeck, J. Gascon, Metal–organic and covalent organic frameworks as single-site catalysts, Chem. Soc. Rev. 46 (2017) 3134–3184, https://doi.org/10.1039/c7cs00033b.

[69] Y. Luan, N. Zheng, Y. Qi, J. Tang, G. Wang, Merging metal–organic framework catalysis with organocatalysis: a thiourea functionalized heterogeneous catalyst at the nanoscale, Catal. Sci. Technol. 4 (2014) 925–929, https://doi.org/10.1039/c3cy00864a.

[70] A.K. Mohammed, S. Gaber, J. Raya, T. Skorjanc, N. Elmerhi, S. Stephen, P.P. Sánchez, F. Gándara, S.J. Hinder, M.A. Baker, K. Polychronopoulou, D. Shetty, Crystallizing covalent organic frameworks from metal organic framework through chemical induced-phase engineering, Sci. Rep. 13 (2023) 19443, https://doi.org/10.1038/s41598-023-46573-3.

[71] J. Guo, D. Jiang, Covalent organic frameworks for heterogeneous catalysis: principle, current status, and challenges, ACS Cent. Sci. 6 (2020) 869–879, https://doi.org/10.1021/acscentsci.0c00463.

[72] M. Pourkhosravani, S. Dehghanpour, F. Farzaneh, Palladium nanoparticles supported on zirconium metal organic framework as an efficient heterogeneous catalyst for the suzuki–miyaura coupling reaction, Catal. Lett. 146 (2016) 499–508, https://doi.org/10.1007/s10562-015-1674-5.

[73] M. Farrag, In situ preparation of palladium nanoclusters in cerium metal-organic frameworks Ce-MOF-808, Ce-UiO-66 and Ce-BTC as nanoreactors for room temperature Suzuki cross-coupling reaction, Micropor Mesopor Mat 312 (2021) 110783, https://doi.org/10.1016/j.micromeso.2020.110783.

[74] K. Zhao, L.-X. Zhang, H. Xu, Y.-F. Liu, B. Tang, L.-J. Bie, Single-ion chelation strategy for synthesis of monodisperse Pd nanoparticles anchored in MOF-808 for highly efficient hydrogenation and cascade reactions, Nanoscale 14 (2022) 10980–10991, https://doi.org/10.1039/d2nr02765h.

[75] L. Mohammadi, M. Hosseinifard, M.R. Vaezi, Stabilization of palladium-nanoparticle-decorated postsynthesis-modified Zr-UiO-66 MOF as a reusable heterogeneous catalyst in C–C coupling reaction, ACS Omega (2023), https://doi.org/10.1021/acsomega.2c07661.

[76] L. Chen, Q. Xu, Metal-organic framework composites for catalysis, Matter 1 (2019) 57–89, https://doi.org/10.1016/j.matt.2019.05.018.

[77] L. Chen, R. Luque, Y. Li, Controllable design of tunable nanostructures inside metal–organic frameworks, Chem. Soc. Rev. 46 (2017) 4614–4630, https://doi.org/10.1039/c6cs00537c.

[78] C. Xu, R. Fang, R. Luque, L. Chen, Y. Li, Functional metal–organic frameworks for catalytic applications, Coord. Chem. Rev. 388 (2019) 268–292, https://doi.org/10.1016/j.ccr.2019.03.005.

[79] C.I. Ezugwu, N.A. Kabir, M. Yusubov, F. Verpoort, Metal–organic frameworks containing N-heterocyclic carbenes and their precursors, Coord. Chem. Rev. 307 (2016) 188–210, https://doi.org/10.1016/j.ccr.2015.06.012.

[80] D. Sun, Z. Li, Double-solvent method to Pd nanoclusters encapsulated inside the cavity of NH 2 –Uio-66(Zr) for efficient visible-light-promoted Suzuki coupling reaction, J. Phys. Chem. C 120 (2016) 19744–19750, https://doi.org/10.1021/acs.jpcc.6b06710.

[81] M. Duan, L. Jiang, G. Zeng, D. Wang, W. Tang, J. Liang, H. Wang, D. He, Z. Liu, L. Tang, Bimetallic nanoparticles/metal-organic frameworks: synthesis, applications and challenges, Appl. Mater. Today 19 (2020) 100564, https://doi.org/10.1016/j.apmt.2020.100564.

[82] D. Sun, M. Xu, Y. Jiang, J. Long, Z. Li, Small-sized bimetallic CuPd nanoclusters encapsulated inside cavity of NH2-UiO-66(Zr) with superior performance for light-induced Suzuki coupling reaction, Small Methods 2 (2018) 1800164, https://doi.org/10.1002/smtd.201800164.

[83] S. Subudhi, S. Mansingh, S.P. Tripathy, A. Mohanty, P. Mohapatra, D. Rath, K. Parida, The fabrication of Au/Pd plasmonic alloys on UiO-66-NH 2 : an efficient visible light-induced photocatalyst towards the Suzuki Miyaura coupling reaction under ambient conditions, Catal. Sci. Technol. 9 (2019) 6585–6597, https://doi.org/10.1039/c9cy01431d.

[84] J. Wang, T. Li, Z. Zhao, X. Zhang, W. Pang, Pd nanoparticles embedded into MOF-808: synthesis, structural characteristics, and catalyst properties for the suzuki–miyaura coupling reaction, Catal. Lett. 152 (2022) 1545–1554, https://doi.org/10.1007/s10562-021-03731-4.

[85] D. Cartagenova, S. Bachmann, J.A.V. Bokhoven, K. Püntener, M. Ranocchiari, Heterogeneous metal–organic framework catalysts for suzuki-miyaura cross coupling in the pharma industry, Chimia Int J Chem 75 (2021) 972–978, https://doi.org/10.2533/chimia.2021.972.

[86] G. Fabrizi, A. Goggiamani, A. Sferrazza, S. Cacchi, Sonogashira cross-coupling of arenediazonium salts, Angew. Chem. Int. Ed. 49 (2010) 4067–4070, https://doi.org/10.1002/anie.201000472.

[87] Y. Liu, J. Wang, T. Li, Z. Zhao, W. Pang, Base-free Pd-MOF catalyzed the Suzuki-Miyaura cross-coupling reaction of arenediazonium tetrafluoroborate salts with arylboronic acids, Tetrahedron 75 (2019) 130540, https://doi.org/10.1016/j.tet.2019.130540.

[88] K. Madankar, J. Mokhtari, Z. Mirjafary, Dichloroimidazolidinedione-activated one-pot Suzuki–Miyaura cross-coupling of phenols, Appl. Organometal. Chem. 34 (2020), https://doi.org/10.1002/aoc.5383.

[89] R. Ma, P. Yang, Y. Ma, F. Bian, Facile synthesis of magnetic hierarchical core–shell structured Fe3O4@PDA-Pd@MOF nanocomposites: highly integrated multifunctional catalysts, ChemCatChem 10 (2018) 1446–1454, https://doi.org/10.1002/cctc.201701693.

[90] A. Dhakshinamoorthy, Z. Li, H. Garcia, Catalysis and photocatalysis by metal organic frameworks, Chem. Soc. Rev. 47 (2018) 8134–8172, https://doi.org/10.1039/c8cs00256h.

[91] M.A. Nasalevich, C.H. Hendon, J.G. Santaclara, K. Svane, B. van der Linden, S.L. Veber, M.V. Fedin, A.J. Houtepen, M.A. van der Veen, F. Kapteijn, A. Walsh, J. Gascon, Electronic origins of photocatalytic activity in d0 metal organic frameworks, Sci. Rep. 6 (2016) 23676, https://doi.org/10.1038/srep23676.

[92] X. Deng, Z. Li, H. García, Visible light induced organic transformations using metal-organic-frameworks (MOFs), Chem. Eur J. 23 (2017) 11189–11209, https://doi.org/10.1002/chem.201701460.

[93] D.A. Reddy, Y. Kim, M. Gopannagari, D.P. Kumar, T.K. Kim, Recent advances in metal–organic framework-based photocatalysts for hydrogen production, Sustain. Energy Fuels 5 (2021) 1597–1618, https://doi.org/10.1039/c9se00749k.

[94] Q. Wang, Q. Gao, A.M. Al-Enizi, A. Nafady, S. Ma, Recent advances in MOF-based photocatalysis: environmental remediation under visible light, Inorg. Chem. Front. 7 (2019) 300–339, https://doi.org/10.1039/c9qi01120j.

[95] F.X.L. i Xamena, A. Abad, A. Corma, H. Garcia, MOFs as catalysts: activity, reusability and shape-selectivity of a Pd-containing MOF, J. Catal. 250 (2007) 294–298, https://doi.org/10.1016/j.jcat.2007.06.004.

[96] C.-H. Wang, W.-Y. Gao, Q. Ma, D.C. Powers, Templating metastable Pd 2 carboxylate aggregates, Chem. Sci. 10 (2018) 1823–1830, https://doi.org/10.1039/c8sc04940h.

[97] T. He, X.-J. Kong, J. Zhou, C. Zhao, K. Wang, X.-Q. Wu, X.-L. Lv, G.-R. Si, J.-R. Li, Z.-R. Nie, A practice of reticular chemistry: construction of a robust mesoporous palladium metal–organic framework via metal metathesis, J. Am. Chem. Soc. 143 (2021) 9901–9911, https://doi.org/10.1021/jacs.1c04077.

[98] S. Parshamoni, R. Nasani, A. Paul, S. Konar, Synthesis of a palladium based MOF via an effective post-synthetic modification approach and its catalytic activity towards Heck type coupling reactions, Inorg. Chem. Front. 8 (2020) 693–699, https://doi.org/10.1039/d0qi01052a.

[99] K. Dedecker, M. Drobek, V. Rouessac, A. Julbe, A palladium-based MOF for the preferential sorption of benzene, ACS Appl. Mater. Interfaces 15 (2023) 6831–6838, https://doi.org/10.1021/acsami.2c20034.

[100] A.J. Rieth, A.M. Wright, M. Dincă, Kinetic stability of metal–organic frameworks for corrosive and coordinating gas capture, Nat. Rev. Mater. 4 (2019) 708–725, https://doi.org/10.1038/s41578-019-0140-1.

[101] J.-P. Zhang, Y.-B. Zhang, J.-B. Lin, X.-M. Chen, Metal azolate frameworks: from crystal engineering to functional materials, Chem. Rev. 112 (2012) 1001–1033, https://doi.org/10.1021/cr200139g.

[102] F. Zheng, S. Cao, Z. Yang, Y. Sun, Z. Shen, Y. Wang, H. Pang, Review: synthesis and catalytic application of MOF complexes containing noble metals, Energy Fuels 38 (2024) 11494–11520, https://doi.org/10.1021/acs.energyfuels.4c01963.

[103] J.A.R. Navarro, E. Barea, J.M. Salas, N. Masciocchi, S. Galli, A. Sironi, C.O. Ania, J.B. Parra H2, N2, CO, and CO2 sorption properties of a series of robust sodalite-type microporous coordination polymers, Inorg. Chem. 45 (2006) 2397–2399, https://doi.org/10.1021/ic060049r.

[104] M. Moharramnejad, A. Ehsani, S. salmani, M. shahi, R.E. Malekshah, Z.S. Robatjazi, H. Parsimehr, Zinc-based metal-organic frameworks: synthesis and recent progress in biomedical application, J Inorg Organomet P 32 (2022) 3339–3354, https://doi.org/10.1007/s10904-022-02385-y.

[105] G.E.M. Schukraft, S. Ayala, B.L. Dick, S.M. Cohen, Isoreticular expansion of polyMOFs achieves high surface area materials, Chem. Commun. 53 (2017) 10684–10687, https://doi.org/10.1039/c7cc04222a.

[106] S.J. Lyle, R.W. Flaig, K.E. Cordova, O.M. Yaghi, Facilitating laboratory research experience using reticular chemistry, J Chem Educ 95 (2018) 1512–1519, https://doi.org/10.1021/acs.jchemed.8b00265.

[107] Z. Mai, D. Liu, Synthesis and applications of isoreticular metal–organic frameworks IRMOFs-n (n = 1, 3, 6, 8), Cryst. Growth Des. 19 (2019) 7439–7462, https://doi.org/10.1021/acs.cgd.9b00879.

[108] Y. Gong, Y.-L. Hou, L. Guo, J. Liu, L. Chen, Y. Gao, Compatible with excellent gold/palladium trap and open sites for green Suzuki coupling by an imidazole-modified MOF, Micropor Mesopor Mat 337 (2022) 111877, https://doi.org/10.1016/j.micromeso.2022.111877.

[109] W. Chen, P. Cai, P. Elumalai, P. Zhang, L. Feng, M. Al-Rawashdeh, S.T. Madrahimov, H.-C. Zhou, Site-isolated azobenzene-containing metal–organic framework for cyclopalladated catalyzed suzuki-miyuara coupling in flow, Acs Appl Mater Inter 13 (2021) 51849–51854, https://doi.org/10.1021/acsami.1c03607.

[110] X. Gong, L. Zhang, H. Zhang, Y. Cui, F. Jin, Y. Liu, Y. Zhai, J. Li, G. Liu, Y. Zeng, Highly active heterogeneous PdCl2/MOF catalyst for suzuki–miyaura cross-coupling reactions of aryl chloride, Z. Anorg. Allg. Chem. 646 (2020) 1336–1341, https://doi.org/10.1002/zaac.202000132.

[111] S. Kim, S. Jee, K.M. Choi, D.-S. Shin, Single-atom Pd catalyst anchored on Zr-based metal-organic polyhedra for Suzuki-Miyaura cross coupling reactions in aqueous media, Nano Res. 14 (2021) 486–492, https://doi.org/10.1007/s12274-020-2885-7.

[112] H. Veisi, M. Abrifam, S.A. Kamangar, M. Pirhayati, S.G. Saremi, M. Noroozi, T. Tamoradi, B. Karmakar, Pd immobilization biguanidine modified Zr-UiO-66 MOF as a reusable heterogeneous catalyst in Suzuki–Miyaura coupling, Sci Rep-Uk 11 (2021) 21883, https://doi.org/10.1038/s41598-021-00991-3.

[113] S. Daliran, M. Ghazagh-Miri, A.R. Oveisi, M. Khajeh, S. Navalón, M. Alvaro, M. Ghaffari-Moghaddam, H.S. Delarami, H. García, A pyridyltriazol functionalized zirconium metal–organic framework for selective and highly efficient adsorption of palladium, Acs Appl Mater Inter 12 (2020) 25221–25232, https://doi.org/10.1021/acsami.0c06672.

[114] R. Sun, B. Liu, B. Li, S. Jie, Palladium(II)@Zirconium-Based mixed-linker metal–organic frameworks as highly efficient and recyclable catalysts for Suzuki and Heck cross-coupling reactions, ChemCatChem 8 (2016) 3261–3271, https://doi.org/10.1002/cctc.201600774.

[115] X. Li, R.V. Zeeland, R.V. Maligal-Ganesh, Y. Pei, G. Power, L. Stanley, W. Huang, Impact of linker engineering on the catalytic activity of metal–organic frameworks containing Pd(II)–Bipyridine complexes, ACS Catal. 6 (2016) 6324–6328, https://doi.org/10.1021/acscatal.6b01753.

[116] X. Li, B. Zhang, R.V. Zeeland, L. Tang, Y. Pei, Z. Qi, T.W. Goh, L.M. Stanley, W. Huang, Unveiling the effects of linker substitution in Suzuki coupling with palladium nanoparticles in metal–organic frameworks, Catal. Lett. 148 (2018) 940–945, https://doi.org/10.1007/s10562-017-2289-9.

[117] H. Furukawa, F. Gándara, Y.-B. Zhang, J. Jiang, W.L. Queen, M.R. Hudson, O.M. Yaghi, Water adsorption in porous metal–organic frameworks and related materials, J. Am. Chem. Soc. 136 (2014) 4369–4381, https://doi.org/10.1021/ja500330a.

[118] A.H. Vahabi, F. Norouzi, E. Sheibani, M. Rahimi-Nasrabadi, Functionalized Zr-UiO-67 metal-organic frameworks: structural landscape and application, Coordin Chem Rev 445 (2021) 214050, https://doi.org/10.1016/j.ccr.2021.214050.

[119] A. Dhakshinamoorthy, A. Santiago-Portillo, A.M. Asiri, H. Garcia, Engineering UiO-66 metal organic framework for heterogeneous catalysis, ChemCatChem 11 (2019) 899–923, https://doi.org/10.1002/cctc.201801452.

[120] J.H. Cavka, S. Jakobsen, U. Olsbye, N. Guillou, C. Lamberti, S. Bordiga, K.P. Lillerud, A new zirconium inorganic building brick forming metal organic frameworks with exceptional stability, J. Am. Chem. Soc. 130 (2008) 13850–13851, https://doi.org/10.1021/ja8057953.

[121] F. Vermoortele, B. Bueken, G.L. Bars, B.V. de Voorde, M. Vandichel, K. Houthoofd, A. Vimont, M. Daturi, M. Waroquier, V.V. Speybroeck, C. Kirschhock, D.E. D. Vos, Synthesis modulation as a tool to increase the catalytic activity of metal–organic frameworks: the unique case of UiO-66(Zr), J. Am. Chem. Soc. 135 (2013) 11465–11468, https://doi.org/10.1021/ja405078u.

[122] Y.-M. Li, L. Cao, H. Ren, C.-Y. Ji, W. Li, L. Cheng, Chiral polymer-mediated Pd@MOF-808 for efficient sequential asymmetric reaction, Catal. Lett. (2022) 1–12, https://doi.org/10.1007/s10562-022-04053-9.

[123] L. Mohammadi, M.R. Vaezi, Palladium nanoparticle-decorated porous metal–organic-framework (Zr)@Guanidine: novel efficient catalyst in cross-coupling (Suzuki, Heck, and Sonogashira) reactions and carbonylative Sonogashira under mild conditions, ACS Omega 8 (2023) 16395–16410, https://doi.org/10.1021/acsomega.3c01179.

[124] Y. Dong, W.-H. Li, Y.-B. Dong, Dual-metal N-heterocyclic carbene complex (M = Au and Pd)-Functionalized UiO-67 MOF for alkyne hydration–suzuki coupling tandem reaction, J. Org. Chem. 86 (2021) 1818–1826, https://doi.org/10.1021/acs.joc.0c02641.

[125] L. Chen, Z. Gao, Y. Li, Immobilization of Pd(II) on MOFs as a highly active heterogeneous catalyst for Suzuki–Miyaura and Ullmann-type coupling reactions, Catal. Today 245 (2015) 122–128, https://doi.org/10.1016/j.cattod.2014.03.074.

[126] L. Chen, S. Rangan, J. Li, H. Jiang, Y. Li, A molecular Pd(ii) complex incorporated into a MOF as a highly active single-site heterogeneous catalyst for C–Cl bond activation, Green Chem. 16 (2014) 3978–3985, https://doi.org/10.1039/c4gc00314d.

[127] X. Li, T.W. Goh, C. Xiao, A.L.D. Stanton, Y. Pei, P.K. Jain, W. Huang, Synthesis of monodisperse palladium nanoclusters using metal–organic frameworks as sacrificial templates, Chemnanomat 2 (2016) 810–815, https://doi.org/10.1002/cnma.201600121.

[128] W. Alsalahi, A.W. Augustyniak, W. Tylus, A.M. Trzeciak, New palladium – ZrO2 nano-architectures from thermal transformation of UiO-66-NH2 for carbonylative Suzuki and hydrogenation reactions, Chem European J 28 (2022) e202103538, https://doi.org/10.1002/chem.202103538.

[129] K.K. Gangu, S. Maddila, S.B. Mukkamala, S.B. Jonnalagadda, A review on contemporary Metal–Organic Framework materials, Inorg. Chim. Acta. 446 (2016) 61–74, https://doi.org/10.1016/j.ica.2016.02.062.

[130] S. Bhattacharya, W.W. Ayass, D.H. Taffa, T. Nisar, T. Balster, A. Hartwig, V. Wagner, M. Wark, U. Kortz, Polyoxopalladate-loaded metal–organic framework (POP@MOF): synthesis and heterogeneous catalysis, Inorg. Chem. 59 (2020) 10512–10521, https://doi.org/10.1021/acs.inorgchem.0c00875.

[131] C. He, J. Liang, Y.-H. Zou, J.-D. Yi, Y.-B. Huang, R. Cao, Metal-organic frameworks bonded with metal N-heterocyclic carbenes for efficient catalysis, Natl. Sci. Rev. 9 (2021) nwab157, https://doi.org/10.1093/nsr/nwab157.

[132] E. Niknam, F. Panahi, A. Khalafi-Nezhad, Immobilized Pd on a NHC functionalized metal–organic framework MIL-101(Cr): an efficient heterogeneous catalyst in Suzuki−Miyaura coupling reaction in water, Appl. Organometal. Chem. 34 (2020), https://doi.org/10.1002/aoc.5470.

[133] M. Bahadori, S. Tangestaninejad, M. Moghadam, V. Mirkhani, A. Mechler, I. Mohammadpoor-Baltork, F. Zadehahmadi, Metal organic framework-supported N-heterocyclic carbene palladium complex: a highly efficient and reusable heterogeneous catalyst for Suzuki-Miyaura C-C coupling reaction, Micropor Mesopor Mat 253 (2017) 102–111, https://doi.org/10.1016/j.micromeso.2017.06.048.

[134] B. Yuan, Y. Pan, Y. Li, B. Yin, H. Jiang, A highly active heterogeneous palladium catalyst for the suzuki–miyaura and ullmann coupling reactions of aryl chlorides in aqueous media, Angew Chem-Ger Edit 122 (2010) 4148–4152, https://doi.org/10.1002/ange.201000576.
[135] V. Pascanu, P.R. Hansen, A.B. Gómez, C. Ayats, A.E. Platero-Prats, M.J. Johansson, M.À. Pericàs, B. Martín-Matute, Highly functionalized biaryls via suzuki–miyaura cross-coupling catalyzed by Pd@MOF under batch and continuous flow regimes, ChemSusChem 8 (2015) 123–130, https://doi.org/10.1002/cssc.201402858.
[136] V. Pascanu, Q. Yao, A.B. Gómez, M. Gustafsson, Y. Yun, W. Wan, L. Samain, X. Zou, B. Martín-Matute, Sustainable catalysis: rational Pd loading on MIL-101Cr-NH2 for more efficient and recyclable suzuki–miyaura reactions, Chem. Eur J. 19 (2013) 17483–17493, https://doi.org/10.1002/chem.201302621.
[137] Y. Huang, Z. Zheng, T. Liu, J. Lü, Z. Lin, H. Li, R. Cao, Palladium nanoparticles supported on amino functionalized metal-organic frameworks as highly active catalysts for the Suzuki–Miyaura cross-coupling reaction, Catal. Commun. 14 (2011) 27–31, https://doi.org/10.1016/j.catcom.2011.07.004.
[138] S. Bhattacharjee, C. Chen, W.-S. Ahn, Chromium terephthalate metal–organic framework MIL-101: synthesis, functionalization, and applications for adsorption and catalysis, Rsc Adv 4 (2014) 52500–52525, https://doi.org/10.1039/c4ra11259h.
[139] S.-H. Lo, D.S. Raja, C.-W. Chen, Y.-H. Kang, J.-J. Chen, C.-H. Lin, Waste polyethylene terephthalate (PET) materials as sustainable precursors for the synthesis of nanoporous MOFs, MIL-47, MIL-53(Cr, Al, Ga) and MIL-101(Cr), Dalton Trans. 45 (2016) 9565–9573, https://doi.org/10.1039/c6dt01282e.
[140] G. Férey, C. Mellot-Draznieks, C. Serre, F. Millange, J. Dutour, S. Surblé, I. Margiolaki, A chromium terephthalate-based solid with unusually large pore volumes and surface area, Science 309 (2005) 2040–2042, https://doi.org/10.1126/science.1116275.
[141] K.K. Tanabe, S.M. Cohen, Postsynthetic modification of metal–organic frameworks—a progress report, Chem. Soc. Rev. 40 (2010) 498–519, https://doi.org/10.1039/c0cs00031k.
[142] M. Kalaj, S.M. Cohen, Postsynthetic modification: an enabling technology for the advancement of metal–organic frameworks, ACS Cent. Sci. 6 (2020) 1046–1057, https://doi.org/10.1021/acscentsci.0c00690.
[143] A. Dhankhar, R.K. Rai, D. Tyagi, X. Yao, S.K. Singh, Synergistic catalysis with MIL-101: stabilized highly active bimetallic NiPd and CuPd alloy nanoparticle catalysts for C–C coupling reactions, Chem 1 (2016) 3223–3227, https://doi.org/10.1002/slct.201600752.
[144] F. Carson, V. Pascanu, A.B. Gómez, Y. Zhang, A.E. Platero-Prats, X. Zou, B. Martín-Matute, Influence of the base on Pd@MIL-101-NH2(Cr) as catalyst for the suzuki–miyaura cross-coupling reaction, Chem European J 21 (2015) 10896–10902, https://doi.org/10.1002/chem.201500843.
[145] O. Singh, A. Agrawal, B.M. Abraham, R. Goyal, C. Pendem, B. Sarkar, Integration of zeolite@metal–organic framework: a composite catalyst for isopropyl alcohol conversion to aromatics, Mater. Today Chem. 24 (2022) 100796, https://doi.org/10.1016/j.mtchem.2022.100796.
[146] Y. Yang, D. Cong, S. Hao, Template-directed ordered mesoporous Silica@Palladium-containing zinc metal–organic framework composites as highly efficient Suzuki coupling catalysts, ChemCatChem 8 (2016) 900–905, https://doi.org/10.1002/cctc.201501314.
[147] D. Saha, R. Sen, T. Maity, S. Koner, Anchoring of palladium onto surface of porous metal–organic framework through post-synthesis modification and studies on Suzuki and stille coupling reactions under heterogeneous condition, Langmuir 29 (2013) 3140–3151, https://doi.org/10.1021/la304147j.
[148] F. Nouri, S. Rostamizadeh, M. Azad, Post-synthetic modification of IRMOF-3 with an iminopalladacycle complex and its application as an effective heterogeneous catalyst in Suzuki-Miyaura cross-coupling reaction in H2O/EtOH media at room temperature, Mol. Catal. 443 (2017) 286–293, https://doi.org/10.1016/j.mcat.2017.10.019.
[149] B. Salahshournia, H. Hamadi, V. Nobakht, Designing a bifunctional metal-organic framework by tandem post-synthetic modifications; an efficient and recyclable catalyst for Suzuki-Miyaura cross-coupling reaction, Polyhedron 189 (2020) 114749, https://doi.org/10.1016/j.poly.2020.114749.
[150] R. Taghavi, S. Rostamnia, Schiff-base post-synthetic modification of IRMOF-3 to encapsulate Pd nanoparticles: it's application in C-C bond formation cross-coupling Suzuki reaction, Chemical Methodologies 6 (2022) 629–638.
[151] S.M.H. Shirazi, J. Mokhtari, Z. Mirjafary, A new method for the synthesis of abiraterone drug catalyzed by Pd-NPs@Zn-MOF as efficient reusable catalyst, Appl. Organometal. Chem. 36 (2022), https://doi.org/10.1002/aoc.6477.
[152] H. Mao, W. Zhang, W. Zhou, B. Zou, B. Zheng, S. Zhao, F. Huo, Hybridization of metal nanoparticles with metal–organic frameworks using protein as amphiphilic stabilizer, Acs Appl Mater Inter 9 (2017) 24649–24654, https://doi.org/10.1021/acsami.7b06754.
[153] M. Položij, M. Rubeš, J. Čejka, P. Nachtigall, Catalysis by dynamically formed defects in a metal–organic framework structure: knoevenagel reaction catalyzed by copper benzene-1,3,5-tricarboxylate, ChemCatChem 6 (2014) 2821–2824, https://doi.org/10.1002/cctc.201402411.
[154] G.H. Dang, T.T. Dang, D.T. Le, T. Truong, N.T.S. Phan, Propargylamine synthesis via sequential methylation and C–H functionalization of N-methylanilines and terminal alkynes under metal–organic framework Cu2(BDC)2(DABCO) catalysis, J. Catal. 319 (2014) 258–264, https://doi.org/10.1016/j.jcat.2014.09.010.
[155] S. Tahmasebi, J. Mokhtari, M.R. Naimi-Jamal, A. Khosravi, L. Panahi, One-step synthesis of Pd-NPs@Cu2(BDC)2DABCO as efficient heterogeneous catalyst for the Suzuki–Miyaura cross-coupling reaction, J. Organomet. Chem. 853 (2017) 35–41, https://doi.org/10.1016/j.jorganchem.2017.10.011.
[156] L. Panahi, M.R. Naimi-Jamal, J. Mokhtari, Ultrasound-assisted Suzuki-Miyaura reaction catalyzed by Pd@Cu2(NH2-BDC)2(DABCO), J. Organomet. Chem. 868 (2018) 36–46, https://doi.org/10.1016/j.jorganchem.2018.04.038.
[157] S. Rostamnia, H. Alamgholiloo, X. Liu, Pd-grafted open metal site copper-benzene-1,4-dicarboxylate metal organic frameworks (Cu-BDC MOF's) as promising interfacial catalysts for sustainable Suzuki coupling, J Colloid Interf Sci 469 (2016) 310–317, https://doi.org/10.1016/j.jcis.2016.02.021.
[158] S.A. Adalikwu, V.S. Mothika, A. Hazra, T.K. Maji, Polar functional groups anchored to a 2D MOF template for the stabilization of Pd(0) nps for the catalytic C–C coupling reaction, Dalton T 48 (2019) 7117–7121, https://doi.org/10.1039/c8dt04766a.
[159] H. Tang, M. Yang, X. Li, M.-L. Zhou, Y.-S. Bao, X.-Y. Cui, K. Zhao, Y.-Y. Zhang, Z.-B. Han, Synthesis of biaryl compounds via Suzuki homocoupling reactions catalyzed by metal organic frameworks encapsulated with palladium nanoparticles, Inorg. Chem. Commun. 123 (2021) 108368, https://doi.org/10.1016/j.inoche.2020.108368.
[160] M. Sanaei, R. Fazaeli, H. Aliyan, Pd/MOF-199: as an efficient heterogeneous catalyst for the Suzukie Miyaura cross-coupling reaction, J Chin Chem Soc-Taip 66 (2019) 1290–1295, https://doi.org/10.1002/jccs.201800428.
[161] A.W. Augustyniak, W. Zawartka, J.A.R. Navarro, A.M. Trzeciak, Palladium nanoparticles supported on a nickel pyrazolate metal organic framework as a catalyst for Suzuki and carbonylative Suzuki couplings, Dalton T 45 (2016) 13525–13531, https://doi.org/10.1039/c6dt02242a.
[162] V. Colombo, C. Montoro, A. Maspero, G. Palmisano, N. Masciocchi, S. Galli, E. Barea, J.A.R. Navarro, Tuning the adsorption properties of isoreticular pyrazolate-based metal–organic frameworks through ligand modification, J. Am. Chem. Soc. 134 (2012) 12830–12843, https://doi.org/10.1021/ja305267m.
[163] L. Peng, S. Yang, S. Jawahery, S.M. Moosavi, A.J. Huckaba, M. Asgari, E. Oveisi, M.K. Nazeeruddin, B. Smit, W.L. Queen, Preserving porosity of mesoporous metal–organic frameworks through the introduction of polymer guests, J. Am. Chem. Soc. 141 (2019) 12397–12405, https://doi.org/10.1021/jacs.9b05967.
[164] Y. Su, Y. Zhang, C. Li, G. Xu, J. Bai, Direct hybridization of Pd on metal–organic framework (MOF)@PAN(C) to catalyze Suzuki reaction, Catal. Lett. 150 (2020) 3196–3205, https://doi.org/10.1007/s10562-020-03213-z.
[165] A. Ghorbani-Choghamarani, Z. Taherinia, M. Mohammadi, Facile synthesis of Fe 3 O 4 @GlcA@Ni-MOF composites as environmentally green catalyst in organic reactions, Environ Technology Innovation 24 (2021) 102050, https://doi.org/10.1016/j.eti.2021.102050.
[166] J. Lim, S. Lee, H. Ha, J. Seong, S. Jeong, M. Kim, S.B. Baek, M.S. Lah, Amine-tagged fragmented ligand installation for covalent modification of MOF-74, Angew. Chem. Int. Ed. 60 (2021) 9296–9300, https://doi.org/10.1002/anie.202100456.
[167] T. Kitao, Y. Zhang, S. Kitagawa, B. Wang, T. Uemura, Hybridization of MOFs and polymers, Chem. Soc. Rev. 46 (2017) 3108–3133, https://doi.org/10.1039/c7cs00041c.
[168] H. Pellissier, Recent developments in enantioselective lanthanide-catalyzed transformations, Coord. Chem. Rev. 336 (2017) 96–151, https://doi.org/10.1016/j.ccr.2017.01.013.
[169] M. Gustafsson, A. Bartoszewicz, B. Martín-Matute, J. Sun, J. Grins, T. Zhao, Z. Li, G. Zhu, X. Zou, A family of highly stable lanthanide Metal−Organic frameworks: structural evolution and catalytic activity, Chem. Mater. 22 (2010) 3316–3322, https://doi.org/10.1021/cm100503q.
[170] R.F. D'Vries, M. Iglesias, N. Snejko, E. Gutiérrez-Puebla, M.A. Monge, Lanthanide metal–organic frameworks: searching for efficient solvent-free catalysts, Inorg. Chem. 51 (2012) 11349–11355, https://doi.org/10.1021/ic300816r.

[171] L.-X. You, L.-X. Cui, B.-B. Zhao, G. Xiong, F. Ding, B.-Y. Ren, Z.-L. Shi, I. Dragutan, V. Dragutan, Y.-G. Sun, Tailoring the structure, pH sensitivity and catalytic performance in Suzuki–Miyaura cross-couplings of Ln/Pd MOFs based on the 1,1′-di(p -carboxybenzyl)-2,2′-diimidazole linker, Dalton T 47 (2018) 8755–8763, https://doi.org/10.1039/c8dt01288a.
[172] D. Dong, Z. Li, D. Liu, N. Yu, H. Zhao, H. Chen, J. Liu, D. Liu, Postsynthetic modification of single Pd sites into uncoordinated polypyridine groups of a MOF as the highly efficient catalyst for Heck and Suzuki reactions, New J. Chem. 42 (2018) 9317–9323, https://doi.org/10.1039/c8nj00518d.
[173] G. Xiong, X.-L. Chen, L.-X. You, B.-Y. Ren, F. Ding, I. Dragutan, V. Dragutan, Y.-G. Sun, La-Metal-Organic Framework incorporating Fe3O4 nanoparticles, post-synthetically modified with Schiff base and Pd. A highly active, magnetically recoverable, recyclable catalyst for CC cross-couplings at low Pd loadings, J. Catal. 361 (2018) 116–125, https://doi.org/10.1016/j.jcat.2018.02.026.
[174] W. Lin, Y. Song, L. Wang, N. Li, Y. Fu, D.-L. Chen, W. Zhu, F. Zhang, Palladium nanoparticles supported on Ce-MOF-801 as highly efficient and stable heterogeneous catalysts for suzuki-miyaura coupling reactions, Catal. Lett. (2022) 1–10, https://doi.org/10.1007/s10562-022-04163-4.
[175] J. Guo, S.-X. Yao, L.-X. You, G. Xiong, I. Dragutan, V. Dragutan, F. Ding, Y.-G. Sun, Pd and Ni NPs@Eu-MOF, an economically advantageous nanocatalyst for C (sp2)-C(sp2) cross-coupling reactions. Key role of Ni and of the metal nanoparticles, Polyhedron 223 (2022) 115950, https://doi.org/10.1016/j.poly.2022.115950.
[176] F. Ding, Y. Li, P. Yan, Y. Deng, D. Wang, Y. Zhang, I. Dragutan, V. Dragutan, K. Wang, Efficient suzuki–miyaura C-C cross-couplings induced by novel heterodinuclear Pd-bpydc-Ln scaffolds, Molecules 23 (2018) 2435, https://doi.org/10.3390/molecules23102435.
[177] J.A. Bobb, A.A. Ibrahim, M.S. El-Shall, Laser synthesis of carbonaceous TiO2 from metal–organic frameworks: optimum support for Pd nanoparticles for C–C cross-coupling reactions, ACS Appl. Nano Mater. 1 (2018) 4852–4862, https://doi.org/10.1021/acsanm.8b01045.
[178] D. Chen, L. Wei, Y. Yu, L. Zhao, Q. Sun, C. Han, J. Lu, H. Nie, L.-X. Shao, J. Qian, Z. Yang, Size-selective suzuki–miyaura coupling reaction over ultrafine Pd nanocatalysts in a water-stable indium–organic framework, Inorg. Chem. 61 (2022) 15320–15324, https://doi.org/10.1021/acs.inorgchem.2c02877.
[179] D. Cartagenova, S. Bachmann, K. Püntener, M. Scalone, M.A. Newton, F.A.P. Esteves, T. Rohrbach, P.P. Zimmermann, J.A. van Bokhoven, M. Ranocchiari, Highly selective Suzuki reaction catalysed by a molecular Pd–P-MOF catalyst under mild conditions: role of ligands and palladium speciation, Catal. Sci. Technol. 12 (2021) 954–961, https://doi.org/10.1039/d1cy01351c.